The Dissertation Committee for Kai-Yin Lo Certifies that this is the approved version of the following dissertation:

Nuclear export and cytoplasmic maturation of the large ribosomal subunit

Committee:

Arlen W. Johnson, Supervisor

Paul M. Macdonald

Makkuni Jayaram

Clarence S. M. Chan

Jaquelin P. Dudley

Nuclear export and cytoplasmic maturation of the large ribosomal subunit

by

Kai-Yin Lo, B.S. ; M.S.

Dissertation

Presented to the Faculty of the Graduate School of

The University of Texas at Austin

in Partial Fulfillment

of the Requirements

for the Degree of

Doctor of Philosophy

The University of Texas at Austin

August, 2009

Dedication

This dissertation is dedicated to my husband and parents for their love and support throughout my graduate study

Acknowledgements

I thank my advisor, Dr. Arlen Johnson, for all his support and effort in training me, allowing me to accomplish my PhD study and develop as a scientist. I also appreciate all the guidance from my committee members**,** Dr. Makkuni Jayaram, Dr. Paul M. Macdonald, Dr. Clarence S. M. Chan, and Dr. Jaquelin P. Dudley, as well as Dr. Scott Steven who has followed my work during joint group meetings. I appreciate all my lab members, past and present, Dr. John Hedeges, Dr. Matthew West, Dr. Lingna Wang, Dr. Nai-Jung Hung, Dr. Peggy Huang, Dr. Simrit Dhaliwal, Cyril Bussiere, Richa Sardana, Joshua White, Kara Helmke, Reed Pfifer, Stafan Bresson, and members of the Stevens Lab for insightful discussion. I also thank Dr. Zhihua Li and Dr. Edward Marcotte for support of the human cell work in the YVH1 project.

I would like to show my sincere gratitude to my husband, Yung-Shin Sun, for his love, understanding, and company. This gives me energy and braveness to complete my PhD study. And I appreciate the support from my beloved parents and sister throughout my graduate career. I am grateful for companionship and friendship from my friends in Austin. Without them, I could not make it through all the difficulties of these years.

I thank E. Hurt, C. Dargemont, E. Lund, J.P. Ballesta, and A. Warren for numerous reagents and helpful comments to my work. This work was supported by NIH GM53655 to A.W. Johnson. Additional support was provided by the Program of Microbiology, the School of Biological Sciences, and the University of Texas at Austin.

Nuclear export and cytoplasmic maturation of the large ribosomal subunit

Publication No._____

Kai-Yin Lo, PhD
The University of Texas at Austin, 2009

Supervisor: Arlen W. Johnson

The work in this thesis addresses the general problem of how ribosomal subunits are exported from the nucleus to mature in the cytoplasm. There are three parts in this dissertation. In the first part, I asked questions about the specificity for export receptors in the nuclear export of the large (60S) ribosomal subunit in yeast. In principle, I tethered different export receptors that are known to work in various unrelated export pathways to the ribosome by fusing them to the trans-acting factor Nmd3. Interestingly, all the chimeric receptors were able to support export, although to different degrees. Moreover, 60S export driven by these chimeric receptors was independent of Crm1, an export receptor that is essential for 60S export in wild-type cells.

The second question I addressed in this project was whether or not a nuclear export signal could be provided in cis on ribosomal proteins (Rpls) rather than in trans by a transacting factor. The nuclear export signal (NES) of Nmd3 was fused to different ribosomal proteins and tested for support of 60S export. Several Rpl-NES fusion constructs worked to promote 60S export. Rpl3 gave the best efficiency. In conclusion, these results imply unexpected flexibility in the 60S export pathway. This may help

explain how different export receptors could have evolved in different eukaryotic lineages.

In the second part of my thesis, I identified the assembly pathway for the base of the ribosome stalk. The stalk is an important functional domain of the large ribosomal subunit because of its requirement for interaction with translation factors. Mrt4 is a nuclear paralog of P0, which is an essential part of the stalk. Here, I identified Yvh1 a novel ribosome biogenesis factor that is required for the release of Mrt4. Yvh1 is a conserved dual phosphatase, but the C-terminal zinc-binding domain rather than the phosphatase function was required for its activity to release Mrt4. Mrt4 localizes in the nucleus and nucleolus in the wild-type cells, but was persistent on cytoplasmic 60S subunits in *yvh1*Δ cells. The persistence of Mrt4 on the 60S subunits blocked the loading of P0 and assembly of the stalk. I also found the binding of Yvh1 depended on Rpl12, a protein that binds together with P0 to form the base of the stalk. Deletion of Rpl12 phenocopied *yvh1*Δ. These data identified the function of Yvh1 as a release factor of Mrt4. I also showed that the function of Yvh1 is conserved in human cells.

In my final project, I analyzed the interdependence and order of the known cytoplasmic maturation events of the 60S subunit. 60S subunits require several maturation steps in the cytoplasm before they become competent in translation. There are four major steps involving two ATPases, Drg1 and Ssa1, and two GTPases, Efl1 and Lsg1. In my study, I ordered these steps into one serial pathway. Drg1 releases Rlp24 in the earliest step of 60S maturation in the cytoplasm. Truncation of the C-terminus of Rlp24 blocked cytoplasmic maturation of the large subunit by preventing the recruitment of Drg1 and led to a secondary defect in the release of Arx1 because of a failure to recruit Rei1. Deletion of REI1 mislocalized Tif6 from the nucleus and nucleolus to the cytoplasm and deletion of ARX1 suppressed the Tif6 mislocalization, indicating that the release of Arx1 was required for Tif6 release downstream.

I found that mutation of efl1 or sdo1, the known release factors for Tif6, also blocked Nmd3 release. Tif6-V192F, which could bypass the growth defects of *efl1* or *sdo1* mutants, suppressed the defect of Nmd3 recycling. These results showed that the release of Tif6 was a prerequisite for Nmd3 release. Thus, the release of Nmd3 is

downstream of the Tif6 release step. In conclusion, I have ordered the events of cytoplasmic maturation with Drg1 as the first step after ribosome export, followed by Rei1/Jji1 and then Sdo1/Efl1. The release of Nmd3 by Lsg1 appears to be the last step of ribosome maturation in the cytoplasm. Thus, the two ATPases Drg1 and Ssa work first and then the two GTPases Efl1 and Lsg1 work in a linear pathway of 60S maturation in the cytoplasm.

Table of Contents

List of Tables

List of Figures

List of Illustrations

Chapter 1
Introduction

1.1 Overview

The ribosome is a large macromolecular complex that is responsible for decoding cellular genetic information into protein. The ribosome itself is composed of both RNA and protein that are assembled into two subunits. In eukaryotes, these are the small subunit (40S) and the large subunit (60S). During translation, the two subunits join together on an mRNA to form the 80S ribosome.

In eukaryotic cells, the assembly of ribosomes occurs in the nucleolus, a subcompartment of the nucleus devoted to ribosome biogenesis. After initial assembly in the nucleolus, ribosomes are exported through the nuclear pore complexes (NPCs) to the cytoplasm where final maturation is completed. My work has focused on late steps of the biogenesis of the 60S subunit: beginning with its export from the nucleus and continuing with maturation of the subunit in the cytoplasm.

In my dissertation work, I have explored several questions related to aspects of ribosome biogenesis. First, I asked about the specificity of receptors for 60S export. In other words, is there a requirement for specific export receptors? For example, specific receptors may help orient the subunit with respect to the nuclear pore complex. Interestingly, I found that 60S subunits show incredible flexibility with respect to the use of different receptors. Export can be driven by virtually any export receptor, even the ones not normally used in 60S export. I also asked about the nature of the nuclear export signal (NES) itself. I show that an NES can be provided in *cis* to the ribosome; this signal does not have to be provided by a trans-acting factor. In the second part of my research, I identified the function of a novel ribosome biogenesis factor, Yvh1. The results from this study outline the pathway for assembly of the ribosomal stalk, an essential structure that recruits translation factors to the ribosome. Finally, in the third portion of my work, I considered all the known cytoplasmic maturation events together and have delineated the pathway of 60S maturation in the cytoplasm. I show that maturation of the subunit

proceeds by a series of steps where an upstream step is required to trigger the next step, similar to a biochemical pathway.

1.2 Ribosome biogenesis in the nucleolus

The ribosome is a huge complex constituted of rRNAs and ribosomal proteins. The bacterial ribosome is around 2.5MDa, and the yeast ribosome is approximately 30% larger in size. The synthesis of ribosomes is the most energy costly activity in an actively growing cell (Warner, 1999). In *Saccharomyces cerevisiae*, 40S and 60S subunits are assembled from a large primary 35S rRNA transcribed by RNA polymerase I. Processing of this rRNA yields 5.8S, 18S, and 25S (Illustration 1.1). The 5S RNA is transcribed by RNA polymerase III separately. 5S, 5.8S, and 25S (28S in higher eukaryotes) rRNA assemble with over 40 ribosomal proteins to make up the 60S subunit (Mager et al., 1997; Planta and Mager, 1998). The 40S contain 18S rRNA and 33 ribosomal proteins (Planta and Mager, 1998; Sengupta et al., 2004).

Ribosome assembly requires many non-ribosomal transacting factors for rRNA processing, rRNA folding, protein loading, and export (Tschochner and Hurt, 2003; Venema and Tollervey, 1999). The rRNAs are extensively modified. Over 100 small nucleolar RNAs (snoRNAs) are required in pre-rRNA cleavage and rRNA modification. In general, they are classified into C/D and H/ACA snoRNAs based on the conserved C (5'-PuUGAUGA-3') and D (5'-CUGA-3') or H and ACA motifs [Reviewed in (Kressler et al., 1999; Venema and Tollervey, 1999)]. SnoRNAs do not have any catalytic function, but direct the methylase or pseudouridine synthase to the RNA substrates by base pairing. Most of the modifications are not essential, suggesting that rRNA modifications serve to fine tune ribosome structure and function.

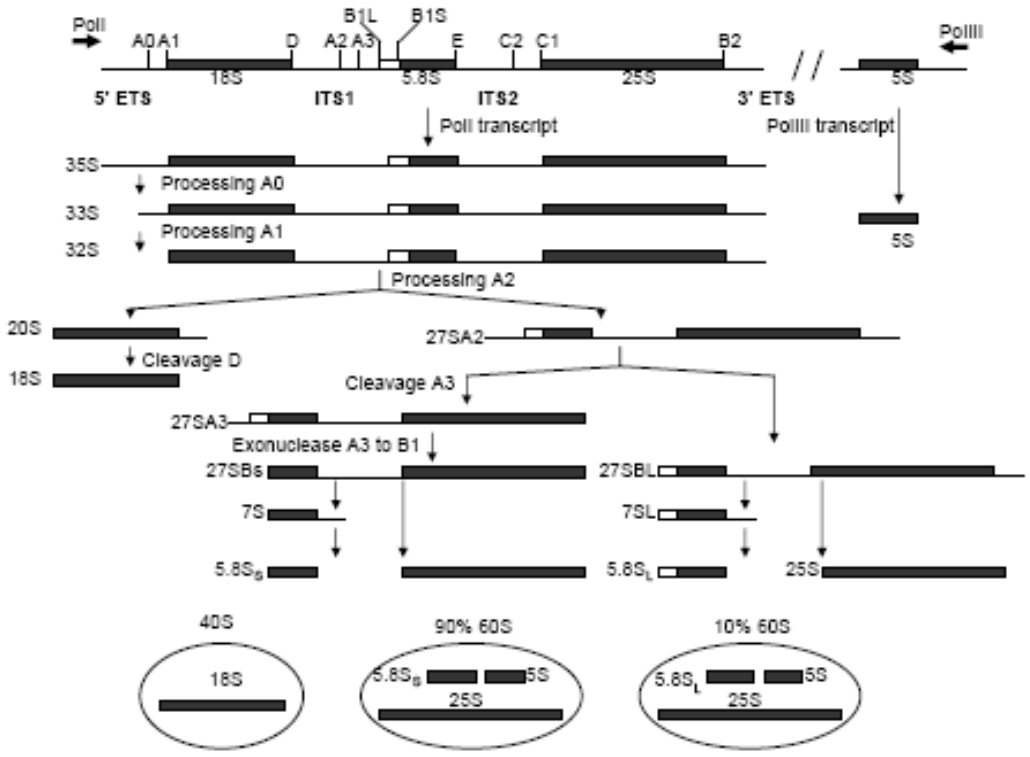

Illustration 1.1 Overview of rRNA maturation pathways in yeast

35S rRNA is transcribed by RNA polymerase I. After it is cleaved into 20S and 27S pre-rRNAs, 20S RNA is exported to the cytoplasm where the 3' end is processed to become mature 18S rRNA. For 27S rRNA, 90% is processed to $5.8S_S$ and 25S, and 10% is processed to $5.8S_L$ and 25S.

1.3 Nuclear Pore Complexes and Nucleocytoplasmic Transport

Transport between the nucleus and cytoplasm occurs via the hydrophobic channel of nuclear pore complexes (NPCs). The NPC is a huge complex with octagonal symmetry composed of three major parts, nuclear basket, central framework, and cytoplasmic filaments. The proteins that make up the NPC are known as nucleoporins (Nups). In yeast, approximately 30 different Nups present in multiple copies comprise the NPCs (Rout et al., 2000). The molecular weight of yeast NPCs is estimated to be from 55 to 72MDa compared to 125MDa in vertebrates (Reichelt et al., 1990; Rout and Blobel, 1993; Yang et al., 1998)

Approximate one third of nucleoporins contain FG repeats, which are made up of 4-48 GLFG, FXFG, SXFG, or PXFG motifs. The interaction between FG repeats and transport receptors is required for mediating transport processes. This interaction involves the phenylalanine ring of the FG-repeat and hydrophobic residues on the surface of the receptor (Bayliss et al., 2000; Bayliss et al., 2002b). However, different transport receptors use different ways to recognize the FG repeats. This may influence the strength and the specificity of the interaction between the cargo complex and the distinct FG-repeat Nups (Bayliss et al., 2002a).

NPCs allow passive diffusion of small molecules less than 9nm in diameter (Paine et al., 1975). Passive diffusion is very slow for bovine serum albumin, which is near the diffusion limit (~7nm diameter, 68 kDa). However proteins less than 20-30 kDa can be exported at a reasonable rate.

Active transport is a selective process for cargos with specific transport signals. The selective permeabilization requires karyopherins, a group of conserved soluble proteins, to recognize the cargo and facilitate the transport of cargo through the channels of NPCs. This carrier-mediated fashion allows transport to occur in a controlled manner (Gorlich and Kutay, 1999). Karyopherins can be divided into importins and exportins, based upon their function in nuclear import or export, respectively. Exportins bind cargos with nuclear export sequences (NESs) and RanGTP cooperatively in the nucleus for transport to the cytoplasm, whereas importins recognize cargos containing nuclear localization signals (NLSs) in the cytoplasm and import the substrates into the nucleus.

The leucine-rich NESs of Crm1, an export receptor (see below for details), are well characterized. The tRNA export receptor Los1 recognizes part of the tRNA structure as an NES (Grosshans et al., 2000). Most NLSs are enriched in basic amino acids and many can be grouped into two classes: bipartite and SV40 large T antigen-like. However, the characterization of most NLSs is still unclear. In yeast, there are 13 β-karyopherins, nine of which are importins and four, Crm1, Los1, Msn5, and Cse1, are exportins (Pemberton and Paschal, 2005).

Crm1 (chromosome region maintenance 1, known as Xpo1 in yeast) mediates export of hundreds of proteins by recognizing leucine-rich NESes. Most NESs are constituted with three to four hydrophobic residues or leucine. The consensus for a leucine-rich NES is: Φ(X2-3)Φ(X2-3)Φ(X)Φ (Φ: L, I, V, F, or M; X: any amino acids) (Fornerod and Ohno, 2002; Kutay and Guttinger, 2005; la Cour et al., 2004). Crm1 is composed of nineteen HEAT (huntingtin, elongation factor3, protein phosphatase 2A and TOR1) repeats, which are important domains that interact with RanGTP, cargos, and also the FG repeats of the Nups. The fungal metabolite leptomycin B (LMB), which alkylates Cys528 of human Crm1, inhibits its export function (Kudo et al., 1999). Cys528 is located in the NES binding groove of Crm1 (Dong et al., 2009b). Covalent addition of LMB to the sulfhydryl group of Cys528 blocks NES access to Crm1. Although this Cys is not conserved in *S. cerevisiae*, mutation of T539 at the corresponding position to Cys makes yeast Crm1 and the yeast cell sensitive to LMB (Neville and Rosbash, 1999).

The structure of Crm1 in complex with SNUPN (also known as snuportin 1) and RanGTP has recently been published (Dong et al., 2009a; Dong et al., 2009b; Monecke et al., 2009). Crm1 is a ring-shaped protein showing a remarkable superhelical twist, as HEAT repeats 2-7 twist away from the plane of the ring with an ~45° rotation. Ran is enclosed in this toroid structure and stabilizes the ring by extensive contacts. SNUPN, and presumably other cargoes as well, rests on the outside of Crm1 allowing its interaction with large cargoes, like the ribosome. Also, the outer surface may provide a larger surface area and variety of binding sites for cargo recognition than the inner face. Crm1 can recognize the nucleotide state of Ran; the structure of RanGDP is incompatible with Crm1 binding. Although the binary binding between Crm1 and NES or RanGTP is

relatively weak, binding of one increases the affinity to the other. GTP hydrolysis of Ran in the cytoplasm results in the dissociation of RanGDP from Crm1, disrupting the cooperative binding to cargo and release into the cytoplasm (Dong et al., 2009a).

Although the export of 40S and 60S subunits are thought to be independent of each other, both pathways seem to rely on Crm1 (Moy and Silver, 1999). Both 40S and 60S subunits are trapped in the nucleus after brief treatment of LMB. While the export pathways of 60S subunits are better defined (see details in the next section), the export pathway of 40S is still vague.

The directionality of transport by the importin-beta family of karyopherins is governed by the RanGTP gradient across the nuclear envelope. The RanGTP gradient is created by the chromatin-associated nucleotide exchange factor, RanGEF/RCC1 (Prp20p) and the cytoplasmic GTPase-activating protein RanGAP [reviewed in (Gorlich and Kutay, 1999)]. Export karyopherins bind cargo with RanGTP in the nucleus to form a stable ternary export complex. Once RanGTP is hydrolyzed by RanGAP and Ran-binding proteins, RanBP1(Yrb1p) or RanBP2 (specific to higher eukaryotes) in the cytoplasm, a conformational change of the exportin occurs, leading to cargo release. The export karyopherins can then recycle back to the nucleus for the next round of export. RanGTP is required for ribosome export (Hurt et al., 1999; Moy and Silver, 1999). If the RanGTP gradient is perturbed by mutation of GSP1 (Ran), *RNA1* (RanGAP), *PRP20* (RanGEF), or *YRB1* (RanBP1), export of both subunits is blocked (Hurt et al., 1999; Moy and Silver, 1999; Stage-Zimmermann et al., 2000).

On the other hand, the import complex is formed between cargo and importin in the cytoplasm without a requirement for Ran. The complex translocates through the NPC channel to the nucleus. Importin α mediates the import of proteins with a classical NLS and binds cargo and importin β in the cytoplasm. Although importin β accounts for interaction with the NPCs, (Gorlich et al., 1995; Gorlich and Laskey, 1995), it can also recognize NLSs directly. The direct binding of nuclear RanGTP to importin β displaces the cargo and importin α (Gorlich et al., 1996). The importin β-RanGTP complex can exit the nucleus for the next round of import (Hieda et al., 1999; Izaurralde et al., 1997).

1.4 Nuclear export of the 60S ribosome

After assembly of the nascent 60S ribosome in the nucleus, 60S subunits are exported to the cytoplasm where they undergo further maturation steps to achieve translationally active status. A yeast cell produces around 4000 ribosome subunits per minute during log phase. Because there are only about 200 NPCs on the nuclear membrane in the yeast cell (Rout and Blobel, 1993), one NPC transports about 20 ribosome subunits per minute.

Several Nups are involved in 60S export, including Nup159, Nup116, Nup1, Nup120, Nup82, Nup49, Nic96, Nsp1, Nup85, Nup133, Nup40, and Gle1 (Gleizes et al., 2001; Stage-Zimmermann et al., 2000). These Nups may act as important interaction sites with export receptors of large subunits or alter the permeability of NPC. For example, Nup120 and Nup133 lack FG repeats and deletion causes NPC clumping.

Translocation of hydrophilic cargo through the hydrophobic NPC channel requires karyopherins to facilitate the interaction of cargo with nucleoporins. The 60S ribosome is highly negatively charged and, potentially, the bulkiest cargo that passes through the NPC in the eukaryotic cell. For efficient transport, 60S subunits, like large cargos, require more than one receptor (Ribbeck and Gorlich, 2001). Three receptors (Crm1, Mex67/Mtr2, and Arx1) have been identified in 60S export pathway. The details will be discussed separately below.

NMD3/CRM1

Crm1 was the first export receptor identified in the 60S export pathway (Gadal et al., 2001; Ho et al., 2000b; Thomas and Kutay, 2003a; Trotta et al., 2003a). Crm1 recognizes the leucine-rich NES of Nmd3, an export adapter of 60S subunits. Nmd3 is a 59 KDa essential protein, which is highly conserved from yeast to humans. The N-terminal domain contains four Cys-X2-Cys zinc-binding motifs that are important for protein-protein or protein-RNA interaction. The C-terminal domain contains an NLS, a coiled coil domain, and NES (Illustration 1.2) (Hedges et al., 2006). When the function of the Nmd3 NES is perturbed, yeast cells show a severe growth defect; 60S subunits are trapped in the nucleus and cells show a 60S deficiency (Ho et al., 2000b). The complete truncation of NES from Nmd3 is lethal (Hedges et al., 2006). During ribosome export,

Nmd3 binds the 60S ribosome in the nucleus and then recruits Crm1 via its NES. Crm1 assists 60S subunits to travel through the channel of NPCs to the cytoplasm (Ho et al., 2000b).

The functional analyses of Nmd3 were also performed in Xenopus oocytes (Trotta et al., 2003a) and HeLa cells (Thomas and Kutay, 2003a). All results demonstrated that the function of Nmd3 as 60S export adapter was conserved from yeast to higher eukaryotes.

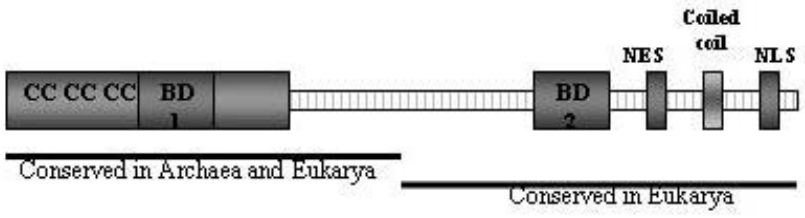

Illustration 1.2 Diagram of Nmd3

The Zinc-binding domains are important for Nmd3 to interact with the 60S subunits. BD1 and BD2 are the proposed 60S-binding sites. The N-terminal 27 KDa is conserved from Archaea to eukarya, whereas the C-terminal domain containing the shuttling sequences is only present in the eukaryotic Nmd3 proteins.

MEX67-MTR2

The Mex67/Mtr2 heterodimer in yeast, and their homologues TAP/P15 in mammals were initially identified as export receptors of most mRNAs (Katahira et al., 1999). The proper formation of Mtr2 and Mex67 dimer is required for optimal interaction between the NTF2-like domain and FG repeats of nucleoporins (Santos-Rosa et al., 1998). The recruitment of Mex67/Mtr2 heterodimers on mRNA depends on the presence of adapter proteins deposited on the mRNA after splicing or 3' end formation (Strasser et al., 2000; Stutz et al., 2000). Unlike the transport pathways using importin-beta karyopherins, mRNA export does not depend on Ran. On the other hand, directionality of mRNA export appears to depend on the RNA helicase Dbp5 (Tran et al., 2007).

The mutant *mtr2-33,* [*mtr2(E106G, R109G)*], has been shown to be defective in ribosomal export at restrictive temperature, but not in the mRNA export pathway (Bassler et al., 2001). Moreover, this allele shows synthetic lethality with *nmd3-1* and strong genetic interaction with 60S ribosome biogenesis factors, Ecm1 and Nug1 (Bassler et al., 2001). Mtr2 can also be detected in Arx1-bound pre-60S complexes. These data suggest that Mtr2 has a role in the ribosomal export process (Bassler et al., 2001). In contrast to the highly conserved sequence between Mex67 and TAP, Mtr2 and p15 share functional and structural homology, but no sequence similarity (Fribourg and Conti, 2003). Compared to other members of the NTF2 family, Mtr2 possesses an NTF2 fold, a cone-like structure constituted with five ß-sheets flanked by one long or two short α-helices, and a unique core domain constituted by three long internal loops. This elongated structure protrudes 20Å from the open end of the cone and serves as another potential substrate binding site. The mutation sites of *mtr2-33*, E106G and R109G, are located in this loop. This specialized domain of Mtr2 is absent in p15 (Senay et al., 2003).

Mex67 and Mtr2 contain several insertions not present in their metazoan orthologs, TAP and P15, which are not involved in 60S export (Yao et al., 2007). These loops are believed to have evolved to interact with the 60S ribosome. Deletion or point mutations introduced within these loops results in severe 60S export defects and lethality.

How is the recognition of mRNA vs 60S subunits by the Mex67/Mtr2 heterodimer regulated? Yao et al (Yao et al., 2008) proposed that the 60S subunit and the Nup84

complex compete for an overlapping binding site on the extended loop Mex67-Mtr2 surface. Functional interaction between Nup85, a subunit in the Nup84 complex, and the Mex67 loop is required for mRNA export, but not for 60S export. Nup85ΔN133, which can disrupt Mex67-Mtr2 association with the Nup84 complex, can rescue the 60S export defects in either *mtr2*(RR>DD) and nmd3ΔNES1 mutants. This suggests that the versatile binding platform on Mex67-Mtr2 could create crosstalk between mRNA and 60S export pathways.

The novel function of Mex67 and Mtr2 in the 60S subunit export pathway in yeast was identified recently in the Hurt lab (Yao et al., 2007) and our lab (see Chapter 3). Overexpression of Mex67 in *nmd3* NES deletion mutant cells can rescue the lethality, but cannot complement the function of an *nmd3* deletion or NLS deletion mutant. This suggests that Mex67 can specifically complement the Nmd3 function in 60S export, but not the function in the 60S biogenesis pathway.

ARX1

Arx1 was identified as a third 60S export receptor (Bradatsch et al., 2007; Hung et al., 2008). *arx1* shows synthetic lethality with *nmd3*(NES) and various *nup* mutants. Deletion of *arx1* traps Nmd3 and 60S subunits in the nucleus. In addition, Arx1 physically interacts with the 60S export complex and also with Nup100, Nup116, and Nup57. Taken together, Arx1 appears to be a noncanonical receptor of the 60S export pathway. However, its human homolog Ebp1 lacks an association with the 60S export pathway or with nucleoporins.

The crystal structure of Ebp1, the human homolog of Arx1, revealed a MetAP (methionine aminopeptidase) fold, which removes methionines from newly synthesized peptides (Kowalinski et al., 2007; Monie et al., 2007). Arx1 was modeled into the Ebp1 structure (Bradatsch et al., 2007). Comparing the model Arx1 structure and MetAPs crystal structure, the residues at the substrate-binding pocket that are essential for catalytic activity in MetAPs are not conserved in Arx1. Consistent with the model, Arx1 does not show aminopeptidase activity. Moreover, Arx1 contains extra loop extensions that are not present in the MetAP (Bradatsch et al., 2007). Interestingly, when the residues in the binding pocket are mutated, *arx1* shows synthetic sickness with *nmd3*

NES mutants and traps 60S subunits in the nucleus. This suggests that the binding pocket of Arx1 interacts with Nups, potentially the FG repeats, not with the methionine of the nascent polypeptides. In conclusion, Arx1 utilizes MetAP fold to interact with 60S subunits, but shows different preference for substrates.

1.5 Maturation of nascent 60S subunit in the cytoplasm

After their export from the nucleus, the 60S subunits undergo further maturation steps in the cytoplasm before they engage in translation. These steps include the release of the three export receptors, and several transacting factors that accompany the 60S subunit during export to the cytoplasm. Also, several ribosomal proteins, including Rpl24 and P0 are loaded in the cytoplasm. So far, four release factors, two GTPases and two ATPases, have been identified in the cytoplasm (Illustration 1.3). A brief introduction for each of these factors is provided here.

Drg1

Drg1 (diazaborine resistance gene 1) is an AAA-protein (ATPase associated with a variety of cellular activities). Inactivation of Drg1 blocks recycling of Rlp24 and several pre-ribosomal proteins, Nog1, Tif6 and Arx1, in the cytoplasm (Pertschy et al., 2007). Drg1 contains two AAA-domains and exhibits ATPase activity in *vitro* (Zakalskiy et al., 2002). Mutations introduced in either of the AAA-domains of Drg1 affect its ATPase activity. Members of this family of ATPase form hexameric ring-like structures upon binding ATP. A conformational change upon ATP hydrolysis enables disassembly of the complex or behaves as an ATP-dependent motor. ATPases are regarded as important in restructuring the 60S subunit at the maturation stage. So far, Drg1 has been shown to be the first release step of 60S trans-acting factors in the cytoplasm (Pertschy et al., 2007).

Rlp24 (Rpl24-like protein) is the nuclear paralog of ribosomal protein, Rpl24. Rlp24 is an essential protein loaded on the pre-60S particle in the nucleolus and then released by Drg1 in the cytoplasm (Pertschy et al., 2007). After Rlp24 is released, Rpl24 binds at the same binding site. Depletion of Rlp24 impairs 27SB processing and decreases 60S subunit levels. Loading of Rlp24 on the 60S subunit is critical for the sequential binding of other trans-acting factors, including Nog1 and Nog2 (Saveanu et al., 2003).

Lsg1

Lsg1 is a GTPase acting in Nmd3 release in the cytoplasm (Hedges et al., 2005). Although GTPase activity has not been shown *in vitro*, mutations in the GTPase domain cause inviability of cells and disrupts the Nmd3 recycling pathway (West et al., 2005).

GTP-hydrolyzing proteins have been shown to play an important role throughout ribosome biogenesis and translation. The GTP hydrolysis cycle behaves as a "molecular switch" in the regulation of cellular processes. When the weak GTPase is activated by regulator or structural cue, the conformational change alters the protein complex function or composition. In ribosome biogenesis, GTPases act at distinct steps and may change protein-protein or protein-rRNA interactions, or alter the protein composition of nascent 60S subunits by releasing some trans-acting factors.

Lsg1 belongs to a "circular permuted GTPase (cpGTPase)" family of proteins (Anand et al., 2006; Hofer et al., 2007). The G domains in regular GTPases are usually arranged G1-G5, however, domains are arranged G4-G5-G1-G2-G3 in the cpGTPase family. cpGTPases always have an "anchoring" C-terminal domain, and some have an additional N-terminal domain. These domains are suggestive of RNA binding. It is possible that RNA-binding modulates GTP binding or *vice versa* (Anand et al., 2006).

Lsg1 is a cytoplasmic protein. Overexpression of a dominant-negative Lsg1 mutant or inactivation of Lsg1 function prevents Nmd3 release from subunits in the cytoplasm and its shuttling into the nucleus (Hedges et al., 2005). This in turn causes the accumulation of pre-60S subunits in the nucleus. Mutations in *nmd3* that decrease its affinity for 60S subunits or overexpression of wild-type *NMD3* alleviates the export defect in *lsg1* mutants. These results suggest that bypassing the block in release of Nmd3 from 60S subunits in the cytoplasm restores 60S export (Hedges et al., 2005; West et al., 2005).

The release of Nmd3 also depends on the loading of ribosomal protein Rpl10 with its chaperone Sqt1 on the 60S subunit in the cytoplasm. It has been proposed that Lsg1 facilitates Rpl10 loading (Hedges et al., 2005; West et al., 2005).

Rei1/Jjj1/Ssa1

Rei1 and Jjj1 are responsible for the recycling process of Arx1. Deletion of either of them relocalizes Arx1 from the nucleus to the cytoplasm and leads to a severe defect in 60S levels detected by sucrose gradient analysis (Demoinet et al., 2007; Hung and Johnson, 2006; Lebreton et al., 2006; Meyer et al., 2007). Rei1 is a C2H2-zinc finger protein, which was reported to be involved in the mitotic signaling pathway (Iwase and Toh-e, 2004). Both Rei1 and Jjj1 localize in the cytoplasm and co-migrate with 60S subunits. Deletion of *JJJ1* shows very similar phenotype to that of deletion of *REI1*: a growth defect and 60S subunits deficiency at lower temperature. Interestingly, the cold-sensitive phenotype can be rescued by deletion of *ARX1* or introduction of mutant *arx1* with decreased 60S binding ability (Demoinet et al., 2007; Hung and Johnson, 2006; Lebreton et al., 2006; Meyer et al., 2007). It implies that Arx1 cannot be released properly from 60S in the absence of Rei1 or Jjj1, and the defect can be easily counteracted by removing Arx1 from 60S subunits.

Jjj1 is a J domain-containing chaperone belonging to the Hsp40 protein family, which are binding partners of Hsp70s (Demoinet et al., 2007; Meyer et al., 2007). There are two classes of Hsp70, Ssas (SSA1-4) and Ssbs (SSB1-2). Purified Jjj1 proteins stimulate the ATPase activity of Ssa1 but not Ssb1 in vitro. The function of Jjj1 depends on its co-chaperone activity. When mutations were introduced in the conserved histidine–proline–aspartic acid (HPD) motif of the J domain, Jjj1 can neither complement the growth in vivo nor stimulate the ATPase activity of Ssa1 in vitro (Meyer et al., 2007).

Efl1 and Sdo1

Eukaryotic translation initiation factor (eIF6) prevents the 60S subunit from joining with the 40S subunit. The yeast homolog, Tif6 (Translation initiation factor 6), also prevents the association between 40S and 60S (Si and Maitra, 1999). However, yeast Tif6 is a ribosome biogenesis factor that binds pre-60S subunits in the nucleolus. Depletion of Tif6 leads to decreased 60S levels and accumulation of halfmer polyribosomes. Furthermore, Tif6-depleted cells show defects for 5.8S and 25S synthesis, but the cell extract is still functional for in translation *in vitro*.

Efl1 (elongation factor-like 1), a cytoplasmic GTPase (Becam et al., 2001; Senger et al., 2001), and Sdo1 play a crucial role in Tif6 recycling (Menne et al., 2007). The

sequence of Efl1 shows high homology to the elongation factors EF-G (prokaryotes) and EF-2 (eukaryotes) (Becam et al., 2001). Deletion of Efl1 confers slow growth, pre-rRNA processing defects, under-accumulation of 60S subunits, 60S subunit export defects, and mislocalization of Tif6. Interestingly, these defects can be rescued by *tif6* suppressor mutants, which show weaker 60S-binding affinity (Senger et al., 2001). Taken together, these results suggest a role for Efl1 in Tif6 recycling. Strikingly, Efl1 does not co-sediment with ribosomes in sucrose gradient analysis but the presence of 60S subunits stimulates the GTPase activity of Efl1 *in vitro* (Senger et al., 2001).

Sdo1 (Shwachman-Diamond syndrome ortholog) is an ortholog to human Shwachman-Bodian syndrome protein (Menne et al., 2007). Mutation of *sdo1* shows a similar phenotype as deletion of *EFL1*: slow-growth, reduced 60S levels, 60S ribosome export block in the nucleus, imbalance of 40S to 60S ratio, and relocalization of Tif6 from the nucleus to cytoplasm. Furthermore, Tif6 gain-of-function mutants can bypass these defects. Unlike Efl1, Sdo1 binds 60S subunits. It has been suggested that Sdo1 loads on the 60S subunit first and helps to recruit Efl1 to the subunit to trigger the releasing of Tif6.

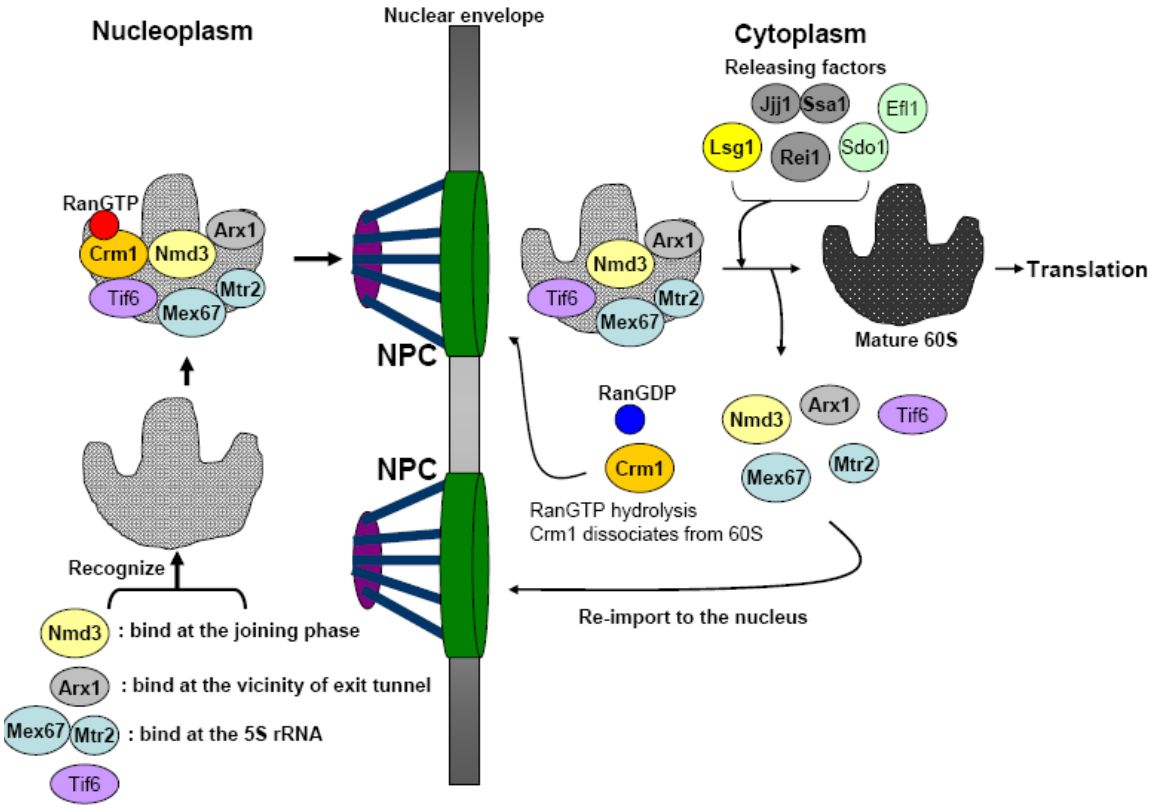

Illustration 1.3 Maturation steps of large subunits in the cytoplasm

1.6 Translation

Following the final maturation steps in the cytoplasm, the two ribosomal subunits become translationally active. Translation itself can be divided into 4 steps: initiation, elongation, termination, and recycling.

Translation initiation is a multi-step process. At least 12 eukaryotic initiation factors (eIFs) help assemble preinitiation complexes [reviewed in (Pestova et al., 2001)]. eIF2 αβγ trimer and tRNAiMet form ternary complex (TC) to assemble a 43S complex from interactions with the 40S subunit and eIF1, eIF1A, eIF3, and eIF5 factors. The 43S pre-initiation complex is recruited to mRNA assisted by the interaction between eIF3, the eIF4G complex, and the 5' m^7G cap and the interaction between the polyA-binding protein (PABP) and the polyA tail. This initiation complex scans along the 5' untranslated region (UTR) of mRNA to the AUG start condon. The recognition between AUG and initiator tRNA triggers the release of eIFs to allow joining of the 60S and 40S subunits.

The open reading frame of an mRNA consists of triplet codons which each encodes a specific amino acid. During elongation, aminoacylated-tRNAs are delivered to the acceptor/aminoacyl (A) site by GTPase EF1A (EF-Tu in bacteria). Upon base-pair recognition of the correct (cognate) tRNA, the EF-1A GTPase is activated and released from the ribosome. Polypeptide-bond formation, between the incoming amino acid and the peptide in the peptidyl-tRNA binding site (P site), is accomplished by the peptidyl-transferase activity of the 60S subunits. The PTC (peptidyl transferase center) is located in the middle of the face of 60S subunit that interacts with the 40S subunit. eEF2 (EF-G in bacteria) then binds to the ribosome to promote translocation peptidyl-tRNA from the A site to the P site as well as movement of the mRNA relative to the ribosome. Consequently, the deacylated tRNA is ejected from the E site. This cycle repeats until the stop codon is reached.

Translation termination is the step that liberates the nascent polypeptide chain. There are three stop codons: UAA, UAG, and UGA. In eukaryotic cells, release factors eRF1 (RF1/RF2 bacteria) recognizes stop codons in the A-site. However, a second release factor, eRF3 (RF3 in bacteria), is needed. eRF3 is a GTPase encoded by *SUP35* in

the *S. cerevisiae*. The stable interaction between eRF1 and the stop codon in the A-site triggers the GTPase activity of eRF3, which leads to the release of the newly synthesized polypeptide from the ribosome (Alkalaeva et al., 2006; Salas-Marco and Bedwell, 2004).

The recruitment of these translation factors to the ribosome requires the stalk of the large subunit. The stalk is a lateral protuberance constituted of a pentameric protein complex containing P0 and two dimers of P1 and P2. In Chapter 4, I identified the maturation pathway of this important functional domain of the ribosome.

In addition, my preliminary results show that the release of Nmd3 is tightly connected to active translation. Blocking translation by inactivation at initiation, elongation, or termination steps also blocks the release of Nmd3 from the 60S subunit in the cytoplasm (see Chapter 5 and Appendices A, B and C). The availability of Nmd3 in the nucleus may directly regulate the rate of export of 60S subunits. Although how translation regulates the last step of ribosome maturation is not understood, this observation suggests a coordination of regulation between the use and the production of ribosome subunits.

1.7 Dissertation objectives

There are five chapters in my dissertation. In Chapter one, I have provided a general introduction about the structure and composition of the ribosomes. I have also described the overview of our current understanding about the ribosome biogenesis with a particular emphasis on factors and events that are related to those biogenesis events that I have studied in my dissertation work. Chapter 2 contains a description of the materials and methods that I used in Chapters 3 through 5.

In Chapter 3, I pursued the question about the flexibility of 60S export pathway. Whereas the function of Nmd3 as an export factor for the 60S subunit is conserved from yeast to humans (Thomas and Kutay, 2003b; Trotta et al., 2003b), Tap/p15, the human orthologs of Mex67/Mtr2, and Ebp1, the human ortholog of Arx1, do not appear to be involved in ribosome export in human cells (Bradatsch et al., 2007; Yao et al., 2007). Ribosome export is a fundamental process in all eukaryotes, and many of the ribosomal proteins and ribosome biogenesis factors are highly conserved. Thus, it is surprising that different eukaryotic lineages have evolved the use of different receptors in the export process of the large subunit. Here, I asked if there are particular requirements for the receptors that are used for 60S export. For example, whether Crm1 must be used or whether other receptors can substitute for Crm1. I found that Crm1 could be replaced by direct recruitment of any of the other known export receptors in yeast. Thus, there does not appear to be a specific requirement for Crm1 in 60S export. In previous work, we asked why the leucine-rich NES for 60S export is contained in a transacting factor rather than in cis on a ribosomal protein (Johnson et al., 2002b). The presence of the NES on a ribosomal protein would seem more economical. I fused the NES of Nmd3 to different ribosomal proteins and found that, in some cases, the NES in cis on a ribosomal protein could drive ribosome export. Thus, there is not an absolute requirement for the NES *in trans* to the ribosome. However, by putting the NES in *trans*, cells could regulate export by regulating Nmd3 shuttling. Like the results shown in Appendices A, B and C, inhibiting translation prevents Nmd3 recycling. This regulation would not function if the NES were on a ribosomal protein.

In Chapter 4, I discovered a new cytoplasmic maturation step of the 60S subunit. The stalk of the ribosome is an essential structure for recruitment of translation factors. In bacteria, L10 and L11 bind cooperatively to helix 43/44 of 23S rRNA to form the stalk base with a tetramer of L7/L12 assembling onto L10. In yeast, P0 and Rpl12 correspond to bacterial L10 and L11, respectively, whereas P1 and P2 replace L7/L12. Mrt4 is a paralog of P0 in eukaryotic cells that localizes to the nucleolus and nucleus; P0 is cytoplasmic. In my study, I identified the function of dual specificity phosphatase Yvh1 in Mrt4 release. Mrt4 must be released to allow P0 binding and the assembly of the ribosomal stalk. I have shown that this pathway is conserved in human cells.

In Chapter 5, I show that the known cytoplasmic maturation steps can be connected into a pathway. Although that there are four major ribosome biogenesis steps driven by two ATPases and GTPases in the cytoplasm, a more complete understanding of the ordering of the action of all four release factors has been lacking. Here, I performed a comprehensive analysis of the potential interdependence of these release events. Failure to release Rlp24 prevents the loading of Rei1 and, consequently, the release of Arx1. The release of Arx1 by Rei1 is upstream of and required for efficient release of Tif6. Finally, I show that *sdo1* and *efl1* mutants block the release of Nmd3 in addition to Tif6. Thus, the release of Tif6 is upstream of the release of Nmd3. My results place all these cytoplasmic maturation steps into a single linear pathway.

Chapter 2
Materials and Methods

The experimental materials and methods used in this thesis are described in detail within this chapter. The strains and plasmids used here for the first time are described in full.

2.1 Materials and Methods for Chapter 3

2.1.1 Strains, plasmids, and media used in Chapter 3

Strains, plasmids, and media

All *S. cerevisiae* strains used in this study are listed in Table 2.1. All strains were grown at 30°C, unless otherwise indicated, in rich medium (yeast extract-peptone) or synthetic dropout medium containing 2% glucose.

Plasmids used in this work are listed in Table 2.2. pAJ1872 (*MEX67*) was made by moving a ClaI-SacI fragment from pAJ528 into pRS423. To create pAJ1882 (*MEX67-nmd3Δ100-GFP*) and pAJ2079 (*mex67-5-nmd3Δ100-GFP*), *MEX67* was amplified with primers AJO994 (CCTGAATTCAGCGGATTTCACAATGTTGG) and AJO995 (GGAGAATTCGTTAATTAAGTTGTTGAACTGCACAAATGCTTC) from either wild type or *mex67-5* genome DNA. The products were digested with EcoRI and ligated into the EcoRI site at nucleotide 4 of the *NMD3* coding sequence in pAJ757 (*nmdΔ100-GFP*). pAJ1892 was made by moving the SstI to XmaI fragment from pAJ1882 to pAJ535. To make pAJ2066 (*nmd3Δ100-MTR2-GFP*), PCR was performed with primers AJO1006 (CCTTTAATTAAAATTTTTAGCAGAGAATCCTCG) and AJO1073 (CCTCCCGGGATGAACACCAATAGTAATACTATG). The fragment was digested with XmaI and PacI and ligated into the same sites of pAJ757. pAJ2076, pAJ2077 and pAJ2078 were made similarly, but with different primer pairs, AJO1106 (CTGCCCGGGAACAACTTAATTAACATGTCCGAT TTGGAAACCGT) and AJO1107 (CAGCCCGGGATTACCAACTAATAATTGAT) for pAJ2076, AJO1108 (CTGCCCGGGAACAACTTAATTAACATGCTAGAA CGGATTCAGCA) and AJO1109 (CAGCCCGGGTTGACCTTGCTTTAAAACAG) for pAJ2077and AJO1110 (CTGCCCGGGAACAACTTAATTAACATGGATTC CACAGGCGCT TC) and

AJO1111 (CAGCCCGGGGTTGTCATCAAAGAGA TTAC) for pAJ2078. The PCR fragments were digested with XmaI and ligated into XmaI-cut pAJ757. pAJ2084, pAJ2085, pAJ2086 pAJ2087, and pAJ2088 were made using the same strategy. The receptor containing fragments were moved as an EcoRI fragment (pAJ1882), XmaI to PacI fragment (pAJ2066), or XmaI fragments (pAJ2076, pAJ2077 and pAJ2078) into the same site(s) of pAJ2083 (*nmd3[L263P F318I]Δ100*). pAJ2089 (*RPL3-NES*), pAJ2090 (*RPL11B-NES*), pAJ2091 (*RPL12B-NES*), and pAJ2094 (*RPL25-NES*) were prepared by PCR amplification of the NES of NMD3 using primers AJO329 (CTGCATCCAGTATACACACCCA) and AJO1118 (GTCTTAATTAACGATGAAGACGCTCCACAA), and ligation of the PacI-HindIII NES-containing fragment into pAJ1090, pAJ1092, pAJ1093 and pAJ1127.

Table 2.1 *S. cerevisiae* strains used in Chapter 3

Strain	Genotype	Source
PSY1687	*MATα ade2 his3 leu2 trp1 ura3 mex67::HIS3 (pUN100: LEU2 mex67-5)*	(Segref et al., 1997)
AJY734	*MAT*α *ade2 ade3 leu2 lys3 ura3 his3 nmd3-4^{ts}*	(Ho and Johnson, 1999a)
AJY1539	*MATa his3*Δ*1 leu2*Δ*0 ura3*Δ*0 met15*Δ*0 crm1(T539C)-HA*	(Hedges et al., 2005)
AJY1950 (SL348)	*MAT*a *leu2 ura3 ade2 ade3 arx1*Δ *nmd3*Δ*C14* (pAJ1029: *ADE3 URA3 ARX1*)	(Hung et al., 2008)
AJY2110	*MAT*a *ura3*Δ*0 his3*Δ*1leu2*Δ*0 lys2*Δ*0 nmd3*::*KanMX* (pAJ112: *URA3 NMD3*)	(Hedges et al., 2006)
AJY2974	*MATa leu2 lys3 ura3 his3 nmd3-4^{ts} crm1(T539C)-HA*	This study
AJY3053	*MAT*a *ura3*Δ*0 his3*Δ*1leu2*Δ*0 lys2*Δ*0 rpl3*Δ:KanMX (*pRPL3-NES* URA3)	This study

Table 2.2 Plasmids used in Chapter 3

Plasmids	Relevant markers	Source
pAJ123	*NMD3* LEU2 CEN	(Ho and Johnson, 1999a)
pAJ1032	*ARX1* LEU2 CEN	Hung, unpublished
pAJ528	*MEX67* URA3 2μ	(Ho et al., 2000c)
pAJ534	*nmdΔ50-myc* LEU2 CEN	(Ho et al., 2000c)
pAJ535	*nmdΔ100-myc* LEU2 CEN	(Ho et al., 2000c)
pAJ538	*NMD3-myc* LEU2 CEN	(Ho et al., 2000c)
pAJ755	*NMD3-GFP* URA3 CEN	Hedges, unpublished
pAJ757	*nmd3Δ100-GFP* URA3 CEN	Hedges, unpublished
pAJ908	*RPL25-GFP* URA3 CEN	(Kallstrom et al., 2003b)
pAJ1025	*ARX1-GFP* LEU2 CEN	(Meyer et al., 2007)
pAJ1121	*GAL:LSG1* LEU2 CEN	West and Johnson, unpublished
pAJ1129	*GAL:LSG1(K349T)* LEU2 CEN	West and Johnson, unpublished
pAJ1359	*nmd3ΔNLS-myc* LEU2 CEN	(Hedges et al., 2006)
pAJ1872	*MEX67* HIS3 2μ	This study
pAJ1882	*MEX67-nmd3Δ100-GFP* URA3 CEN	This study
pAJ1892	*MEX67-nmd3Δ100-myc* LEU2 CEN	This study
pAJ2066	*nmd3Δ100-MTR2 -GFP* URA3 CEN	This study
pAJ2076	*nmd3Δ100-CSE1 -GFP* URA3 CEN	This study
pAJ2077	*nmd3Δ100-LOS1 -GFP* URA3 CEN	This study
pAJ2078	*nmd3Δ100-MSN5 -GFP* URA3 CEN	This study
pAJ2079	*(mex67-5)-nmd3Δ100-GFP* URA3 CEN	This study
pAJ2084	*MEX67-nmd3[L263P F318I]Δ100-GFP* URA3 CEN	This study
pAJ2085	*nmd3[L263P F318I]Δ100-MTR2-GFP* URA3 CEN	This study
pAJ2086	*nmd3[L263P F318I]Δ100-CSE1-GFP* URA3 CEN	This study
pAJ2087	*nmd3[L263P F318I]Δ100-LOS1-GFP* URA3 CEN	This study
pAJ2088	*nmd3[L263P F318I]Δ100-MSN5-GFP* URA3 CEN	This study
pAJ2089	*RPL3-NES* LEU2 CEN	This study
pAJ2090	*RPL11B-NES* LEU2 CEN	This study
pAJ2091	*RPL12B-NES* LEU2 CEN	This study
pAJ2093	*RPL8B-NES* LEU2 CEN	This study
pAJ2094	*RPL25-NES* LEU2 CEN	This study
pAJ2095	*RPL32-NES* LEU2 CEN	This study
pAJ2218	*MEX67-GFP* LEU2 CEN	This study
pAJ2221	*RPL3* LEU2 CEN	This study
pAJ2226	*nmd3Δ100-MSN5-myc* LEU2 CEN	This study

pAJ2227	*nmd3*Δ*100-LOS1-myc* LEU2 CEN	This study
pAJ2456	*RPL3-NES(*Δ*14)* LEU2 CEN	This study

2.1.2 Microscopy

Overnight cultures of cells were diluted to an OD_{600}~0.1 in fresh media and then incubated for 5-6 hours at appropriate temperatures. Hoechest dye was added at a final concentration of 4μM to stain the nucleus. For LMB experiments, cells were concentrated ten-fold, and LMB (LC Laboratories, Cambridge, MA) was added at a final concentration of 0.1μg/ml. Fluorescence was visualized on a Nikon E800 microscope fitted with an 100X objective and a Photometrics CoolSNAP ES digital camera controlled with the NIS-Elements AR 2.10 software.

2.1.3 Sucrose gradient analysis

For polysome profile assays, cultures were collected at OD_{600} ~0.2-0.3. Cycloheximide (200 μg/ml final concentration) was then added, and cells were immediately harvested by pouring onto ice and centrifugation. Extracts were prepared by glass bead extraction in polysome lysis buffer (10mM Tris-HCl pH 7.5, 100 mM KCl, 10 mM $MgCl_2$, 6 mM BME, 200 μg/ml cycloheximide). 9 OD_{260} units of protein extract were loaded onto linear 7% to 47% sucrose gradients in polysome lysis. After a 2.5 hour spin at 40,000 rpm in a Beckman SW40 rotor, gradient fractions were collected on an ISCO density gradient fractionator, continuously measuring absorbance at 254 nm.

To determine the ratio between 60S and 40S subunits, cell lysis buffer and sucrose solutions were made in low magnesium buffer (50 mM Tris pH 7.4, 50 mM NaCl, and 1 mM DTT). Subsequent conditions for sucrose gradient sedimentation and analysis were exactly as described above.

2.1.4 Immunoprecipitation

For immunoprecipitations, 200 ml cultures were grown to an OD_{600} of ~0.4-0.5 in drop-out medium. Cells were resuspended in IP buffer (20 mM Tris pH 7.5, 100 mM NaCl, 6 mM $MgCl_2$, 10% glycerol, 0.1% NP40, 1 mM PMSF and 1 μM leupeptin and 1 μM pepstatin A) and cell extracts were made by glass bead lysis. Anti-c-Myc antibody was added to the supernatants, and protein complexes were pulled down by BSA-blocked protein A agarose beads (Invitrogen). Samples were eluted in 25 μl of 1x Laemmli sample buffer and proteins were detected by Western blotting.

2.2 Materials and Methods for Chapter 4

2.2.1 Strains, plasmids, and media used in Chapter 4

Strains, plasmids, and media

All *S. cerevisiae* strains used in this study are listed in Table 2.3. All strains were grown at 30°C, unless otherwise indicated, in rich medium (yeast extract-peptone) or synthetic dropout medium, containing 2% glucose. AJY2551 (*mrt4*Δ) and AJY2976 (yvhΔ) are haploid strains derived from the heterozygous diploid deletion collection (Research Genetics). The KanMX cassette of AJY2977 (*yvh1*Δ::KanMX) was switched to NAT^r to give AJY2547. AJY2553 and AJY3048 were derived from crossing AJY2551 with AJY2547 and AJY3040 with AJY2977, respectively.

Plasmids used in this work are listed in Table 2.4, and the sequences of oligos are listed in Table 2.5. pAJ2002 (RLP24-myc) contained 330 nucleotides upstream of the start codon plus the entire open reading frame of RLP24 fused in frame to a 13-myc tag in pRS415. For making pAJ2020 (Yvh1-myc) and pAJ2026 (Yvh1ΔC-myc), *YVH1* was amplified by PCR with primers AJO1148 and AJO1182 and AJO1148 and AJO1194, respectively. The PCR products were digested with SstI and PacI and ligated into the same sites of pAJ1026 (Hung et al., 2008). pAJ2024 (Yvh1C117S-myc) and pAJ2025 (Yvh1ΔN-myc) were made by fusion PCR. First round PCR, using primers AJO1148XAJO1196 and AJO1195XAJO1149 for pAJ2024 and AJO1148XAJO1193 and AJO1192XAJO1149 for pAJ2025, generated two fragments. PCR products were then used as templates in the second round PCR with outer primers only. Final PCR products were digested with SstI and PacI and ligated into the same sites of pAJ1026. Primers AJO1227 and AJO1228 were used to amplify *MRT4* and ligated into pAJ1025 (Meyer et al., 2007) to create pAJ2457. pAJ2463 was constructed with fusion PCR. Primers AJO1227 and AJO1237 and AJO1236 and AJO1229 were used in the first round PCR, and outside primers were used in the second round. PCR products were digested with SstI and BamHI and ligated into the same sites of pAJ907 (Hedges et al., 2005). pAJ2464 was made by moving *YVH1* as an SstI to PacI fragment from pAJ2020 into pAJ1025 (Meyer et al., 2007)

Table 2.3 Yeast strains used in Chapter 4

Strain	Genotype	Source
BY4741	*MATa his3Δ1 leu2Δ0 ura3Δ0 met15Δ0*	
W303	*MATa leu2-3, 112 trp1-1 his3-11,15 ura3-1 ade2-1 can1-100*	
6EA1	*MATa leu2-3, 112 trp1-1 his3-11,15 ura3-1 ade2-1 can1-100 rpl12aΔ::KanMX rpl12bΔ::HIS3*	(Briones et al., 1998)
AJY543	*MATa ade2 ade3 leu2 lys2-801 ura3-52 nmd3-1*	(Johnson and Kolodner, 1995)
AJY1539	*MATa ura3Δ0 his3Δ1leu2Δ0 lys2Δ0 CRM1(T539C)-HA*	(West et al., 2007)
AJY2547	*MATα ura3Δ0 his3Δ1leu2Δ0 lys2Δ0 yvh1Δ::NAT^r*	This study
AJY2551	*MAT*a *ura3Δ0 his3Δ1leu2Δ0 lys2Δ0 mrt4Δ::KanMX*	This study
AJY2553	*MATa ura3Δ0 his3Δ1leu2Δ0 lys2Δ0 yvh1Δ::NAT^r mrt4Δ::KanMX*	This study
AJY2976	*MAT*a *ura3Δ0 his3Δ1leu2Δ0 lys2Δ0 yvh1Δ::KanMX*	This study
AJY2977	*MATα ura3Δ0 his3Δ1leu2Δ0 lys2Δ0 yvh1Δ::KanMX*	This study
AJY2982	*MAT*a *ura3Δ0 his3Δ1leu2Δ0 lys2Δ0 YVH1-GFP::HIS3*	Open Biosystems
AJY3040	*MAT*a *ura3Δ0 his3Δ1leu2Δ0 lys2Δ0 MRT4-GFP::HIS3*	Open Biosystems
AJY3048	*MAT*a *ura3Δ0 his3Δ1leu2Δ0 lys2Δ0 MRT4-GFP::HIS3 yvh1Δ::KanMX*	This study

Table 2.4 Plasmids used in Chapter 4

Plasmids	Relevant markers	Source
pAJ538	*NMD3-myc* LEU2 CEN	(Ho et al., 2000b)
pAJ2002	*RLP24-myc* LEU2 CEN	This study
pAJ2020	*YVH1-myc* LEU2 CEN	This study
pAJ2024	*YVH1C117S-myc* LEU2 CEN	This study
pAJ2025	*YVH1*Δ*N-myc* LEU2 CEN	This study
pAJ2026	*YVH1*Δ*C-myc* LEU2 CEN	This study
pAJ2457	*MRT4-GFP* LEU2 CEN	This study
pAJ2458	*RPL12B* URA3 2μ	This study
pAJ2461	*MRT4(G68D)-GFP* LEU2 CEN	This study
pAJ2463	*MRT4(G68D)* LEU2 CEN	This study
pAJ2464	*YVH1-GFP* LEU2 CEN	This study
pAJ2469	*P0-GFP* LEU2 CEN	This study
pAJ2475	*MRT4-HA* URA3 CEN	This study
pAJ2476	*pGPD-DUSP12* LEU2 CEN	This study
pAJ2477	*pGPD-Flag-MRTO4* URA3 CEN	This study
phNMD3	hNMD3-GFP	(Trotta et al., 2003a)

Table 2.5 Oligonucleotides used in Chapter 4

Oligo	Sequence
Used in cloning	
AJO1148	CTGGAGCTCCCATATTAAGAGGCCAGGTG
AJO1149	CAGTTAATTAAGAGGAATTGGACTAGGGAGA
AJO1182	CAGTTAATTAATCTATTTACTTTCTCGGATTCA
AJO1192	CAAGAAATTACAGGGACCATGGACTTGGATAAATTAACTGAAG
AJO1193	AGTCCATGGTCCCTGTAATTTCTTGCT
AJO1194	CGCTTAATTAACTATTGGATCCGCGACGACTCCGAATCTTT
AJO1195	CAAGCAGGCCTCTCGAGATC
AJO1196	TCTCGAGAGGCCTGCTTGAGAATGAGCAAAAAC
AJO1227	CTGGAGCTCTCAAAGCTATTCCCCTTTCC
AJO1228	CTGTTAATTAATTCCATGTTGATGTTAGTGC
AJO1229	CTGGGATCCTCCTGCTCTCACGTTCTTCC
AJO1236	GGCAGGCTCTAAGTTAATTATGGATAAGAGGAAAGTTTTACAAAAAG
AJO1237	CTTTTTGTAAAACTTTCCTCTTATCCATAATTAACTTAGAGCCTGCC
Used in Northern botting	
AJO249	TCTGGTAGATATGGCCGCAACC
AJO190	GTCTGGACCTGGTGAGTTTCCC
AJO130	TCTTGCCCAGTAAAAGCTCTCATGC
AJO603	TGTTACCTCTGGGCCCCGATTG
AJO313	TCCAGTTACGAAAATTCTTGTTTTTGACAA
AJO191	CGCTGCGTTCTTCATCGATGCG
AJO282	GGCCAGCAATTTCAAGTTA
AJO214	GTTCGCCTAGACGCTCTCTTC
AJO192	CCCGCCGTTTACCCGCGCTTGG
AJO317	CGTGTCTAGCCGCGAGGAAGGATTTGTTCC
AJO962	GCGACCAAAGTAAAAGTCAAGAACGACTCCACAAGTGCGAGGGTCGCGAC

2.2.2 Northern blotting

Cells were cultured to an OD_{600} of ~0.2-0.3. Total RNA was extracted by the hot phenol method (Kohrer and Domdey, 1991). Briefly, cells were resuspended in buffer AE (50 mM NaOAc, 10 mM EDTA) with hot acid phenol and heated at 65°C for 60 min. After centrifugation, the aqueous phase was recovered and extracted with phenol and chloroform twice. RNA was resolved in 1% formaldehyde gels or 6% Novex TBE-Urea polyacryamide gels (Invitrogen) for small RNAs, transferred to nylon membrane (Zetaprobe, BioRad) and probed with P^{32}-labeled oligonucleoides.

2.2.3 Sedimentation through sucrose cushions

Cultures were grown to an OD_{600} of ~0.4-0.5 in the medium. Protein extracts were prepared by vortexing with glass beads in extraction buffer (20 mM Tris pH 7.5, 6 mM $MgCl_2$, 10% glycerol, 0.1% NP40, 1 mM PMSF and 1 μM leupeptin and 1 μM pepstatin A) at different NaCl concentrations indicated in the figure legends. Protein extracts (200µl) were overlaid on 500 µl 1M sucrose in 20 mM Tris, 8 mM $MgCl_2$, and 100 mM KCl in 1.5ml ultracentrifuge tubes (Beckman). Samples were centrifuged at 80,000 rpm in a TLA100.3 rotor (Beckman) at 4°C for 60 min. Proteins in the top layer (free protein) or the pellet (ribosome pool) were separated by SDS-PAGE and detected by Western.

2.2.4 Sucrose gradient analysis

For polysome profile assays, cultures were collected at OD_{600} ~0.2-0.3. Cycloheximide (200 µg/ml final concentration) was then added, and cells were immediately harvested by pouring onto ice and centrifugation. Extracts were prepared by glass bead extraction in polysome lysis buffer (10 mM Tris-HCl pH 7.5, 100 mM KCl, 10 mM $MgCl_2$, 6 mM BME, 200 µg/ml cycloheximide). Protein extract (9 OD_{260} units) were loaded onto linear 7% to 47% sucrose gradients in polysome lysis. After a 2.5 hour spin at 40,000 rpm in a Beckman SW40 rotor, gradient fractions were collected on an ISCO density gradient fractionator, continuously measuring absorbance at 254 nm.

2.2.5 Microscopy

Overnight cultures of cells were diluted with fresh media to an OD_{600} ~0.1 and then were incubated for another 3-4 hours at 30°C. For use of leptomycin B (LMB) with yeast,

cells were concentrated ten-fold, and LMB was added at a final concentration of 0.1 μg/ml. Fluorescence was visualized on a Nikon E800 microscope fitted with a 100X objective and a Photometrics CoolSNAP ES digital camera controlled with the NIS-Elements AR 2.10 software. Images were prepared using Adobe Photoshop 7.0.

2.2.6 Immunoprecipitation

For immunoprecipitations, 200-250 ml cultures were grown to an OD_{600} of ~0.4-0.5 in selective medium. Cells were resuspended in IP buffer (20 mM Tris pH 7.5, 100 mM NaCl, 6 mM $MgCl_2$, 10% glycerol, 0.1% NP40, 1 mM PMSF and 1 μM leupeptin and 1 μM pepstatin A) and cell extracts were prepared by glass bead lysis. c-myc monoclonal antibody (9e10) was added to the supernatants, and protein complexes were pulled down with BSA-blocked protein-A agarose beads (Invitrogen). Samples were eluted in 25 μl of 1x Laemmli sample buffer and detected by Western blotting.

2.2.7 Immunofluorescence in HeLa cells

HeLa cells were grown to approximately 30% confluence on sterile cover slips. 10nM siRNA specific to DUSP12 was transfected by using RNAiMax (Invitrogen). As controls, cells were either untreated or transfected with control siRNA. After 48 hours, cells were fixed with 4% formaldehyde and permeabilized with cold methanol. MRTO4 was detected with ani-MRTO4 antibody (Santa Cruz Biotechnology).

HeLa cells were treated with 10 nM LMB or vehicle alone as a control and incubated at 37°C for 18 hours. The localization of DUSP12 or P0 was detected by using anti-DUSP12 antibody (Novus) or anti-P0 antibody (Abnova).

2.3 Materials and Methods for Chapter 5

2.3.1 Strains, plasmids, and media used in Chapter 5

Strains, plasmids, and media

All *S. cerevisiae* strains used in this study are listed in Table 2.6. All strains were grown at 30°C, unless otherwise indicated, in rich medium (yeast extract-peptone) or synthetic dropout medium, containing 2% glucose. AJY2474, AJY2467, AJY2956, and AJY2957 were obtained by transforming the indicated plasmids into the appropriate heterozygous diploid deletion strain (Research Genetics) followed by sporulation. The GAL1 promoter and 3xHA tag was amplified from pFA6A (Longtine KanMX pGAL-3HA) and integrated into W303 to generate AJY2981. AJY3005 and AJY3006 were derived from crossing BSY28 and AJY1699 (tif6Δ pTIF6), and AJY3013 and AJY3014 were from crossing AJY2981 with AJY1700 (tif6Δ pTIF6).

Plasmids used in this work are listed in Table 2.7. To make pAJ1875, *RLP24* was amplified with primers AJO585 (GGCGTCGACTACGTTGATTCAAATGGC) and AJO613 (GCGCGACGTCACATCTCTAACTCCTAAG). The fragment was digested with SmaI and SalI and ligated into the same sites of pRS413. To make pAJ1895, PCR was performed with primers AJO582 (GCGACTCGAGTGATATCTATCGCTTTTCTAGGA) and AJO1005 (GAATTAATTAATTTAGCCAACTTTCTGGC). The fragment was digested with SalI and PacI and ligated into the same sites of pAJ1139 (RLP24-HA). pAJ2064 (*GAL:RLP24-HA*) and pAJ2065 (*GAL:rlp24ΔC-HA*) were performed with the same primers but different templates. AJO1064 (GCGGAATTCATGAGAATTTATCAATGCCA) and AJO1037 (GCTACGGCTAGAGCTCTGGAGCTTTTGAATC) were used to amplify rlp24ΔC from pAJ1139 or RLP24 from pAJ1895. The PCR products were digested with EcoRI and PacI and ligated into pAJ1810. pAJ2074 (*NOG1-myc*) was made by PCR amplification using AJO1097 (CGTGAGCTCCTCTGGCTGTCTTGCAGATT) and AJO1098 (ACGTTAATTAAACGGAAATCTGTCTTACCGAC), and ligating the SstI and PacI-cut fragment into the same sites of pAJ1026. To make pAJ2075 (*DRG1-myc*), *DRG1* was amplified with AJO1099 (CGTCGGCCGAGTGGGCCCGTGGTTTATCA)

and AJO1100 (ACGTTAATTAACGAAGATGAACCGCTTCTTAG). The PCR fragment was digested with EagI and PacI and ligated into the same sites of pAJ1026.

Table 2.6 Yeast strains used in Chapter 5

Strain	Genotype	Source
W303	*MATa ade2 his3Δ leu2Δ trp1Δ ura3Δ*	
BY4741	*MATa his3Δ1 leu2Δ0 ura3Δ0 met15Δ0*	
FWY111	*MATa ade2 his3Δ leu2Δ trp1Δ ura3Δ afg2-18* (*drg1ts*)	(Pertschy et al., 2007)
S288C	*MATα can1Δ::MFA1pr-HIS3 lyp1Δ his3Δ1 leu2Δ0 ura3Δ0 met15Δ0*	(Menne et al., 2007)
BSY28	*MATα can1Δ::MFA1pr-HIS3 lyp1Δ his3Δ1 leu2Δ0 ura3Δ0 met15Δ0 sdo1ts*	Goyenechea and Warren, unpublished
AJY1699	*MATa his3Δ1 leu2Δ0 ura3Δ0 tif6Δ::KanMX with pAJ1194 (GAL:TIF6-myc URA3 CEN)*	This study
AJY1700	*MATα his3Δ1 leu2Δ0 ura3Δ0 tif6Δ::KanMX with pAJ1194 (GAL:TIF6-myc URA3 CEN)*	This study
AJY1903	*MATa his3Δ1 leu2Δ0 ura3Δ0 met15Δ0 arx1:KanMX rei1Δ:KanMX*	(Hung and Johnson, 2006)
AJY1909	*MATa ade2 his3Δ leu2Δ trp1Δ ura3Δ ARX1-GFP::HIS3MX*	(Hung and Johnson, 2006)
AJY1917	*MATa his3Δ1 leu2Δ0 ura3Δ0 met15Δ0 rei1Δ::KanMX*	(Hung and Johnson, 2006)
AJY1948	*MATa his3Δ1 leu2Δ0 ura3Δ0 met15Δ0 ARX1-GFP::HIS3MX*	Hung, unpublished
AJY2467	*MATa his3Δ1 leu2Δ0 ura3Δ0 met15Δ0 rlp24Δ::KanMX with pAJ898 (RLP24-HA URA3 CEN)*	This study
AJY2474	*MATa his3Δ1 leu2Δ0 ura3Δ0 met15Δ0 jjj1Δ::KanMX*	This study
AJY2909	*MATa his3Δ1 leu2Δ0 ura3Δ0 met15Δ0 TIF6-GFP::HIS3MX*	ResGene
AJY2981	*MATa ade2 his3Δ leu2Δ trp1Δ ura3Δ KanMX::GAL:3XHA-EFL1*	This study
AJY3005	*MATα his3Δ1 leu2Δ0 ura3Δ0 met15Δ0 sdo1ts tif6Δ::KanMX with pAJ2451 (TIF6 LEU2 CEN)*	This study
AJY3006	*MATα his3Δ1 leu2Δ0 ura3Δ0 met15Δ0 sdo1ts tif6Δ::KanMX with pAJ2250 (TIF6(V192F) LEU2 CEN)*	This study
AJY3013	*MATα his3Δ leu2Δ ura3Δ KanMX::GAL:3XHA-EFL1X tif6Δ::KanMX with pAJ2451 (TIF6 LEU2 CEN)*	This study
AJY3014	*MATα his3Δ leu2Δ ura3Δ KanMX::GAL:3XHA-EFL1 tif6Δ::KanMX with pAJ2250 (TIF6(V192F) LEU2 CEN)*	This study
AJY3072	*MATa his3Δ1 leu2Δ0 ura3Δ0 met15Δ0 jjj1Δ:KanMX TIF6-GFP::HIS3MX*	This study

AJY3075	*MATa his3Δ1 leu2Δ0 ura3Δ0 met15Δ0 rei1Δ:KanMX TIF6-GFP::HIS3MX*	This study
AJY3078	*MATa ade2 his3Δ leu2Δ trp1Δ ura3Δ TIF6-GFP::HIS3MX*	This study
AJY3079	*MATa ade2 his3Δ leu2Δ trp1Δ ura3Δ drg1ts TIF6-GFP::HIS3MX*	This study
AJY3088	*MATa ade2 his3Δ leu2Δ trp1Δ ura3Δ drg1ts ARX1-GFP::HIS3MX*	This study
AJY3093	*MATa his3Δ1 leu2Δ0 ura3Δ0 met15Δ0 arx1:KanMX rei1Δ:KanMX TIF6-GFP::HIS3MX*	This study

Table 2.7 Plasmids used in this study

Plasmids	Relevant markers	Source
pAJ582	NMD3-GFP LEU2 CEN	(Hedges et al., 2005)
pAJ754	NMD3(AAA)-GFP LEU2 CEN	(Hedges et al., 2005)
pAJ901	*LSG1-myc* URA3 CEN	(Kallstrom et al., 2003a)
pAJ903	*LSG1-myc* LEU2 CEN	(Kallstrom et al., 2003a)
pAJ1003	TIF6-GFP LEU2 CEN	This study
pAJ1004	TIF6-GFP URA3 CEN	This study
pAJ1025	ARX1-GFP LEU2 CEN	This study
pAJ1018	*REI1-myc* URA3 CEN	(Hung and Johnson, 2006)
pAJ1028	*REI1-myc* LEU2 CEN	This study
pAJ1139	*RLP24-HA* HIS3 CEN	This study
pAJ1875	*RLP24* HIS3 CEN	This study
pAJ1895	*RLP24*Δ*C-HA* HIS3 CEN	This study
pAJ2064	*GAL:RLP24* URA3 CEN	This study
pAJ2065	*GAL:rlp24*Δ*C-HA* URA3 CEN	This study
pAJ2074	*NOG1-myc* LEU2 CEN	This study
pAJ2075	*DRG1-myc* LEU2 CEN	This study
pAJ2218	MEX67-GFP LEU2 CEN	This study
pAJ2239	*DRG1-myc* URA3 CEN	This study

2.3.2 Microscopy

Overnight cultures of cells were diluted with fresh media to an OD_{600} ~0.1 and then were incubated for another 3-4 hours at permissive temperature. The temperature sensitive strains and isogeneic wild type strains were shifted to 37°C for the indicated times, as described in the figure legends, before cell harvest. For leptomycin B (LMB) treatment, cells were concentrated ten-fold, and LMB was added to a final concentration of 0.1 μg/ml. Fluorescence was visualized on a Nikon E800 microscope fitted with an X100 objective and a Diagnostic Instruments SPOT II camera controlled by NIS-Elements AR2.10 software. Images were prepared using Adobe Photoshop 7.0.

2.3.3 Immunoprecipitation

For immunoprecipitations, 200-250 ml cultures were grown to an OD_{600} of ~0.4-0.5 in dropout medium. Detailed culture conditions are given in the figure legends. The *rei1* and *jjj1* mutants were grown continuously at room temperature. Temperature-sensitive mutants were shifted to 37℃ before cell harvest: the *Drg1ts* mutant was shifted for 1 hour, *sdo1ts* for 30 minutes and *lsg1-1* for 3 hours.

Cells were resuspended in IP buffer (20 mM Tris pH 7.5, 100 mM NaCl, 6 mM $MgCl_2$, 10% glycerol, 0.1% NP40, 1 mM PMSF and 1 μM leupeptin and 1 μM pepstatin A), lysed by vortexing with glass beads and clarified by centrifugation. c-myc or HA-specific antibodies were added to the supernatants and protein complexes were precipitated by addition of BSA-blocked protein A agarose beads (Invitrogen). Proteins were eluted in 25 μl of 1x Laemmli sample buffer and detected by Western blotting.

Chapter 3
Reengineering 60S export

3.1 Introduction

Extensive studies on nucleo-cytoplasmic export of the ribosomes have shown Nmd3 to be an export adaptor for the large subunit of the ribosome (Gadal et al., 2001; Ho et al., 2000b; Thomas and Kutay, 2003a; Trotta et al., 2003a). Nmd3 binds to 60S subunits in the nucleus and recruits the export receptor Crm1, which recognizes the nuclear export signal (NES) at the C-terminus of Nmd3. Crm1 facilitates translocation of the ribosome through the nuclear pore complex (NPC) by interacting directly with nucleoporins. The NES of Nmd3 is critical for its function, and its deletion results in a block in 60S export and cell inviability.

The mRNA export receptor Mex67 was found to be a high copy suppressor of an Nmd3 NES deletion mutant (Ho et al., 2000b). The Mex67/Mtr2 heterodimer was also identified as an export receptor for 60S subunits (Yao et al., 2007). In addition to Nmd3/Crm1 and Mex67/Mtr2, Arx1 was also identified as a noncanonical export receptor that directly interacts with 60S subunits and nucleoporins (Bradatsch et al., 2007; Hung et al., 2008; Yao et al., 2007). Deletion of *ARX1* partially blocks the export of Nmd3-bound 60S subunits from the nucleus. Interestingly, the homologues of Mex67/Mtr2 and Arx1 in higher eukaryotic cells lack a role in 60S export. Ribosomes and their assembly pathway are highly conserved throughout eukaryotes. However, ribosomes appear to have evolved to use different receptors in the export pathways of yeast and humans.

Results of my initial experiments to understand how MEX67 suppressed an *nmd3* mutant showed that overexpression of Mex67 restored the growth of an *nmd3* mutant in which the Crm1-dependent nuclear export signal (NES) was deleted and modestly improved the 60S export. This led me to test whether recruitment of Mex67 more efficiently to ribosomal subunits would enhance their export. A related question, I addressed whether the recruitment of other export receptors, whose biological function is not related to 60S export, would also facilitate the export of large subunits. Surprisingly, ribosome export could indeed be reengineered. The fusion of Mex67, Mtr2, and other

export receptors (Cse1, Los1, and Msn5) to an Nmd3 NES-deficient mutant, respectively, suppressed the lethality of a conditional *nmd3-4* mutant. Furthermore, these chimeric proteins restored 60S export. Finally, I determined if the Crm1-dependent NES for the 60S subunit is required by an adapter protein in trans, since an NES integral to the ribosome seems more economical. To ask this, I fused the NES of Nmd3 to different ribosomal proteins to introduce an NES in cis on 60S subunits. I found that the adapter function of Nmd3 could be substituted by fusion of NES to rproteins, although, to a reduced extent compared to Nmd3 and Arx1. These results imply the flexibility in the nature of the export receptor and export signal for exporting the large ribosomal subunit.

3.2 Background

The synthesis of ribosomal subunits starts in the nucleolus, a subcompartment of the nucleus that is organized around the rRNA transcription units. After RNA polymerase I transcribes 35S rRNA, ribosomal proteins and trans-acting factors assemble as a single 90S ribonucleoprotein (RNP) precursor. The 90S is then cleaved to yield a 43S (pre-40S) complex, and assembly of large subunit proteins and processing factors on the remaining 3' portion of the primary transcript yields a 66S (pre-60S) subunit. Although they are assembled from the same primary transcript, the two ribosomal subunits are exported independently of one another. The particles that are exported are not yet fully mature: additional rRNA processing and protein assembly events occur in the cytoplasm. Furthermore, both subunits are exported with a small complement of non-ribosomal trans-acting factors.

The nuclear export of most proteins and RNAs is mediated by karyopherins (Fried and Kutay, 2003; Gorlich and Kutay, 1999; Weis, 2003), a conserved group of soluble factors that facilitate the unidirectional transport of cargo molecules through the NPC in the nuclear envelope (Macara, 2001; Mattaj and Englmeier, 1998). Four karyopherins in yeast are known to be involved in export. These are Crm1, which recognizes leucine-rich nuclear export signals (NESs), Los1, the tRNA exporter, Cse1 which exports importin alpha and Msn5, involved in the export of certain protein cargoes and tRNAs (Pemberton and Paschal, 2005). The binding of these exportins to their

substrates in the nucleus depends on the formation of a ternary complex with RanGTP, which stabilizes the exportin-cargo interaction. Upon translocation to the cytoplasm, hydrolysis of GTP on Ran, stimulated by a cytoplasmic GTPase-activating protein (GAP) and Ran-binding protein 1 (Yrb1), results in a conformational change necessary for disassembly of the export complex (Petosa et al., 2004). The directionality of export is controlled by the high concentration of Ran-GTP in the nucleus versus cytoplasm, which promotes assembly of exportins with their cargo only in the nucleus.

The 60S ribosomal subunit is one of the largest nuclear export cargos in yeast. Its efficient export through the hydrophobic channel of the NPC is likely to require more than one receptor. Crm1 was the first export receptor to be identified for the 60S subunit. Crm1 is recruited to the large subunit in the nucleus by the leucine-rich NES of Nmd3, an adapter protein that is essential protein for 60S export from yeast to humans (Gadal et al., 2001; Ho et al., 2000b; Thomas and Kutay, 2003a; Trotta et al., 2003a). Nmd3 shuttles between the nucleus and cytoplasm, and the steady state protein distribution is in both nucleus and cytoplasm.

Recently, two other 60S export receptors were identified: Arx1 (Bradatsch et al., 2007; Hung et al., 2008) and Mex67 (Yao et al., 2007). Unlike Crm1, the direction of transport of these two receptors is not controlled by the RanGTP gradient. In addition, three receptors interact directly with both the 60S subunit and nucleoporins. Arx1 was first identified on the Nmd3-containing 60S complex. Deletion of *ARX1* causes a cold-sensitive phenotype and a 60S export defect. Further characterization showed that *arx1*Δ exhibits synthetic lethality with *nup120* and *nmd3*Δ*C14* and physically interacts with nucleoporins. These results identified the function of *ARX1* as an export receptor.

Mex67 and Mtr2 act as a heterodimer that is responsible for the majority of mRNA export in yeast (Santos-Rosa et al., 1998; Segref et al., 1997). Interestingly, *mtr2-33* only blocks 60S export, but not mRNA export (Senay et al., 2003). In addition *MEX67* and *MTR2* have strong genetic interactions with factors involved in 60S export; high copy *MEX67* can suppress the growth defect of *nmd3* export mutants (Lo and Johnson, 2009; Yao et al., 2007). *mex67-5* is synthetic lethal with *nmd3-1,* a mutant lacking the NES at the C-terminus (Ho et al., 2000b). Also, Mex67 and Mtr2 have been shown to

interact with nascent 60S subunits. A comparison of the sequences of Mex67/Mtr2 to their human homologues, Tap/p15, reveals several insertions in the yeast proteins. Deletions of these loops of Mex67 and Mtr2 were shown to specifically block 60S export and may have evolved in yeast to facilitate 60S export. Therefore, the Mex67 and Mtr2 heterodimer was identified as a 60S export receptor.

Recently, three receptors are known to be required for the efficient export of 60S subunits through the NPC. However, only the function of Crm1 in 60S export is conserved in higher eukaryotes. Considering that ribosome export is an essential pathway in eukaryotes, and that many ribosome biogenesis factors are highly conserved, such flexibility in the export receptors used for 60S subunit export is surprising. Here, I asked if there is a specific requirement of export receptors in ribosome export. Interestingly, Mex67, Mtr2, and any other export karyophrins, Cse1, Los1, and Msn5, could support 60S export if recruited directly to the subunit. These results suggest that there is no requirement for a specific export receptor for the large subunit. Directionality of most export events is determined by nucleotide hydrolysis to release export receptors. However, fusing export receptors to Nmd3 should make their release dependent on the machinery specific to releasing Nmd3. Indeed, the Msn5-Nmd3 fusion protein was mislocalized to the cytoplasm by expression of a dominant *LSG1* mutant that we have shown previously traps Nmd3 on 60S subunits in the cytoplasm.

Finally, I asked if export could be driven by adding an NES to the ribosome *in cis*, through fusion of the Nmd3 NES sequence to a ribosomal protein. Indeed, fusing the NES of Nmd3 to Rpl3 supported ribosome export. These results imply remarkable flexibility in the nature of the export receptor and export signal for the large ribosomal subunit and may help explain how different export receptors could have evolved in different eukaryotic lineages.

3.3 Results

3.3.1 Genetic interaction between Mex67, Mtr2 and Nmd3

MEX67 showed genetic interaction with *NMD3*. *MEX67* was identified as a high copy suppressor of *nmd3-1*, and *mex67-5* was also shown to be synthetic lethal with

nmd3-1 (Ho et al., 2000b). Since the *nmd3* mutant lacked an mRNA export defect or decreased expression levels of *MEX67* (data not shown), *MEX67* may bypass the ribosome export defect caused by mutant *NMD3*. To determine how *MEX67* suppresses *nmd3-1*, I tested the ability of high copy *MEX67* to suppress a panel of *nmd3* mutants (Fig 3.1A). Surprisingly, *MEX67* could rescue the growth defects of *nmd3* export mutants, even the ones lacking the entire NES (Fig 3.1B). However, MEX67 could not suppress the growth defect of an *nmd3* mutant deleted of its nuclear localization signal (*nmd3*Δ*NLS*). Also, *MEX67* could not replace *NMD3* (Fig 3.1B Vector, 5FOA), consistent with the idea that Nmd3 has a function in ribosome biogenesis beyond its role in export.

Mtr2 was reported to have a dual role in both mRNA and ribosome export pathways. Mex67 and Mtr2 form a heterodimer that recognizes mRNA and directly interacts with nuclear pore complex to export mRNA from the nucleus (Strasser et al., 2000). Mtr2 was also found in an Arx1-containing 60S complex (Nissan et al., 2002), and *mtr2-33* is specifically defective in ribosome export (Bassler et al., 2001). Together, these observations suggest that Mtr2 is also involved in ribosome export. To further dissect out the function of Mtr2 in ribosome export pathway, genetic interactions were tested between *NMD3* mutants and *MTR2*. Interestingly, expression of *MTR2* from a high copy vector did not suppress the growth defect of the *nmd3*Δ*50* mutant and also did not relieve the dominant-negative effect of *nmd3*Δ*50* (data not shown). *nmd3(AA)* contains two point mutations within its NES that by themselves have a very modest effect on Nmd3 function [(Fig 3.1A) and (Hedges et al., 2006)]. Surprisingly, overexpression of *MTR2* in this mutant was mildly toxic (Fig 3.1C). In addition, *mtr2-33* and *nmd3(AA)* showed a strong synthetic sick interaction (Fig 3.1D). Thus *MEX67* and *MTR2* both show strong genetic interactions with *NMD3* that are specific to its function in nuclear export of the 60S subunit, although overexpression of *MEX67* or *MTR2* differentially affects the growth of *nmd3* mutants.

The NES of Nmd3 is a critical functional domain involved in ribosome export. Point mutations within the NES partially disrupt Crm1 binding, whereas deletion of the entire NES is expected to completely block Crm1 binding (West et al., 2007).

Remarkably, high copy *MEX67* could rescue the growth defect of *nmd3* NES truncation mutants. This suggests that Mex67 can drive ribosome export independent of the NES of Nmd3, most probably by interacting with the NPC directly, as in the case of mRNA export. Mtr2 might work as an accessory factor to help Mex67 to recruit the ribosome to the NPC rather than directly bridging this interaction since a high level Mtr2 could not rescue nmd3 export mutants.

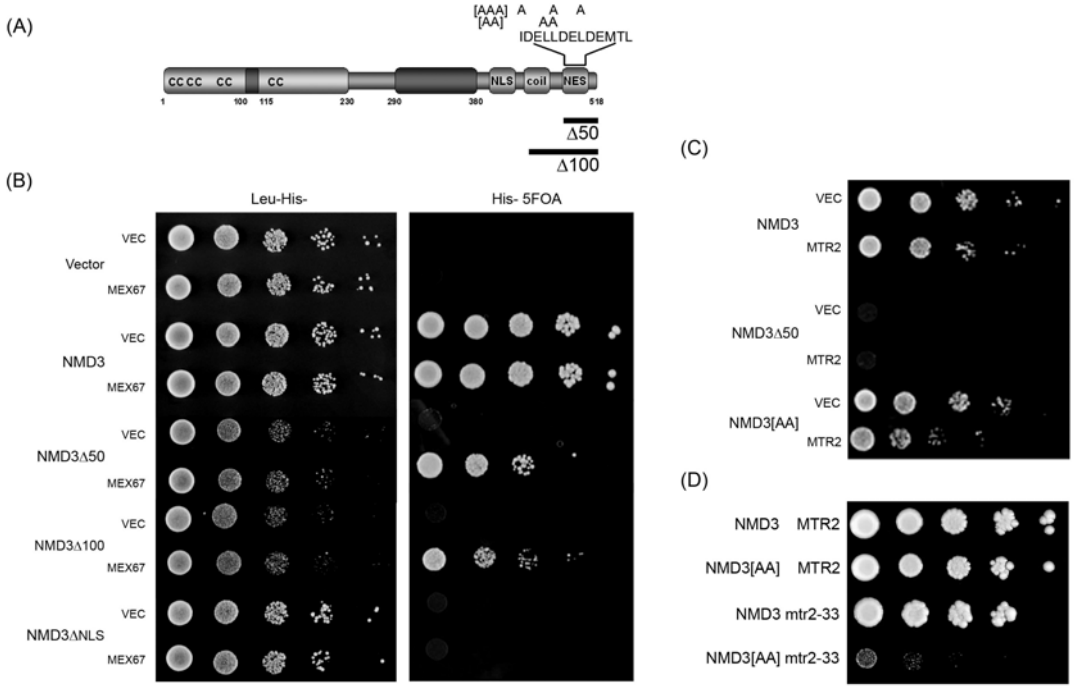

Figure 3.1 Genetic interactions among *MEX67*, *MTR2* and *NMD3*.

(A) Schematic diagram showing Nmd3 functional domains and mutants. (B, C) Growth analysis of AJY2110 (*nmd3*::KanMX pAJ112 *NMD3*) expressing different mutant *nmd3* alleles and high-copy *MEX67* (pAJ1872) (B) or high-copy *MTR2* (pAJ1877) (C). Ten-fold dilutions of AJY2110 (*nmd3*Δ) transformed with vector (pRS415), *NMD3* (pAJ538), *nmd3*Δ*50* (pAJ534), *nmd3*Δ*100* (pAJ535), and *nmd3*Δ*NLS* (pAJ1359) in combination with vector (pRS423) or high-copy *MEX67* or *MTR2* were spotted onto His^- Leu^- drop-out or His^- 5FOA medium and incubated at 30°C. (D) AJY2110 and AJY2466 (*nmd3*::KanMX *mtr2*::HIS3 with pAJ112 and pAJ1367 *mtr2-33*) with wild-type *NMD3* (pAJ538) or *nmd3(AA)* (pAJ751) were spotted on 5FOA medium.

3.3.2 *MEX67* rescues the 60S export defect in *nmd3* NES mutants

Since only Mtr2 is reported to bind the late 60S ribosome, I tested whether Mex67 also shows interaction with the 60S ribosome. Consistent with a previous result (Yao et al., 2007), Mex67 can be detected in Nmd3-13myc immunoprecipitated subunits (data not shown).

To characterize the role of Mex67 in 60S export, Rpl25-GFP and Nmd3-GFP were used as reporters to detect whether Mex67 can rescue the 60S export defect of cells expressing *nmd3*Δ50, which poorly supports growth and shows a severe 60S export defect. Consistent with previous results, both Nmd3Δ50-GFP and Rpl25-GFP signal were trapped in the nucleus (Fig 3.2A). Although over-expression of *MEX67* did not alter the nuclear accumulation of Nmd3Δ50-GFP, the distribution of Rpl25-GFP was shifted toward the cytoplasm. This discrimination may be from the dynamic difference between these two reporters. Truncation of the C-terminal NES of Nmd3 would dramatically reduce its rate of export. However, its NLS is intact and the protein will be efficiently imported, giving a strongly nuclear bias. A modest increase in export would not be observed if the rate of import were higher. On the other hand, Rpl25 does not recycle to the nucleus and a modest increase in its rate of export will yield a corresponding change in the distribution of Rpl25 between the nucleus and cytoplasm

Cells expressing Nmd3Δ50 showed lower 60S levels and halfmers (Fig 3.2B; compare WT with vector and Nmd3Δ50 with vector). Similar to the modest improvement of 60S export, high copy Mex67 only modestly suppressed the polysome defect of nmd3Δ50 (Fig 3.2B; compare Nmd3Δ50 with vector and 2μ *MEX67*). There was a slight, reproducible increase in polysomes, but no obvious change in free subunit levels (Fig 3.2B, 60S). In addition, analysis of total subunit levels by sucrose gradient sedimentation under subunit dissociating conditions revealed no detectable difference in the ratio of 60S to 40S subunit levels with or without high-copy *MEX67* (Fig 3.2C). Thus, high copy *MEX67* significantly enhances the growth of cells containing NES-deficient *NMD3*, but at the cellular level, this corresponds to a very modest improvement in subunit export.

This result could indicate that cell growth can be supported even with very limiting ribosomal subunit levels. FACS data showed that the export-defective *nmd3*

mutants affect progression through the cell cycle that leads to a modest shift to 1N in haploid cells (data not shown). This cell cycle phenotype is nearly completely reversed by high-copy *MEX67* (data not shown), perhaps explaining why the suppression of the growth defect of nmd3Δ50 was much more significant than the suppression of the 60S export defect.

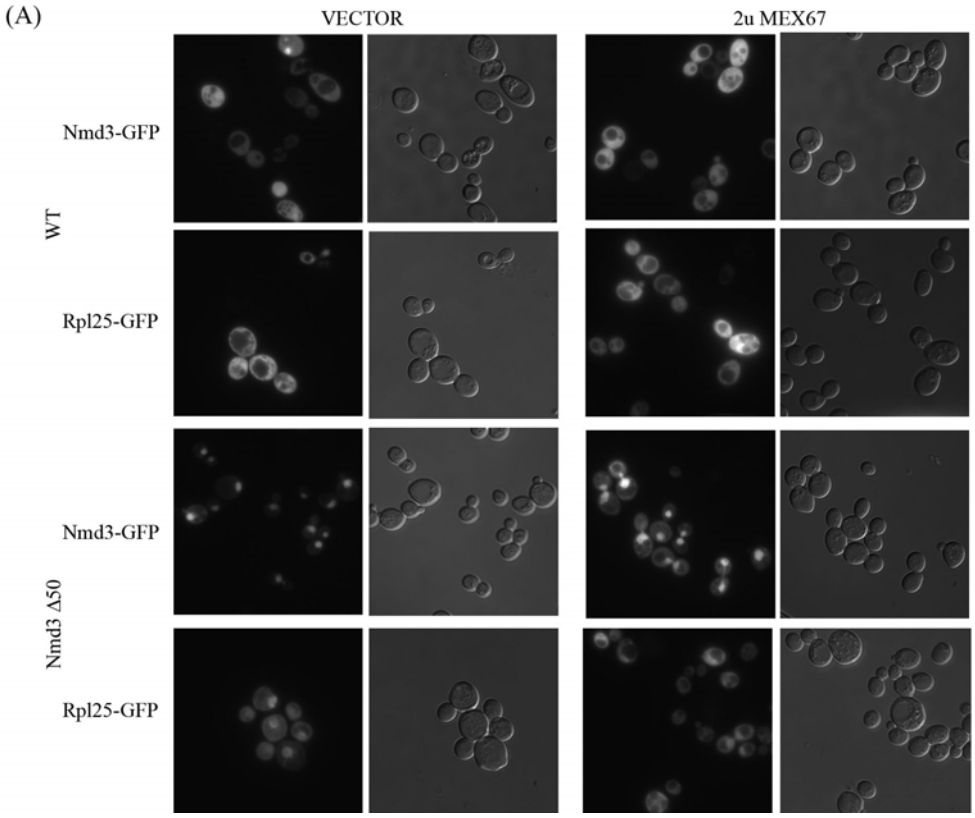

Figure 3.2 High-copy *MEX67* modestly increases ribosome export in an export-deficient *nmd3* mutant.

(A) Cells were cultured in selective medium, collected at OD_{600} ~0.3 and GFP and whole cells were visualized by fluorescence and DIC (differential interference contrast) microscopy, respectively. (B) AJY2110 (*nmd3*Δ) with wild-type or *nmd3*Δ*50* in combination with vector alone or high copy (2μ) *MEX67* were grown in selective medium at 30°C and harvested at an OD_{600} ~ 0.3. Cell extracts were fractioned on 7% to 47% sucrose gradients containing 10 mM Tris, pH7.5, 100 mM KCl, 6 mM βME, 10 mM $MgCl_2$ and 200 μg/ml cycloheximide. (C) Cell extracts and gradients were prepared similar to that described in (B), but without cycloheximide and $MgCl_2$.

3.3.3 A Mex67-Nmd3△100 Fusion protein can complement the Nmd3 export function

To further test whether Mex67 can replace the NES function of Nmd3, full-length *MEX67* was fused to the N-terminus of *nmd3*Δ100 (Fig 3.3A). Interestingly, *MEX67-nmd3*Δ*100* could rescue the growth of *nmd3-4ts*, a temperature-sensitive lethal mutant that fails to export 60S subunits and shows a severe instability of 25S rRNA at non-permissive temperature (Ho et al., 2000a; Ho et al., 2000b) (Fig 3.3B). However, this fusion could not complement the lethality of *mex67-5* (Santos-Rosa et al., 1998), a mutant that is defective for mRNA export (Fig 3.3C). This result indicates that this fusion protein cannot support mRNA export, but rather does support 60S export. Although 2μ *MEX67* can rescue *nmd3* export mutants, it cannot restore the growth defect of *nmd3-4ts* (Fig 3.3B). This is consistent with the result that 2μ *MEX67* cannot replace *NMD3* function in an *nmd3* deletion strain (Fig 3.1B). At non-permissive temperature, *nmd3-4ts* may not only lose function as an export adapter, but also potential roles in ribosome biogenesis pathway that cannot be replaced by Mex67. As further controls to demonstrate that this fusion protein required both the 60S binding function of Nmd3 and the export function of Mex67, I introduced specific mutations into the fusion protein. Mutations of L263P and F318I in Nmd3 have been shown to impair 60S binding (Hedges et al., 2006) and render the protein nonfunctional. The introduction of these two point mutations into the Mex67-Nmd3Δ*100* fusion protein abolished its ability to complement the growth of *nmd3-4* (Fig3.3D), suggesting that this fusion protein requires the Nmd3Δ100 moiety to bind 60S subunits. I also replaced *MEX67* with *mex67-5,* which loses interaction with Mtr2 at restrictive temperature (Santos-Rosa et al., 1998). The introduction of *mex67-5* to the chimeric protein reduced complementation of *nmd3-4* significantly (Fig3.3D). Thus, the Mex67 moiety also contributes to function of the chimeric protein.

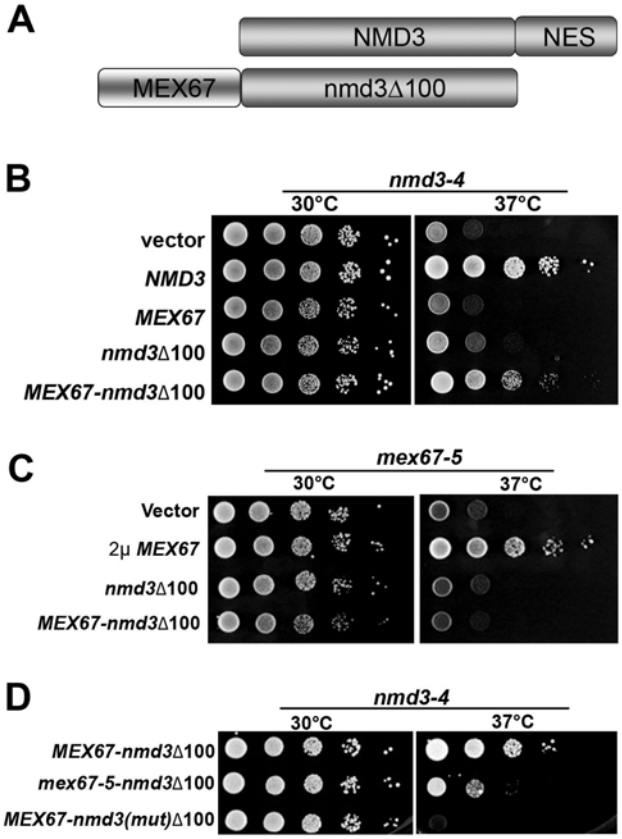

Figure 3.3 Fusion of Mex67 to NES-deficient Nmd3 suppresses *nmd3-4ts* at non-permissive temperature

(A) Schematic diagram showing the MEX67-*nmd3*Δ100 construct. (B) Ten-fold serial dilutions of AJY734 (*nmd3-4*) transformed with empty vector, *NMD3* (pAJ409), *MEX67* (pAJ528), *nmd3*Δ*100-GFP* (pAJ757), and *MEX67-nmd3*Δ*100 -GFP* (pAJ1882) were spotted onto selective medium and incubated for 3 days at the indicated temperature. (C) Growth test of AJY1231 (*mex67-5*) transformed with empty vector, *MEX67* (pAJ528), *nmd3*Δ*100-GFP* (pAJ757) or *MEX67-nmd3*Δ*100- GFP* (pAJ1882) were spotted onto selective medium and incubated at 30°C or 37°C. (D) *MEX67-nmd3*Δ*100-GFP* (pAJ1882), *(mex67-5)-nmd3*Δ*100-GFP* (pAJ2079) or *MEX67-nmd3[L263P F318I]*Δ*100-GFP* (pAJ2084) were transformed into AJY1231 and tested for complementation as in (B).

I next examined 60S export in cells using Mex67-Nmd3Δ100 as a 60S subunit export receptor. The localization of Rpl25-eGFP was monitored in *nmd3-4* with wild-type *NMD3*, *nmd3Δ100*, and *MEX67-nmd3Δ100*. Consistent with previous results, Rpl25-eGFP was in the cytoplasm when cells expressed wild-type Nmd3 at both permissive and nonpermissive temperature. Nmd3Δ100 is a C-terminal deletion of one hundred amino acids. This region contains the NES and a coiled-coil domain of *NMD3,* which is not related to 60S subunits binding ability. The expression of *nmd3*Δ100 causes a strong dominant negative-effect by preventing 60S export (Ho et al., 2000a). Cells expressing Nmd3Δ100 showed a block in 60S export at 30°C and the defects were more prominent at 37°C (Fig 3.4A). In contrast, the chimeric Mex67-Nmd3Δ100 fusion protein supported an intermediate level of export (Fig 3.4A, bottom panel), with 64±7% cells showing cytoplasmic Rpl25-eGFP signal. This result is comparable to the growth test, implying that the Mex67-Nmd3Δ100 fusion protein can partially complement Nmd3 export function. This was also reflected in increased 60S subunit levels detected by sucrose gradient analysis of free subunits and polysomes (Fig 3.4B). Halfmers were present in cells with Nmd3Δ100 at both 30°C and 37°C. The halfmers in cells expressing *MEX67-nmd3*Δ100 fusion protein were reduced compared with Nmd3Δ100 (Fig 3.4B). Altogether, these results show that a chimeric MEX67-*nmd3*Δ100 fusion protein could support 60S export.

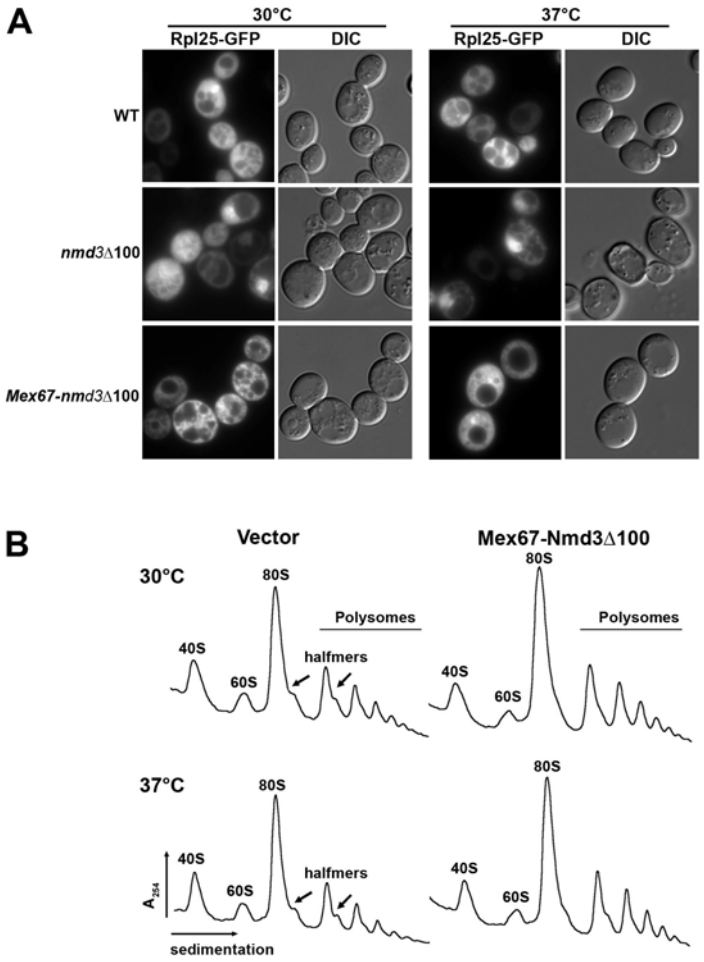

Figure 3.4 The Mex67-Nmd3Δ100 fusion protein restores export and 60S levels in an *nmd3-4* mutant.

(A) AJY734 (*nmd3-4*) with *NMD3-myc* (pAJ538), *nmd3Δ100-myc* (pAJ535), and *MEX67-nmd3Δ100-myc* (pAJ1892) were grown to early log phase and then shifted to 37°C for 120 min. The localization of Rpl25-GFP (pAJ908) was detected by fluorescence microscopy (B) AJY734 (*nmd3-4*) with *nmd3Δ100-myc* (pAJ535) and *MEX67-nmd3Δ100-myc* (pAJ1892) were grown in selective medium to an OD_{600} ~ 0.3 at 30°C or shifted to 37°C for 30 min before harvest. Cell extracts were fractionated on 7% to 47% sucrose gradients containing 10 mM Tris, pH 7.5, 100 mM KCl, 6 mM βME, 10 mM $MgCl_2$ and 200 μg/ml cycloheximide.

Wild-type Nmd3 utilizes Crm1 for nuclear export. If Mex67 substitutes for the function of CRM1 in the Mex67-Nmd3Δ100 fusion protein, its localization should not be sensitive to the Crm1-inhibitor leptomycin B (LMB). Yeast Crm1 is not sensitive to LMB so I used the Crm1(T539C) mutant, which has been shown sensitive to LMB. As expected, in the absence of LMB, wild-type Nmd3 was distributed throughout the whole cell, whereas Nmd3Δ100 only localized to the nucleus. Mex67, being an export receptor, is localized to the nuclear envelope (Santos-Rosa et al., 1998). Mex67-Nmd3Δ100 has a unique distribution in nucleoplasm, cytoplasm, and nuclear envelope (Fig 3.5). During a time course of LMB treatment, where wild-type Nmd3 was trapped in the nucleus after 15 min of LMB treatment, Mex67-Nmd3Δ100 was not trapped in the nucleus even after 1 hr (Fig 3.5). This result suggested that the Mex67-Nmd3Δ100 fusion protein can bypass the requirement of Crm1 in 60S export. In conclusion, Mex67 can replace Crm1 in 60S export, if recruited directly to the subunit through fusion to Nmd3. In this situation, the ribosome likely carries two molecules Mex67; one wild-type Mex67 is at its native binding site, and one is recruited as a fusion protein by Nmd3. To test this assumption that the subunit now contains two molecules of Mex67, I immunoprecipitated 60S subunits containing the Mex67-Nmd3Δ100 fusion protein and probed for endogenous Mex67 by Western blotting. Indeed, I could detect native Mex67 in the immunoprecipitate, indicating that the subunit was loaded with two molecules Mex67 (Fig 3.6).

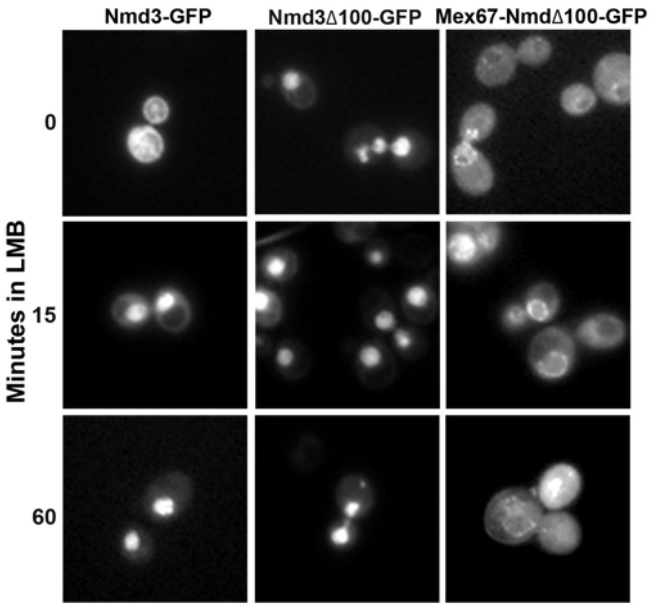

Figure 3.5 The localization of the Mex67-Nmd3ΔNES chimeric protein is resistant to LMB treatment.

AJY1539 (*crm1*T539C) with *NMD3-GFP* (pAJ755), *nmd3Δ100-GFP* (pAJ757), *MEX67-nmd3Δ100-GFP* (pAJ1882) were treated with 0.1 μg/ml LMB for the indicated timeS, fixed with 3.7% formaldehyde and visualized by fluorescence microscopy.

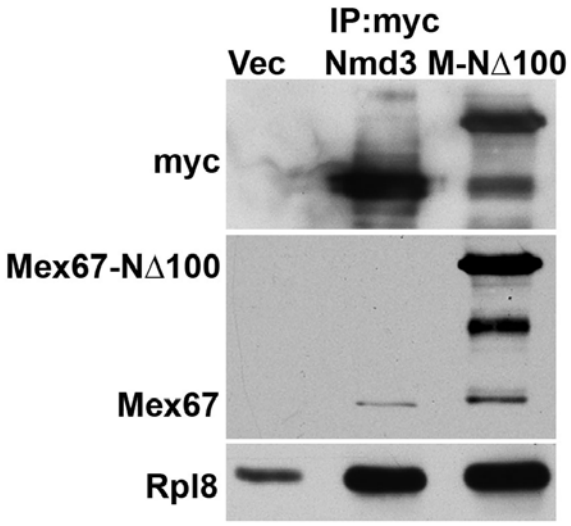

Figure 3.6 Two molecules of Mex67 are recruited to the subunit.

Immunoprecipitation was done with with anti-c-myc antibody directed against Nmd3-myc (pAJ538) or Mex67-Nmd3Δ100-myc (pAJ1892) expressed in BY4741. Vec represents an empty vector control. The immunoprecipitates on Western blots were incubated with c-myc, Mex67 and Rpl8-specific antibodies.

3.3.4 Other receptor fusion proteins can also support 60S export defect

Next, the ability of the large subunit to use other export receptors for transport through the NPC was tested. MTR2, required for mRNA export, CSE1, the exporter of importin α, LOS1, the tRNA receptor, and MSN5, a nuclear export receptor of several proteins, were individually fused at the C-terminal end of *nmd3*△100 (Fig 3.7A). Each fusion restored Nmd3-like function in *nmd3-4* mutant at non-permissive temperature, but to varying degrees (Fig 3.7B). Msn5 and Los1 showed the best complementation, whereas the Mtr2 fusion was considerably weaker in activity and the Cse1 fusion was further compromised. In each case, complementation was lost when these export receptors were fused to the *nmd3* double point mutant (L263P, F318I) (Fig 3.7B) indicating that binding to the 60S subunit was required for function. In addition, each fusion protein was able to complement the lethality of an *nmd3*Δ mutant (data not shown), indicating that they were functional as the sole copies of Nmd3.

To have further evidence for support of 60S export by these chimeric receptors and Nmd3Δ100 fusion proteins, I assayed Rpl25-eGFP localization in these strains. Consistent with the growth test (Fig 3.7B), 60S subunits were no longer trapped in the nucleus in *nmd3-4* strains with LOS1 and MSN5 fusion proteins (Fig 3.7C). In summary, export receptors from other pathways could function in 60S export when recruited to the subunit.

Like the Mex67 fusion protein, the localization of these chimeric proteins also depended on the nature of the receptor that was fused to Nmd3. The Cse1 and Msn5 fusion proteins localized predominantly in the nucleus, whereas the Los1 fusion protein was present in the nucleus, cytoplasm, and nuclear envelope (Fig 3.8).

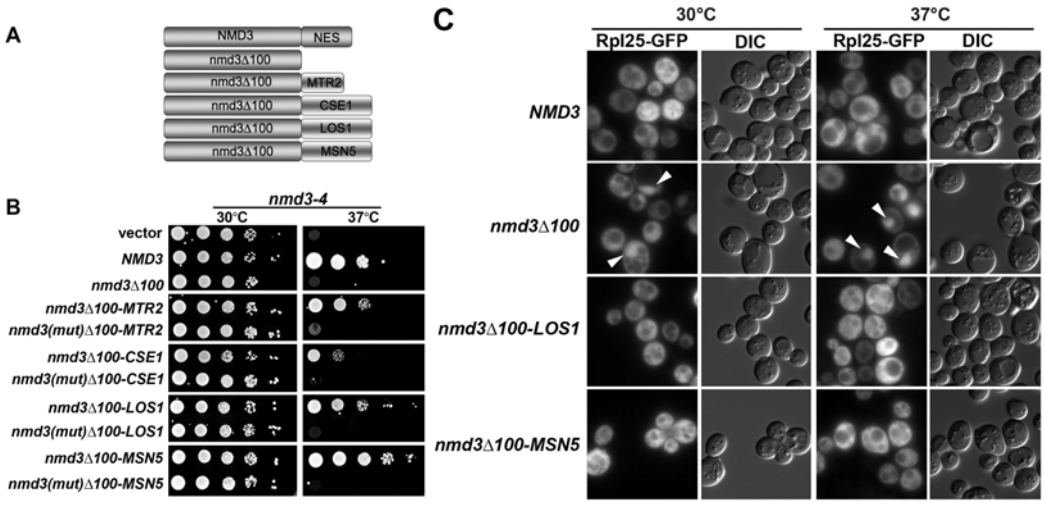

Figure 3.7 Fusion of other receptors to NES-deficient Nmd3 supports ribosome export.

(A) Schematic diagram showing the fusion protein constructs between different receptors and the NES-deficient *nmd3*. (B) Ten-fold serial dilutions of AJY734 (*nmd3-4*) containing empty vector, *NMD3* (pAJ409), *nmd3Δ100-GFP* (pAJ757), *nmd3Δ100-MTR2 -GFP* (pAJ2066), *nmd3(mut)Δ100-MTR2-GFP* (pAJ2085), *nmd3Δ100-CSE1 –GFP*(pAJ2076), *nmd3(mut)Δ100-CSE1-GFP* (pAJ2086), *nmd3Δ100-LOS1 -GFP* (pAJ2077), *nmd3(mut)Δ100-LOS1-GFP* (pAJ2087), *nmd3Δ100-MSN5 -GFP* (pAJ2078), and *nmd3(mut)Δ100-MSN5-GFP* (pAJ2088) were spotted onto selective medium and incubated for 6 days at the indicated temperature. *nmd3(mut)* is *nmd3[L263P F318I]*. (C) AJY734 (*nmd3-4*) expressing Rpl25-GFP (pAJ908) and wild-type *NMD3-myc* (pAJ538), *nmd3Δ100-myc* (pAJ535), *nmd3Δ100-LOS1-myc* (pAJ2227), and *nmd3Δ100-MSN5-myc* (pAJ2226) was grown in selective medium to early log phase at 30°C and then shifted to 37°C for 60 min before visualizing GFP.

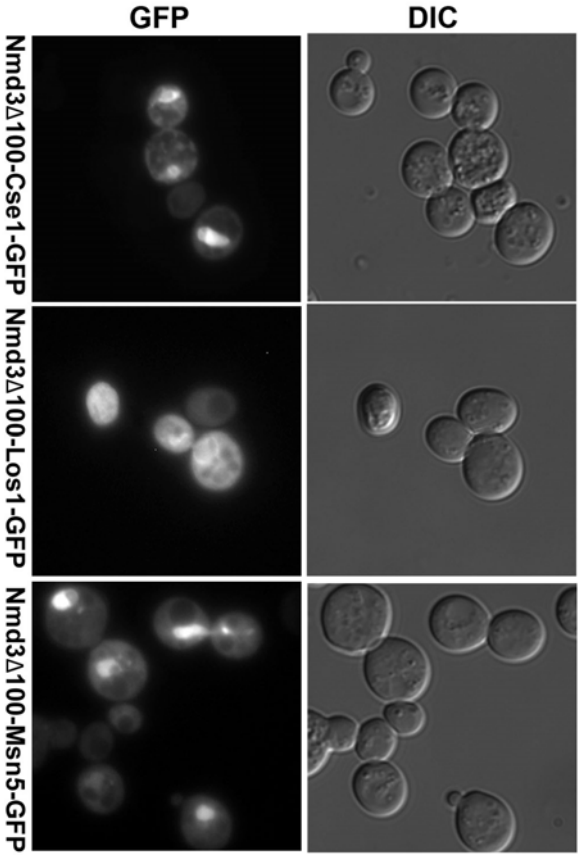

Figure 3.8 Localization of chimeric proteins is dependent on the nature of the receptor.

AJY734 (*nmd3-4*) with *nmd3*Δ*100*-Cse1-*GFP* (pAJ2076), *nmd3*Δ*100-LOS1-GFP* (pAJ2077), or *nmd3*Δ*100-MSN5-GFP* (pAJ2078) were cultured to early log phase at 30°C before microscopy.

To ensure that these receptors did bind to the 60S subunits and work as export receptors, the sedimentation of Mex67-Nmd3Δ100 and Nmd3Δ100-Msn5 were detected across the fractions of sucrose gradients. Indeed, both proteins were found exclusively at the position of free 60S (Fig 3.9), as we have previously observed for Nmd3 (Ho et al., 2000b). Although I only examined the sedimentation of Mex67 and Msn5 fusions, all the fusion proteins were expected to cosediment with 60S subunits, reflecting the function of their Nmd3 domains. The genetic evidence that mutations disrupting Nmd3 binding to 60S rendered these fusions non-functional supports this assumption (Fig 3.7B).

If 60S export is driven by the chimeric receptors and not dependent on Crm1, export should be insensitive to LMB. I tested LMB sensitivity of 60S export in an *nmd3-4ts crm1(T539C)* mutant containing chimeric receptor fusion proteins. To confirm that 60S export depended only on the chimeric receptors, cells were shifted to nonpermissive temperature at early log phase to inactivate the function of Nmd3 and then tested for LMB sensitivity. In wild-type cells, Rpl25-eGFP was cytoplasmic in the absence of LMB but trapped in the nucleus, after LMB treatment. In the presence of Nmd3Δ100, Rpl25-eGFP was blocked in the nucleus regardless of LMB treatment (Fig 3.10, first two panels from top). Mex67-Nmd3Δ100 and Nmd3Δ100-Msn5 supported the most efficient growth in *nmd3-4*, so I only tested cells with these two chimeric receptors. In cells with either of the chimeric receptors, the percentage of cells showing nuclear localization of Rpl25-GFP did not change upon treatment with LMB (Fig 3.10, lower two panels). Thus, 60S export by the chimeric fusion proteins was insensitive to Crm1.

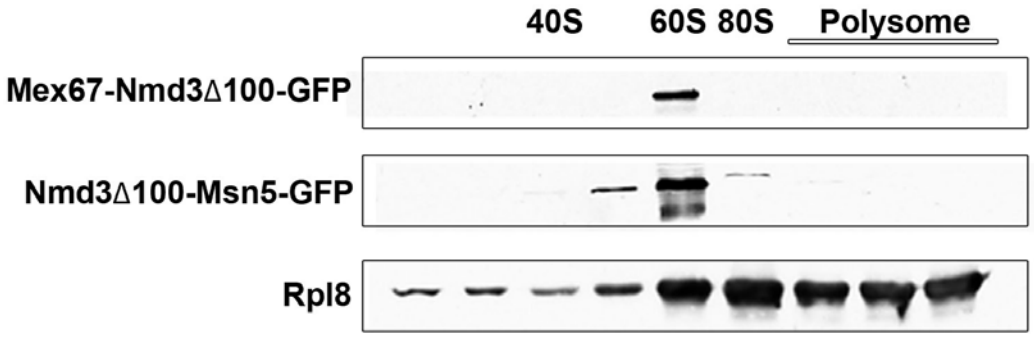

Figure 3.9 Chimeric proteins cosediment with 60S ribosomes.

AJY734 (*nmd3-4*) with *MEX67-nmd3Δ100-GFP* (pAJ1882) or *nmd3Δ100-MSN5-GFP* (pAJ2078) were cultured to early log phase at 30°C. Extracts were prepared and sedimented through 7% to 47% sucrose gradients by ultracentrifugation as described in Materials and Methods. Fractions were collected, proteins separated by SDS-PAGE and visualized by Western blotting using rabbit anti-GFP as the primary antibody and anti-Rpl8 antibodies.

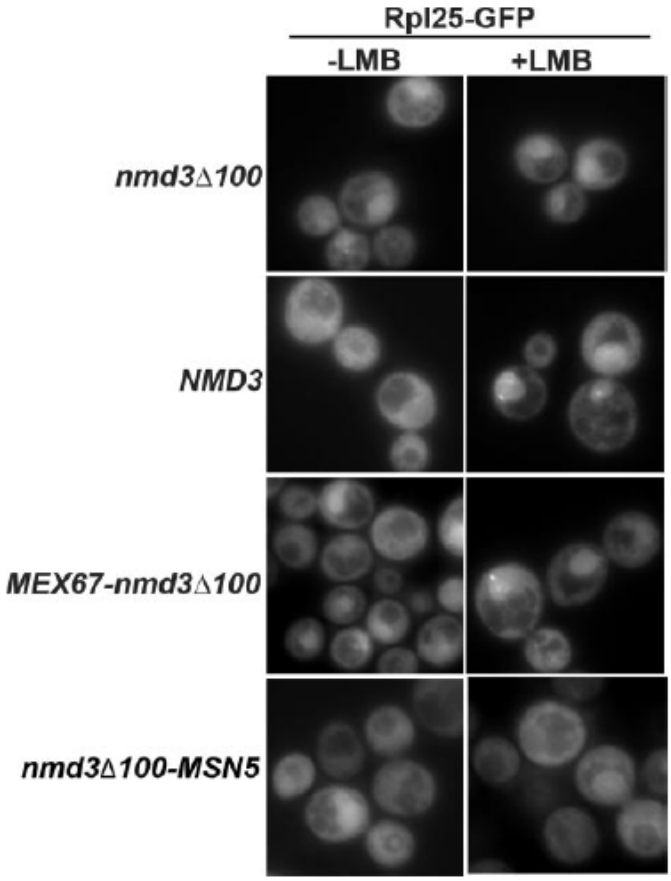

Figure 3.10 60S export by the chimeric Mex67-nmd3Δ100 fusion protein is insensitive to LMB. Rpl25-GFP (pAJ908) was monitored in AJY2974 (*nmd3-4 crm1*T539C) with pAJ535 (*nmd3*Δ100), pAJ538 (*NMD3*), pAJ1892 (*MEX67-nmd3*Δ*100*), or pAJ2226 (*nmd3*Δ-*MSN5*). The cells were diluted into fresh medium from overnight cultures and incubated at 30°C for 30 min. After the temperature shift to 37°C for 1.5 h, LMB (0.1 μg/ml) was added and the cultures were incubated at 37°C for another 30 min before microscopy.

3.3.5 Lsg1 determines the transport direction of these novel export receptors

The RanGTP gradient determines the direction of nucleocytoplsmic transport. Export cargo is bound by an export receptor only in the presence of RanGTP in the nucleus and dissociates from its receptor upon GTP hydrolysis in the cytoplasm. In the case of the chimeric receptors, the binding to the ribosome depends on the 60S binding moiety of Nmd3. Because GTP hydrolysis on Ran is not expected to release Nmd3 from the ribosome, the RanGTP gradient cannot determine the direction of transport of these chimeric proteins.

Wild-type Nmd3 is released from ribosomes by the cytoplasmic GTPase Lsg1 (Hedges et al., 2005) and not by hydrolysis of GTP on Ran. Expression of the dominant-negative *LSG1(K349T)* mutant traps wild-type Nmd3 on cytoplasmic 60S ribosomes (Hedges et al., 2005). I tested if this mutant could also trap the chimeric receptors in the cytoplasm. Since the Mex67-Nmd3Δ100 and Nmd3Δ100-Los1 fusion proteins were localized in both the nucleus and the cytoplasm with nuclear envelope decoration, their mislocalization could not be easily detected. Consequently, I took advantage of the nuclear localization of Nmd3Δ100-Msn5. The localization of Nmd3Δ100-MSN5 was monitored in conditions where *LSG1* or *LSG1(K349T)* was overexpressed. Whereas 32$\pm$3% of cells showed cytoplasmic localization of Nmd3Δ100-Msn5 before expression of the dominant-negative *LSG1* (Fig 3.11, lower panel, *LSG1(K349T)* Raf) after 2 hr of induction in galactose, the fraction of cells showing cytoplasmic Nmd3Δ100-Msn5 rose to 89$\pm$1% (Fig 3.11, lower panel, *LSG1(K349T)* Gal). As a control, I observed similar results with *nmd3(AAA)*, a mutant version of Nmd3 that displays a nuclear bias (Hedges et al., 2005). Thus, the chimeric Nmd3Δ100-Msn5 protein, and likely the other chimeric proteins as well, require functional Lsg1 for their release in the cytoplasm.

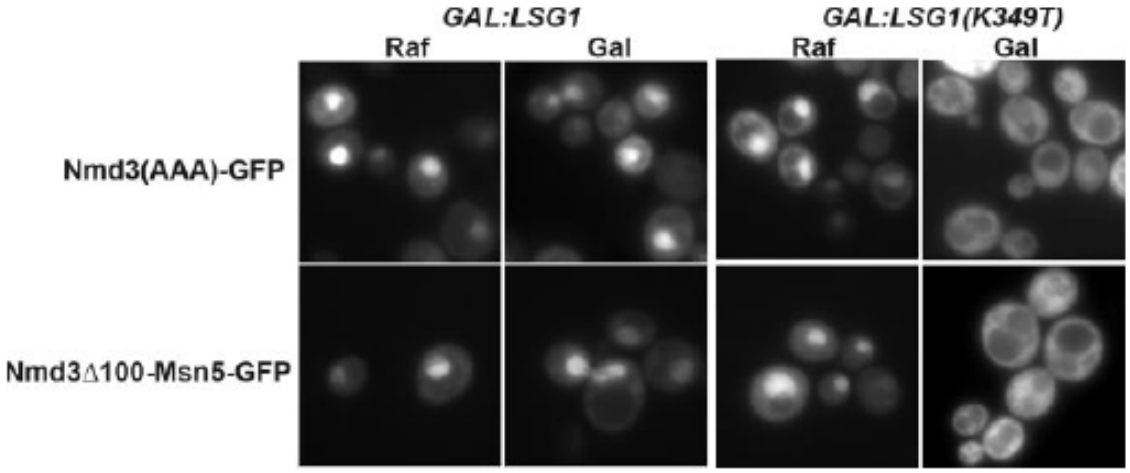

Figure 3.11 Release of the chimeric Nmd3Δ100-Msn5 fusion protein from the ribosome in the cytoplasm requires the GTPase Lsg1.

AJY734 (*nmd3-4*) with pAJ758 (*nmd3AAA-GFP*) or pAJ2078 (*nmd3*Δ*-MSN5-GFP*) were grown in raffinose-containing medium to early log phase at 30°C. Either wild-type *LSG1* (pAJ1121) or dominant-negative mutant *LSG1(K349T)* (pAJ1129) was over expressed by adding 1% galactose. The cultures were then shifted to 37°C for another 2 hrs.

3.3.6 The ribosome can carry an NES in *cis*

Nmd3 is an adapter protein that supplies the NES to bridge the interaction between the 60S subunit and Crm1. The advantage of using an adapter to direct 60S export may be better regulation of export. However, it seems more economical to use an NES *in cis*. The question addressed in this subaim is whether or not the NES can be provided *in cis* by a ribosomal protein.

The NES from Nmd3 was fused to the C-terminus of Rpl3, Rpl8B, Rpl11B, Rpl12B, Rpl25 and Rpl32. These proteins are dispersed around the subunit (Fig 3.12A). These NES-fusion rproteins were tested for complementation of growth in AJY1950. This strain is very sensitive for assaying enhanced 60S export because it is deleted for the export receptor Arx1 and contains an export-defective *NMD3* (*nmd*3Δ14). The double mutant is lethal unless export function is provided by another gene that supports 60S export, like *ARX1*, *NMD3*, or possibly an *RPL*-NES fusion. Among the proteins that I tested, the Rpl3-NES construct gave the strongest complementation (Fig 3.12B). Rpl25 and Rpl12B complemented less well, and Rpl11B was only slightly better than empty vector (Fig 3.12B and data not shown). Other fusions showed no difference from an empty vector control (data not shown). To provide evidence that the *RPL*-NES proteins were incorporated into subunits, extracts of cells expressing Rpl3-NES and Rpl12B-NES were fractionated through sucrose density gradients. Western blotting using Nmd3-specific antibody, which can recognize specifically the NES motif, was performed to detect the distribution of Rpl-NES proteins. The majority of Nmd3 cosedimented with free 60S subunits (Fig 3.12C). For the Rpl-NES proteins, the signals could be detected in 60S, 80S and polysome fractions, demonstrating fusion protein incorporation into the large ribosomal subunit. In addition, complementation of *arx1*Δ *nmd3*Δ*C14* required a functional NES on Rpl3. RPL3 alone or with mutant NES could not support the growth of *arx1*Δ *nmd3*Δ*C14* mutants, although Rpl3 with either a functional or mutant NES complemented an rpl3Δ mutant (Fig 3.13B). Thus, all the Rpl3 constructs were functional for Rpl3 function, but only the fusion of a functional NES could provide export functionality.

To ask more directly if the Rpl3-NES fusion supported export, I assayed Rpl25-GFP localization in cells expressing the Rpl3-NES construct. In this analysis, an empty vector control could not be used because of lethality. Consequently, I used the strain with *RPL12B*-NES, which complemented poorly for a basal level of export. This strain showed a severe 60S export defect (Fig 3.12D). The *RPL3*-NES construct, which showed the strongest complementation of *arx1 nmd3*Δ*C14* among the rprotein fusions also partially rescued the block of 60S export. In the presence of *NMD3* or *ARX1*, only 10% to 20% of cells showed nuclear accumulation of Rpl25-GFP, indicating relatively efficient export. On the other hand, the strain with *RPL3*-NES showed that 30-40% of cells had Rpl25-GFP trapped in the nucleus (Fig 3.12D), whereas in the Rpl12B-NES fusion, the majority of the cells retained Rpl25-GFP in the nucleus. These results show that the NES sequence can be supplied *in cis* on the ribosome and is not necessarily required *in trans* on a ribosome-associated factor.

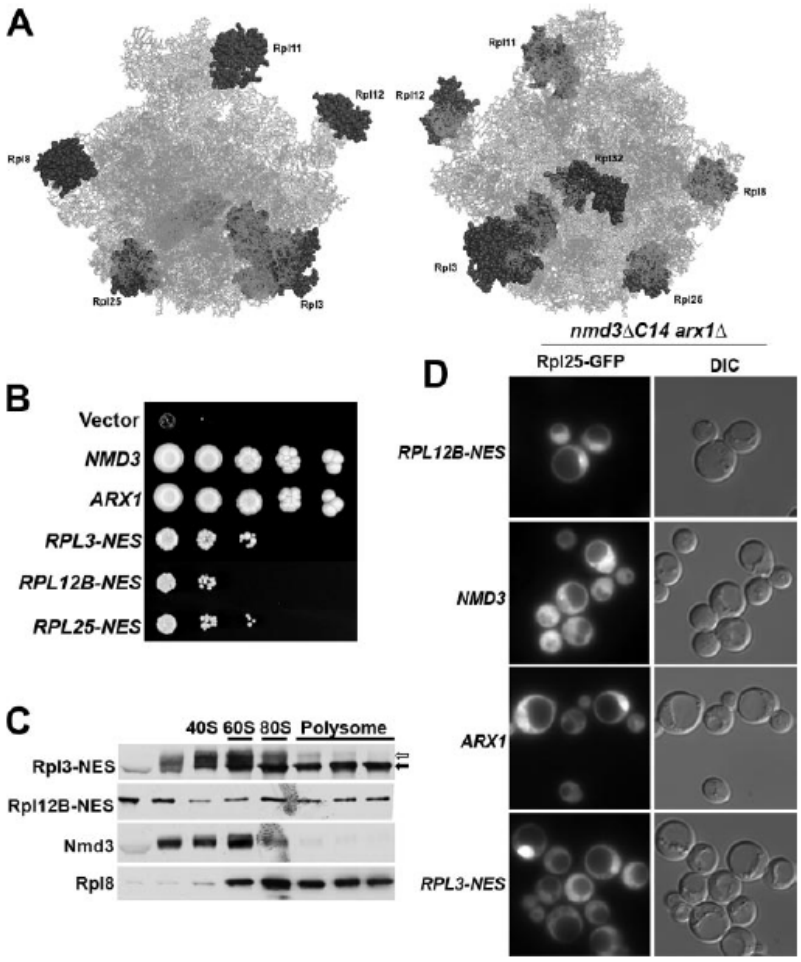

Figure 3.12 An NES added to the ribosome in cis bypasses an *nmd3* mutant defect

(A) Cartoon of the 60S subunit showing the positions of six ribosomal proteins to which NESs were fused. (B) Ten-fold serial dilutions of cultures of AJY1950 with vector, *NMD3* (pAJ123), *ARX1* (pAJ1032), *RPL3-NES* (pAJ2089), *RPL12B-NES* (pAJ2091), and *RPL25-NES* (pAJ2094) on 5FOA plates and incubated at 30°C for 6 days. (C) Rpl3-NES (pAJ2089) and Rpl12b-NES (pAJ2091) were expressed in AJY1950 and their co-sedimentation with ribosomes was analyzed using sucrose gradients. The NES fusions were detected by Western blotting using an antibody against Nmd3 that is specific for the NES of Nmd3. The distributions of Rpl8 and Nmd3 are shown for comparison. (D) The localization of Rpl25eGFP were detected in AJY1950 containing *RPL12B-NES* (pAJ2091), *NMD3* (pAJ123), *ARX1* (pAJ1032), or *RPL3-NES* (pAJ2089).

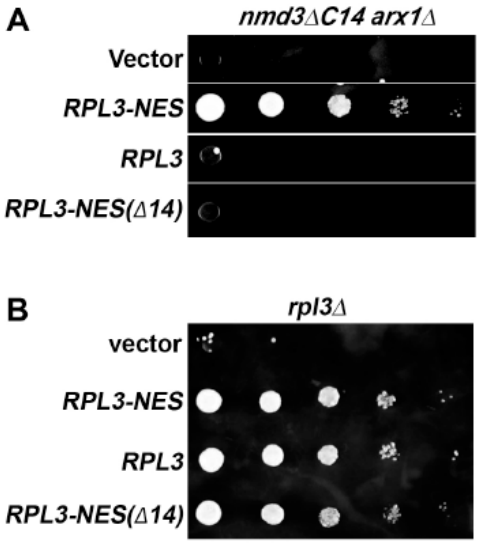

Figure 3.13 Only Rpl3 with a functional NES supports 60S export.

A. AJY1950 with vector, pAJ2289 (*RPL3-NES LEU2*), pAJ2221 (*RPL3 LEU2*), and pAJ2456 (*RPL3-NES(Δ14)*) were spotted on the 5FOA plate. B. Ten-fold dilutions of AJY3053 (*rpl3*Δ) with pAJ2289, pAJ2221, and pAJ2456 were spotted on the 5FOA plate.

3.4 Discussion

Overexpression of Mex67 restored the growth of an *nmd3* export mutant

My results have shown that overexpression of the mRNA export factor Mex67 can restore growth of a cell in which the 60S export adapter Nmd3 has been deleted of its Crm1-dependent NES. When *MEX67* was identified as a high-copy suppressor of mutant *nmd3* (Ho et al., 2000b), it was thought that this might be from an indirect effect, i.e., increasing mRNA stability or increasing mRNA export to enhance translation. However, when 2μ *MEX67* supported the growth of *nmd3*ΔNES, but not *nmd3*Δ or *nmd*3ΔNLS, it suggested that *MEX67* is directly involved in ribosome export.

The improved growth rate correlated with a modest improvement in polysome profiles, and a modest increase in 60S export, monitored by Rpl25-GFP. These results suggest that Mex67 is a limiting factor for 60S export. The Mex67/Mtr2 heterodimer has recently been described as an essential export receptor that works in parallel with Crm1 (Yao et al., 2007). In contrast to published results in (Yao et al., 2007), the relocalization of Nmd3 NES export mutants upon overexpresion of MEX67 was not observed. I also could not detect an improved subunit ratio.

More than one receptor is required for efficient 60S export

Translocation of hydrophilic cargo molecules through the hydrophobic channel of the NPC requires receptors to partition into such an environment. Whereas relatively small cargo molecules accomplish this with single receptors, it has been speculated that large cargo molecules require multiple receptors (Ribbeck and Gorlich, 2001). This has been experimentally demonstrated for protein import in HeLa cells, where a dimeric maltose-binding protein containing a single import receptor was not efficiently translocated. On the other hand, the addition of a second import receptor synergistically stimulated import (Ribbeck and Gorlich, 2001). The 60S ribosomal subunit may be the bulkiest cargo to pass through the NPC. In addition, it is highly electro-negative, due to the large amount of RNA on the surface of the subunit. Thus, the 60S subunit is likely to require multiple receptors for translocation. The current evidence suggests that Nmd3, Arx1, and Mex67 are distributed over the surface of the large subunit. Preliminary results

suggest that Arx1 binds in the vicinity of the exit tunnel (Hung and Johnson, 2006), whereas Nmd3 appears to bind to the joining surface on the opposite face of the subunit (Bussiere, Sengupta, Johnson and Frank, unpublished) and Mex67 binds at 5S rRNA (Yao et al., 2007). This distribution may allow the entire surface of the ribosome to partition into the NPC.

Is there specificity for receptors in the 60S export pathway?

Except for Nmd3/Crm1, Arx1 and Mex67 do not have conserved functions in 60S export in higher eukaryotic cells (Bradatsch et al., 2007; Hung et al., 2008; Yao et al., 2007). This suggests that the ribosome export pathway might be very flexible. To test this idea, I tried to replace Crm1 by fusing different receptors with an Nmd3ΔNES truncation mutant to determine if these chimeric receptors could mediate 60S export. There are four importin β-like export receptors in yeast: Crm1, Los1, Cse1, and Msn5. Except for Crm1, each of them was fused to an Nmd3 NES mutant and tested for their ability to complement an *nmd3* temperature-sensitive mutant. Surprisingly, these chimeric proteins all complemented Crm1 function in 60S export, but to different degrees. This suggested that any export karyopherin, if recruited to the 60S subunit, can support 60S export. Similarly, it has been shown that the Rev-dependent export of genomic RNA of HIV viruse can be transported independently of Rev and Crm1 by tethering of other receptors. It may be not surprising that the 60S can be transported through the NPC by receptors recruited from other pathways, but it is striking that this transport works in vivo. In the case of the chimeric fusion proteins used here, the loading of receptor is controlled by Nmd3, but the receptor and nucleoporin binding preferences are totally changed. In conclusion, the number of karyopherins binding on the cargo seems more crucial than which type of karyopherin is employed.

Do the multiple receptors have to be different?

In the Mex67-Nmd3Δ100 fusion case, if multiple receptors can work, why have cells evolved different receptors in ribosome export? One simple explanation is to avoid competition between receptors for common binding sites. It is also possible that the

utilization of different export receptors represents cross talk between different cellular export pathways. The translational capacity of a cell is determined by its ribosome content. mRNA export may be regulated in response to translation capacity. Lastly, different receptors may provide a complex mechanism of regulation at the level of ribosome export.

Reasons for inefficient export by chimeric receptors and Rpl-NES fusions

Several explanations could account for the fact that the receptor-fusion proteins did not provide wild-type efficiency. The fusion of Nmd3Δ100 on the receptors might partially impair the interaction between the receptor and the NPC. Or, these chimeric receptors may cause defects at the Nmd3 biogenesis step. It is also possible that the ribosomal subunits in the novel export pathways compete for the nucleoporin-binding sites with the native substrates of these receptors.

Although the fusion of an NES to several ribosomal proteins supported 60S export, it should be noted that none of the Rpl-NES fusions worked efficiently. Various explanations could account for the relatively weak function of the NES fusions to ribosomal proteins. The fusion protein must assemble into the subunit and not drive premature export of the pre-60S. The NES must be accessible to Crm1 once on the subunit. In addition, the position of the NES on the subunit may be important. Preliminary results suggest that Nmd3 binds to the joining face of the large subunit (Sengupta, Bussiere, Johnson, and Frank, unpublished). Efficient export may require recruitment of a receptor to this large RNA surface to facilitate partitioning the ribosome into the hydrophobic channel of the NPC. As the joining face of the large subunit is highly constrained by its requirement to engage properly with the small subunit, the evolution of a trans-acting factor on this surface may have been favored over the acquisition of an NES on a ribosomal protein in the subunit interface.

CHAPTER 4

Assembly of the ribosome stalk requires the dual specificity phosphatase Yvh1 for the exchange of Mrt4 with P0

4.1 Introduction

A recent genome-wide screen for protein-protein interactions in yeast identified the dual phosphatase Yvh1 as a potential interactor for Lsg1, Tif6 and Rei1 (Tarassov et al., 2008). These factors are all involved in late steps of 60S biogenesis, suggesting that Yvh1 is also involved in this pathway. This initiated my interest to further characterize Yvh1 potential function in the 60S biogenesis pathway. In this study, I identified Yvh1 as the release factor for Mrt4, a nuclear paralog of the essential ribosomal stalk protein P0. Deletion of *YVH1* relocalizes Mrt4 to the cytoplasm and causes the persistence of Mrt4 on 60S subunits. A mutation in Mrt4 at the protein/RNA interface significantly weakens the affinity of Mrt4 for the ribosome, and thereby bypasses the requirement for Yvh1. Yvh1 shuttles, and pre-60S subunits associated with Yvh1 contain Rpl12, but lack both Mrt4 and P0. Furthermore, deletion of Rpl12 abolishes Yvh1 binding to 60S subunits. These results suggest a linear series of events in which Yvh1 binds to Rpl12 and displaces Mrt4 in the nucleus. Once in the cytoplasm P0 loads onto the subunit to assemble the mature stalk and Yvh1 is released. The release of Mrt4 by Yvh1 controls Rpp0 loading and stalk formation on the 60S subunits. The initial interaction of the subunit with Mrt4 may ensure that translation factors do not precociously associate with the pre-60S subunit during assembly, and provides functional compartmentalization of ribosome assembly as well as spatial separation afforded by the nuclear envelope.

4.2 Background

Ribosome maturation is a complicated process. rRNA is transcribed in the nucleolus by RNA polymerases I and III. The ribosomal proteins and numerous trans-acting factors are needed to process and modify the rRNAs as they are assembled into

ribosomal subunits. After the ribosomes mature to a certain stage, various factors enable their transport to the cytoplasm where they undergo further maturation steps leading to translationally competent ribosomes.

During ribosome biogenesis, the paralogs of several mature ribosomal proteins are initially incorporated into the subunits as trans-acting factors to assist the ribosome assembly process. Thereafter, the proteins are replaced by their mature ribosomal protein counterparts. These paralogs usually share conserved ribosome-binding motifs. This is the case for Rpl24 and its paralog, Rlp24. The loading of Rlp24 happens in the nucleolus and is required for 27S rRNA processing (Saveanu et al., 2003). Rlp24 is exported out of the nucleus on the 60S subunit, and is released in the cytoplasm by the ATPase Drg1 (Pertschy et al., 2007). Rpl24 binds the large subunit in the cytoplasm after release of Rlp24 and acts as a protein component of the mature 60S ribosome. Similarly, ribosomes are first assembled with Mrt4, which is subsequently replaced by the essential ribosomal protein P0 during assembly of the stalk. Here, I report that Yvh1 is required for the release of Mrt4 to allow the assembly of P0 in the subunit.

Yvh1 was identified as a dual-specificity phosphatase, which can recognize both phosphoserine/phosphothreonine and phosphotyrosine (Guan et al., 1992). Yvh1 is a highly conserved protein. The human ortholog of Yvh1 is able to complement the phenotype of a Yvh1 deletion in S. *cerevisiae* (Muda et al., 1999). In budding yeast, a *yvh1* deletion is slow growing and shows a sporulation defect (Park et al., 1996). Yvh1 has a conserved N-terminal phosphatase domain and a C-terminal zinc-binding domain. Yeast Yvh1 interacts with Nop7, an early ribosomal biogenesis factor, via its N-terminal domain (Sakumoto et al., 2001), suggesting that Yvh1 is involved in ribosome biogenesis.

The ribosomal stalk is required for recruitment of translation factors and is essential for ribosome activity. The stalk is composed of five proteins. Rpp0 (or P0) is a large protein that forms the stalk base. P0 interacts directly with 25S rRNA at the GTPase center. A P1/P2 hetero-tetrameric complex forms the rest of the stalk and binds to the ribosome via P0 (Hanson et al., 2004; Krokowski et al., 2006; Krokowski et al., 2005). P0 is an essential protein, whereas P1 and P2 are non-essential small acidic proteins. In

bacterial ribosomes, L10 and L11, corresponding to eukaryotic P0 and Rpl12, bind cooperatively to helices 43 and 44 in domain II of 23S rRNA (Rosendahl and Douthwaite, 1995). It is likely that in the eukaryotic ribosome P0 and Rpl12 show similar cooperative binding to 25S rRNA as loss of Rpl12 reduces the affinity of P0 for the ribosome (Briones et al., 1998). The C-terminal domain of bacterial L10 interacts with the translation factors IF2, EF-Tu, EF-G and RF3 (Diaconu et al., 2005), and this is likely the critical function of L10 and P0.

Mrt4 localizes to the nucleus with enrichment in the nucleolus. The amino acid sequence of Mrt4 is similar to P0 (Zuk et al., 1999). Their N-terminal domains are conserved. However, P0 has an extended C-terminus not present in Mrt4, and Mrt4 has a short extension at its extreme N-terminus, which contains a potential NLS. Mrt4 is observed in the 66S ribosome complex, but not on the mature 60S subunits (Collins et al., 2007; Gavin et al., 2006). These results suggest that Mrt4 binds ribosomes at an early stage of assembly in the nucleolus. On the contrary, P0 is cytoplasmic and is present in mature 60S subunits (Hanson et al., 2004). Based on these findings, Mrt4 is assumed to be the nuclear paralog of P0 (Rodriguez-Mateos et al., 2009) which exchanges for P0 during assembly. The mechanism for Mrt4 release to allow the assembly of P0 is not known.

4.3 Results

4.3.1 Yvh1 is required for ribosome biogenesis

YVH1 was recently identified as a new 60S biogenesis factor (Liu and Chang, 2008). In a protein complementation assay, Yvh1 showed interaction with several transacting factors, Tif6, Lsg1 and Rei1 (Tarassov et al., 2008). Also, Yvh1 interacts with the nucleolar 60S biogenesis factor Nop7 in a yeast two-hybrid assay (Sakumoto et al., 2001). However, the actual function of Yvh1 in 60S biogenesis is unknown.

To further characterize Yvh1 function, rRNA processing was monitored by Northern blotting, comparing pre-rRNA species from wild-type and *yvh1*Δ cells. Compared to wild type, *yvh1*Δ cells showed accumulation of 35S, 27S and 23S rRNAs, depletion of 25S, and no significant change in 20S, 18S, and small rRNAs (Fig 4.1).

*yvh1*Δ cells harbor an imbalance of 40S and 60S subunits (Fig 4.2A) to yield halfmers, which are the result of 60S deficiency and represent unbound 48S translation initiation complexes on mRNAs [data not shown and (Liu and Chang, 2008)]. Also, deletion of *YVH1* blocked 60S subunit export [data not shown and (Liu and Chang, 2008)]. These results suggest that Yvh1 function is required for 60S synthesis.

Yvh1 has a phosphatase domain at its N-terminus and a Zn^{2+} binding domain at its C-terminus (Fig 4.2B). To determine which domain(s) of Yvh1 is necessary and sufficient for its function in 60S biogenesis, mutants were constructed (Figure 4.2B). Consistent with previous results, mutation of a conserved residue in the phosphatase domain (yvh1C117S), or truncation of the N-terminal domain (yvh1ΔN), complemented a yvh1 deletion and restored growth comparable to wild type [data not shown and (Liu and Chang, 2008)]. In contrast, the zinc-binding domain deletion mutant (yvh1ΔC) did not complement a *yvh1* deletion [data not shown and (Liu and Chang, 2008)]. Polysome profiles revealed *yvhC117S* and *yvh1*Δ*N* to have wild-type profiles, whereas *yvh1*Δ*C* had severely reduced 60S levels [data not shown and (Liu and Chang, 2008)]. These results clearly link the growth defect of *yvh1* mutants to a 60S biogenesis defect.

The growth defects observed in these mutants could be due to a lesser affinity of the Yvh1 mutants for 60S. A sucrose cushion assay was used to analyze the ribosome binding capabilities of different Yvh1 mutants. Both wild-type Yvh1 and Yvh1C117S cosedimented with 60S. However, only 30% of Yvh1ΔN cosedimented with 60S (Fig 4.2 C). This result was inconsistent with the data published previously (Liu and Chang, 2008) where, in a sucrose gradient, Yvh1ΔN was solely observed with the 60S peak. The difference might be due to the more stringent conditions used in the cushion assay. In contrast to the N-terminal mutants, Yvh1ΔC did not bind to 60S (Fig 4.2 C). Taken together, these observations indicate that the C-terminal domain of Yvh1 is necessary for interaction with the 60S subunit. Thus, the putative N-terminal phosphatase domain of Yvh1 does not provide the primary function of Yvh1.

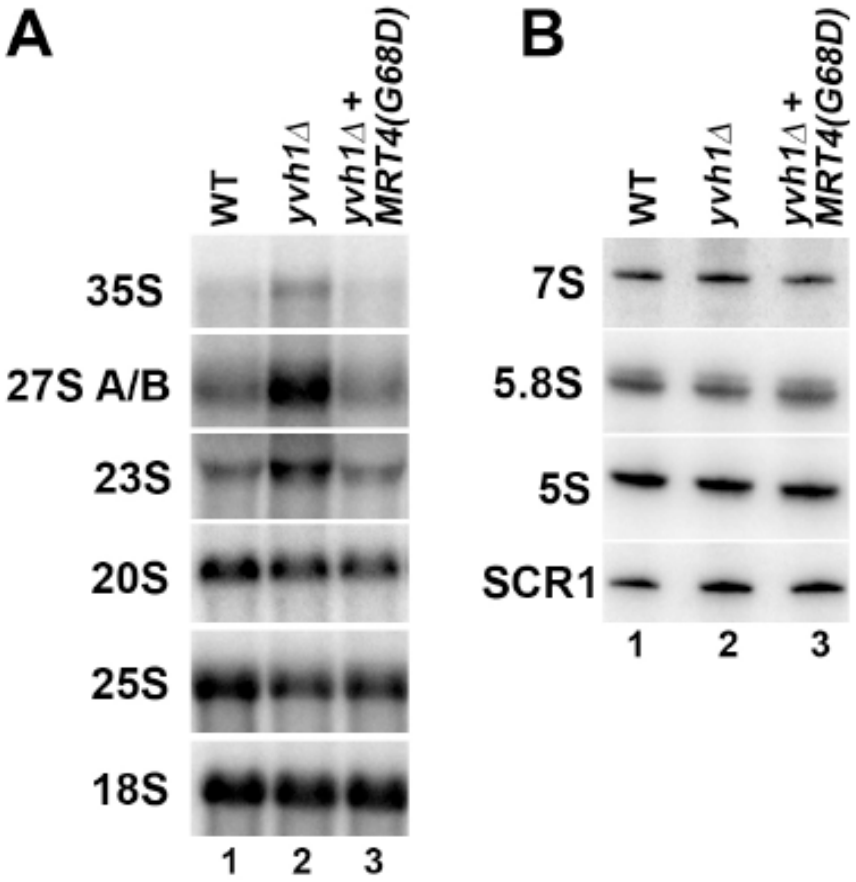

Figure 4.1 Northern blot analysis of rRNA processing intermediates.

BY4741 (wild-type, WT), AJY2976 (*yvh1*Δ) with empty vector or pAJ2461 (MRT4G68D) were cultured at 30°C until early log phase. Total RNA was prepared, and the various rRNAs and processing intermediates were detected by Northern blotting using P^{32}-labeled oligonucleotides.

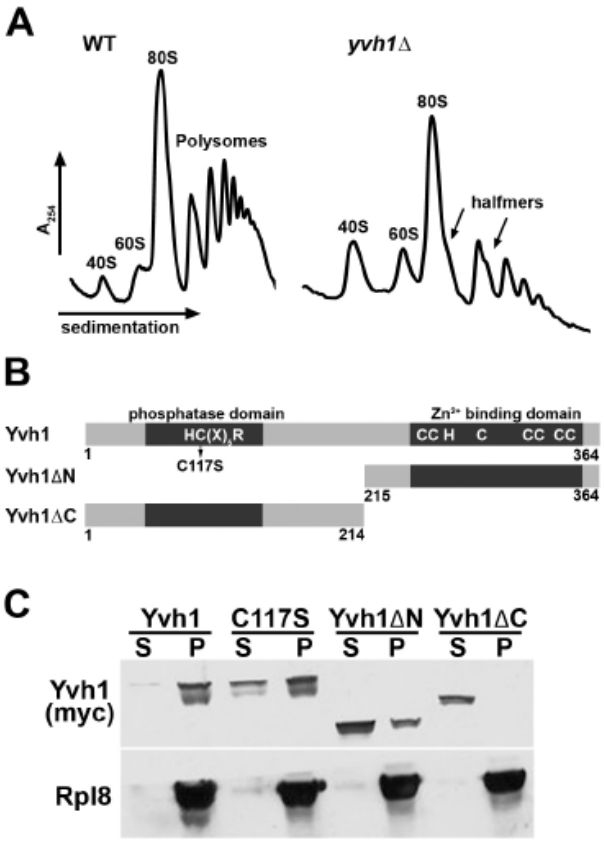

Figure 4.2 The Dual-specificity phosphatase Yvh1 is a ribosome biogenesis factor and its C-terminal domain is crucial for 60S interaction.

(**A**) Extracts were prepared from wild-type (BY4741) and *yvh1*Δ (AJY2976) cells and fractionated by sedimentation through 7-47% sucrose density gradients as described in Materials and Methods. (**B**) Cartoon of Yvh1 and various mutant constructs. Dark bars indicate the conserved phosphatase and zinc-binding domains. Numbers indicate amino acid positions. (**C**) Protein extracts were prepared from AJY2976 (*yvh1*Δ) with pAJ2020 (Yvh1-myc), pAJ2024 (Yvh1-C117S-myc), pAJ2025 (Yvh1ΔN-myc) and pAJ2026 (Yvh1ΔC-myc) and overlayed on 1M sucrose cushions. Samples were centrifuged at 80,000 rpm for 60 min at 4°C in a Beckman TLA100 rotor to separate free protein and ribosome particles. Equal amounts of supernatant (S) and pellet (P) fractions were separated by SDS-PAGE, and Western blots were performed using c-myc (Yvh1) and Rpl8-specific antibodies.

4.3.2 RPL12 is a high copy suppressor of yvh1Δ

To better understand the function of Yvh1, a screen for high copy suppressors of yvh1Δ was conducted. (This screen was carried out by a rotation student, Feng Wang, under my supervision.) RPL12B was identified as a suppressor of yvh1Δ (Fig 4.3A). Previous studies suggested that Yvh1 is involved in other pathways besides ribosome biogenesis (Beeser and Cooper, 2000; Hanaoka et al., 2005; Liu and Chang, 2008; Park et al., 1996; Sakumoto et al., 2001). Thus, this suppressor was tested specifically for complementation of Yvh1 function in 60S biogenesis. Extracts prepared from yvh1Δ cells with vector or high copy RPL12 were separated on 7% to 47% sucrose density gradients. As expected, the vector control showed halfmers. Increasing the copy number of RPL12B modestly improved the polysomes and, surprisingly, reduced the levels of free 60S (Fig 4.3B). This result implies that increasing the levels of Rpl12B enhances the utilization of free 60S subunits in the cytoplasm.

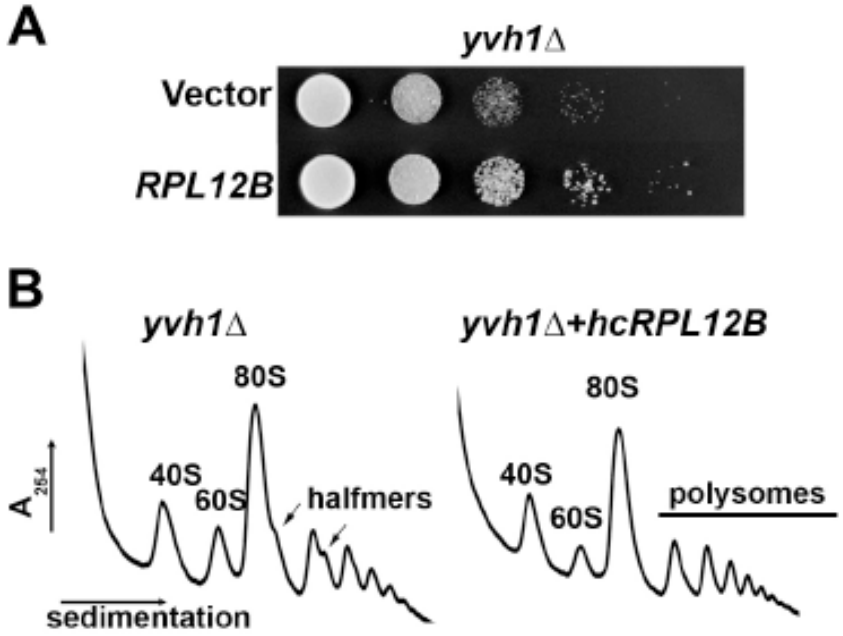

Figure 4.3 RPL12B is a high copy suppressor of *yvh1*Δ.

(**A**) Serial ten fold dilutions of AJY2976 (*yvh1*Δ) with vector or pAJ2458 (2μ RPL12B) were spotted onto Ura dropout medium and incubated at 30°C for 2 days. (**B**) Extracts from AJY2976 (*yvh1*Δ) with vector or pAJ2458 were fractioned on sucrose gradients as described in the legend to Figure 1.

4.3.3 Yvh1 is required to release Mrt4

Yeast Rpl12 corresponds to bacterial L11 which, together with L10, form the base of the stalk (Diaconu et al., 2005; Gonzalo and Reboud, 2003). The binding of L11 and L10 to domain II of 23S rRNA is cooperative (Rosendahl and Douthwaite, 1995). This interaction between bacterial L11 and L10 led me to consider if high copy suppression of yvh1Δ by RPL12B was the result of a defect in stalk assembly in the yvh1 mutant. I tested if P0 was also a high copy suppressor of yvh1Δ, however, it was not (data not shown).

Mrt4, a highly conserved protein in eukaryotes, is closely related to P0 in sequence (Fig 4.4). Sequence alignment and the atomic structure of bacterial stalk base (Kavran and Steitz, 2007) indicate that the conserved N-terminal domain of P0 and Mrt4 is responsible for RNA binding. Additionally, Mrt4 and P0 bind to the 60S subunit in a mutually exclusive fashion (Rodriguez-Mateos et al., 2009), further supporting the notion that the two proteins bind to the same site on the ribosome. However, these two proteins localize in distinct compartments: Mrt4 shows nuclear and nucleolar localization while P0 shows predominantly a cytoplasmic signal. Furthermore, Mrt4 is only on the nascent 60S subunits; P0 is a component in the mature ribosome. Mrt4 is suggested to be assembled into the ribosome during early assembly and is later replaced by P0 (Rodriguez-Mateos et al., 2009).

MRT4(G68D) is a dominant suppressor of yvh1Δ (Satya Nugroho, 2003). The links between Yvh1, Mrt4 and Rpl12 hint at Yvh1 playing a role in the formation of the stalk. I considered that Yvh1 is required to release Mrt4. This would predict that in the absence of Yvh1, Mrt4 would fail to be released and remain on subunits in the cytoplasm. To explore this possibility, the localization of Mrt4 was detected in wild-type versus *yvh1*Δ cells. In wild type, Mrt4 was localized in the nucleus with nucleolus enhancement. Surprisingly, in the *yvh1* deletion strain, Mrt4 was mislocalized to the cytoplasm (Fig 4.5A). However, Nop7, the N-terminal interaction factor of Yvh1, Nog1, and Rlp24, maintained nuclear and nucleolar localization (data not shown). This implies that the mislocalization of Mrt4 is not from an indirect defect of loss of nuclear integrity, but that Yvh1 is specifically required for Mrt4 recycling.

To test if the 60S binding or the phosphatase activity of Yvh1 is required for Mrt4 release, I monitored Mrt4 localization in the different *yvh1* mutants. While Mrt4 localization was restored in *yvh1*Δ*N* and *yvh1(C117S)*, mutants which complement the slow growth phenotype of *yvh1*Δ, Mrt4 was still mislocalized in *yvh1*Δ*C* cells (Fig 4.5B). This result strongly connected the growth phenotype of yvh1Δ cells and Mrt4 mislocalization. The slow growth and 60S biogenesis defects of yvh1Δ may result from a failure to recycle Mrt4 to the nucleus to support nascent 60S subunits assembly or from a failure to release Mrt4 and load P0, or both.

To know whether mislocalized Mrt4 remains bound to the large subunit, indicating a failure in its release, or if it is off the subunit, indicating a failure in reimport of Mrt4, Mrt4 sedimentation pattern was analyzed across a sucrose gradient. Mrt4 cosedimented exclusively at the 60S peak in wild-type cells (Fig 4.5C), consistent with its function as a trans-acting factor of the large subunits. In *yvh1*Δ cells, Mrt4 sedimentation pattern did not change (Fig 4.5C), suggesting that Mrt4 persists on the 60S subunits in the cytoplasm in the absence of Yvh1.

Rlp24, Nmd3 and Lsg1 are trans-acting factors in 60S ribosome biogenesis. Rlp24 and Nmd3 shuttle, but their steady state distributions are primarily nuclear and cytoplasmic, respectively. On the other hand, Lsg1 is restricted to the cytoplasm. To gain further evidence that Mrt4 remained on subunits in the cytoplasm in *yvh1*Δ cells, I determined whether altered levels of Mrt4 on Rlp24, Nmd3 and Lsg1-bound complexes could be detected. As shown in Fig 4.5D, Mrt4 was depleted from the Rlp24 complex, but accumulated in Nmd3 and Lsg1 immunoprecipitated complexes in a *yvh1*Δ mutant. Thus, in the absence of Yvh1, Mrt4 is not efficiently released from the subunit and mislocalizes to the cytoplasm.

Altogether, these results suggest that Mrt4 cannot be released properly from 60S subunits in *yvh1*Δ cells. In other words, Yvh1 is a release factor of Mrt4.

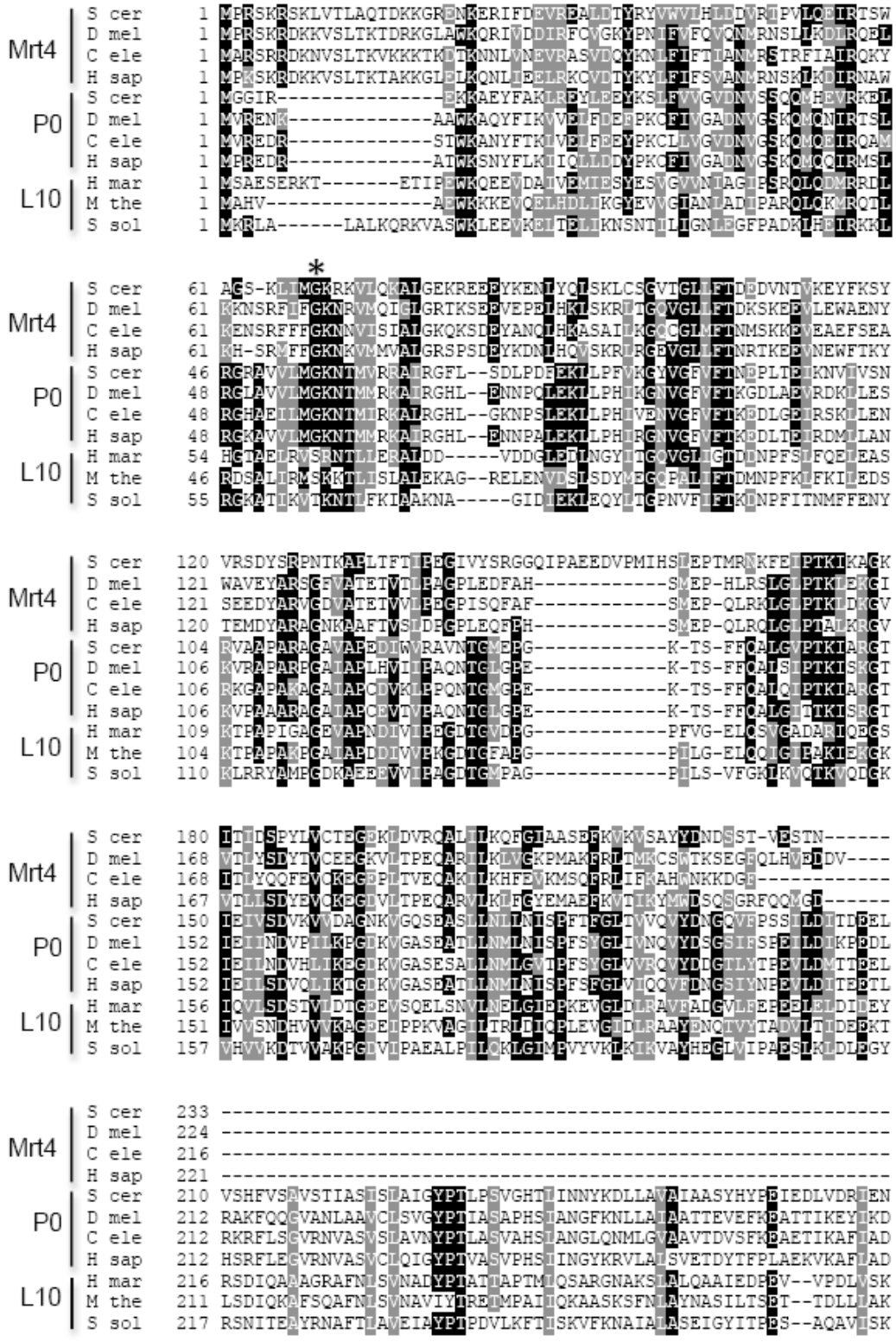
Mrt4
P0
L10
S cer
D mel
C ele
H sap
H mar
M the
S sol

Figure 4.4 Multiple sequences alignment of Mrt4, P0 and L10.

Multiple sequence alignment was performed on the amino acid sequences of Mrt4, P0, and L10 from different organisms indicated on the figure using ClustalW and BoxShade (S cer: *Saccharomyces cerevisiae*, D mel: *Drosophila melanogaster*, C ele: *Caenorhabditis elegans*, H sap: *Homo sapiens*, H mar: *Haloarcula marismortui*, M the: *Methanothermobacter thermautotrophicus*, S sol: *Sulfolobus solfataricus*). The position of Glycine 68 has been indicated with an asterisk (*).

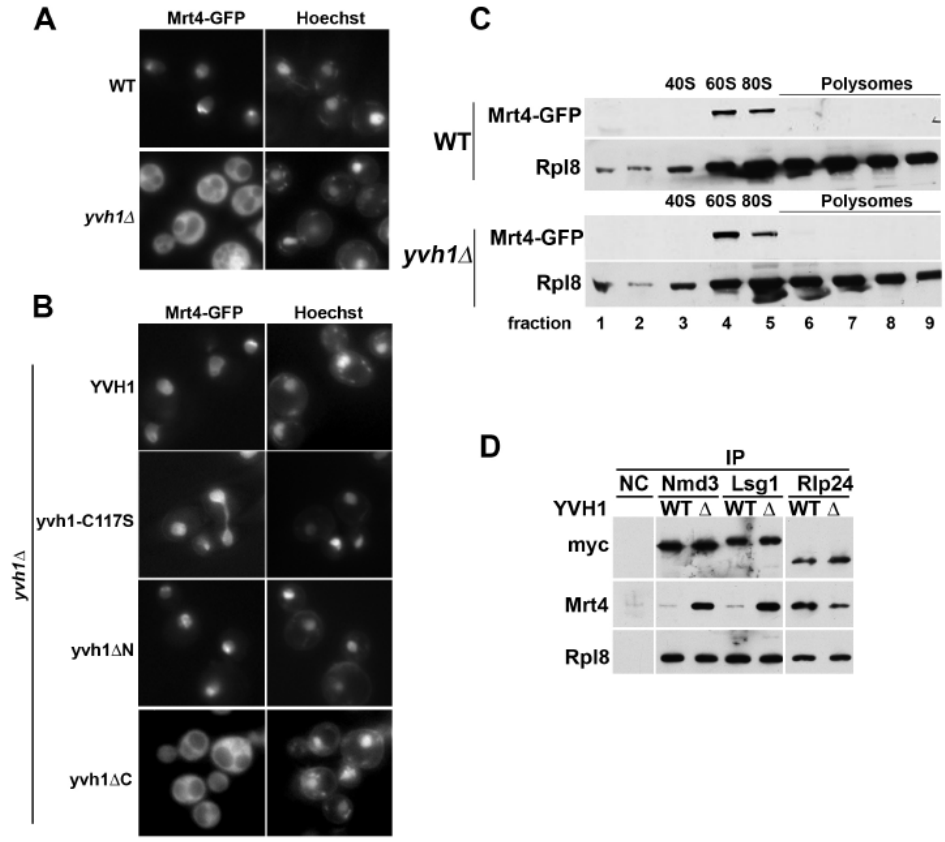

Figure 4.5 Mrt4 persists on cytoplasmic ribosomes in the absence of Yvh1.

(**A**) The localization of genomic Mrt4-GFP was visualized in AJY3040 (MRT4-GFP) and AJY3048 (MRT4-GFP *yvh1*Δ). DNA was stained with Hoechst 33342 (**B**) Localization of Mrt4-GFP in various *yvh1* mutants: AJY3048 with pAJ2020 (Yvh1), pAJ2024 (Yvh1-C117S), pAJ2025 (Yvh1ΔN) or pAJ2026 (Yvh1ΔC). (**C**) Extracts of AJY3040 (MRT4-GFP) and AJY3048 (MRT4-GFP *yvh1*Δ) were fractioned on 7% to 47% sucrose gradients. Fractions were precipitated with TCA, separated by SDS-PAGE, and the presence of Mrt4, P0, Rpl12 and Rpl8 across the gradients was detected by Western blotting. (**D**) Immunoprecipitation and Western blotting was used to detect altered levels of Mrt4 in Rlp24, Nmd3 and Lsg1 complexes from wild-type and *yvh1*Δ cells. Nmd3-myc (pAJ538), Lsg1-myc (pAJ903), and Rlp24-myc (pAJ2020) were immunoprecipitated from AJY3040 and AJY3048. Proteins were separated by SDS-PAGE and detected by Western blotting with myc (bait proteins), GFP (Mrt4), and Rpl8-specific antibodies.

4.3.4 MRT4G68D bypasses the requirement for Yvh1

If the persistence of Mrt4 on the subunit is the reason for the slow growth of *yvh1*Δ cells, elimination of Mrt4 may alleviate the problem. I deleted *MRT4* in *yvh1*Δ cells. As seen in Figure 4.6A, the *mrt4*Δ and *yvh1*Δ single mutants were almost indistinguishable from the *mrt4*Δ *yvh1*Δ double mutant in growth rate.

I also tested the effects of increasing the levels of Mrt4 in *yvh1*Δ cells. Overexpressing Mrt4 could restore the nuclear pool of Mrt4 to support 60S biogenesis. On the other hand if Yvh1 were absolutely required for release of Mrt4, increasing Mrt4 levels would be expected to drive more Mrt4 onto nascent subunits without a mechanism for its release. This would exacerbate the defect of a *yvh1* mutant. In fact, overexpression of MRT4 strongly inhibited cell growth (Fig 4.6B), implying that in the absence of Yvh1, the persistence of Mrt4 on subunits is detrimental. Overexpression of Mrt4 did not cause any dominant negative effects of wild type cells (data not shown).

MRT4(G68D) improved the growth of yvh1Δ strain [Fig 4.6C and (Satya Nugroho, 2003)] and complemented the growth defect of mrt4Δ cells (data not shown). Since the growth defect of yvh1Δ is from the persistence of Mrt4 on the 60S subunits, Mrt4(G68D) may bypass the requirement of Yvh1 for release. Indeed, Mrt4(G68D) was predominantly nuclear in the absence of Yvh1 (Fig 4.6D). Thus, this mutant Mrt4 appears to bypass Yvh1 function while maintaining Mrt4 function.

To further confirm that Mrt4(G68D) suppresses 60S ribosome biogenesis defects of yvh1Δ, the polysome profile of yvh1Δ with Mrt4(G68D) cells was analyzed. Compared to the profile with yvh1Δ cells, yvh1Δ with Mrt4(G68D) did not show halfmers or an imbalance between 40S and 60S subunits and the height of polysome peaks was increased (Fig 4.6E). The rRNA processing defect in yvh1Δ was also rescued by Mrt4(G68D) (Fig 4.1).

Because of the similarity in sequence between Mrt4 and bacterial L10 (Fig 4.4), the Mrt4(G68D) mutation was modeled into the L10 structure of the *Haloarcula* 50S subunit [PDB structure 2QA4 (Kavran and Steitz, 2007)] (Fig 4.7A and B). Gly68 is in a region of Mrt4 that is highly conserved among Mrt4, P0 and bacterial L10 (Fig 4.4). In this structure model, Gly68 is on a loop interacting with 25S rRNA (Fig 5A 5B). The

amino acid change from neutral Gly to Asp may weaken the interaction between Mrt4 and the ribosome subunit because of electrostatic repulsion or distortion of the local structure from introducing a bulkier amino acid. A weakened interaction with the ribosome could allow Mrt4 to bypass the requirement of Yvh1 for release, explaining the mechanism of suppression. Such a suppressing mechanism has been observed previously; mutations in Tif6 weaken its interaction with 60S subunits and bypass the need for the release factors, Sdo1 and Efl1 (Menne et al., 2007; Senger et al., 2001).

To test the idea that Mrt4(G68D) has weaker affinity for large subunits, the binding of Mrt4 and Mrt4(G68D) to 60S subunits was tested by salt titration. At 100 mM NaCl, wild-type Mrt4 and Mrt4(G68D) both stayed on the 60S subunit. However, at 200 mM and 300 mM NaCl, the majority of Mrt4(G68D) was released from the subunit whereas wild-type Mrt4 binding was largely unaffected (Fig 4.7C). Mrt4(G68D) fully complemented the growth defect of an *mrt4*Δ mutant (data not shown). The affinity of this mutant for the ribosome must be finely balanced between binding strongly enough to support ribosome biogenesis and not too strongly so that it does not require Yvh1 for its release.

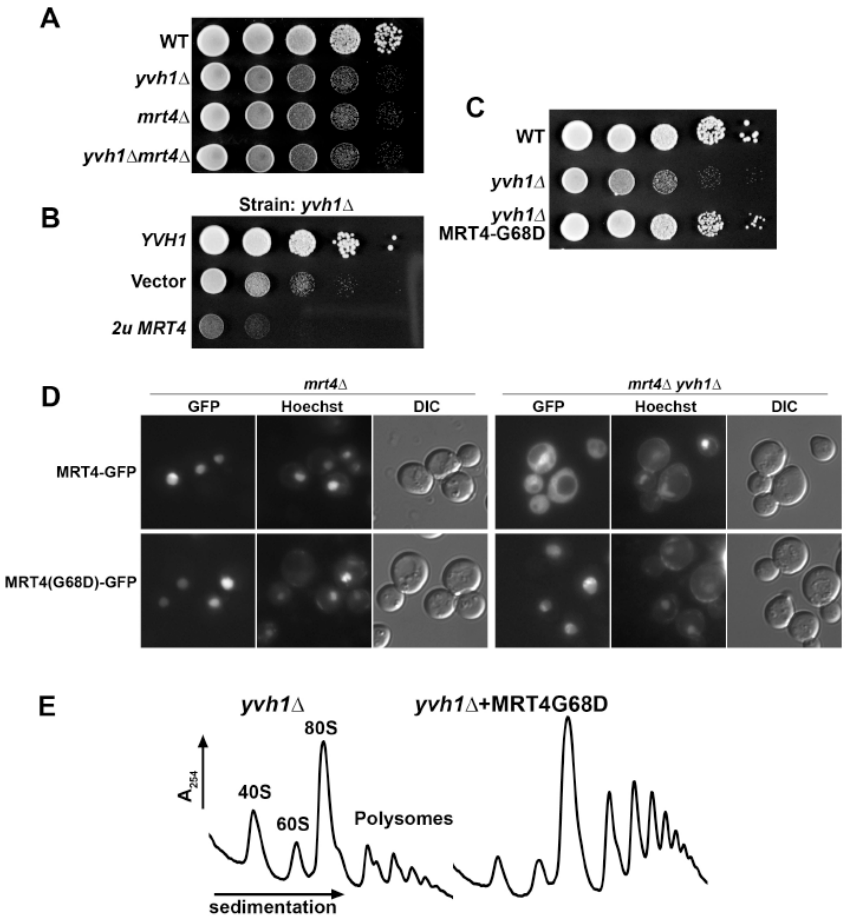

Figure 4.6 Genetic interaction between *MRT4* and *YVH1*.

(**A**) Ten-fold serial dilutions of cultures of BY4741 (wild-type), AJY2976 (*yvh1*Δ), AJY2551 (*mrt4*Δ), and AJY2553 (*yvh1*Δ *mrt4*Δ) were spotted on YPD and incubated at 30°C for 2 days. (**B**) Serial dilutions of AJY2976 (*yvh1*Δ) containing *YVH1*(pAJ2020), vector and 2μ *MRT4* (pAJ2486) were spotted on a Leu drop-out plate and incubated at 30°C for 3 days. (**C**) Serial dilutions of BY4741 and AJY2976 (*yvh1*Δ) with vector or pAJ2461 (MRT4G68D) were spotted onto selective media and incubated at 30°C (**D**) The localization of MRT4-GFP (pAJ2457) and MRT4G68D-GFP (pAJ2461) was visualized in AJY2551 (*mrt4*Δ) and AJY2553 (*mrt4*Δ *yvh1*Δ) cells. DNA was stained with Hoechst; DIC: differential image contrast. (**E**) Polysome profiles of AJY2976 (*yvh1*Δ), AJY2553 with pAJ2461 (MRT4G68D) were analyzed on 7% to 47% sucrose gradients.

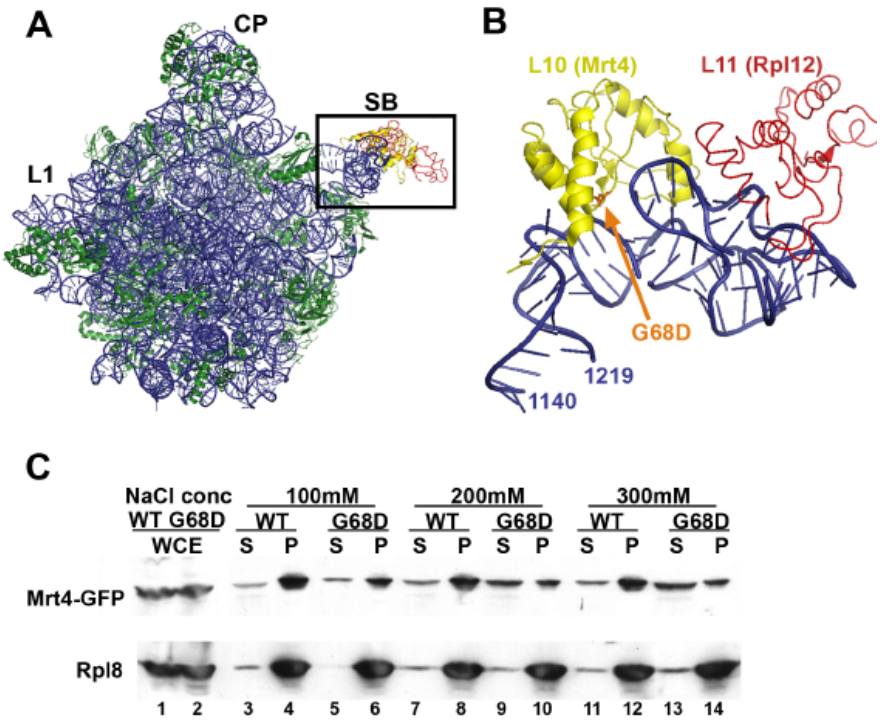

Figure 4.7 G68D introduces an acidic residue at the interface of Mrt4 and 25S rRNA and reduces the affinity of Mrt4 for 60S subunits.

(**A**) Crystal structure of the entire 50S subunit from *Haloarcula marismortui*, adapted from PDB 2QA4 (Kavran and Steitz, 2007). CP: central protuberance; L1: L1 stalk; SB, stalk base. The proteins in yellow and red are L10 and L11 respectively. Rectangle indicates the region magnified in B. (**B**) Enlarged view of the stalk base, looking down from the central protuberance. Yellow: 23S (corresponding to 25S), Blue: rRNA; Red: L11 (corresponding to Rpl12). (The expected position of the G68D mutation in Mrt4 in the context of L10 is indicated in orange.) (**C**) Cell extracts were prepared from AJY2553 (*yvh1*Δ *mrt4*Δ) with MRT4-GFP (pAJ2457) (WT) or MRT4G68D-GFP (pAJ2461) (G68D) at the indicated salt concentrations. Free and ribosome-bound proteins were separated by sedimentation through sucrose cushions. Equal amounts of supernatant (S) and pellet (P) were separated by SDS-PAGE, and the presence of Mrt4 and Rpl8 (as a marker for 60S) were detected by Western blotting using anti-GFP or anti-Rpl8. Lanes 1 and 2: whole cell extracts as loading controls.

4.3.5 Rpl12 is required for Yvh1 binding to the ribosome

Rpl12 is a high-copy suppressor of yvh1Δ (Fig 4.3A). Based on the structure of the archaeal 50S subunit (Fig 4.7A and B), Rpl12 binds to the GTPase-associated domain of 25S rRNA, adjacent to Mrt4 in the pre-60S or P0 in the mature 60S subunit. Rpl12 and P0 form the stalk base. Since Mrt4 is released by Yvh1, but Rpl12 remains in the Yvh1-60S complex (see below), Rpl12 might be required for Yvh1 binding to the 60S subunits. There are two Rpl12 homologues in yeast, Rpl12a and Rpl12b. Deletion of both alleles (rpl12ΔΔ) is viable, but has a very slow growth phenotype. I immunoprecipitated Yvh1 from wild-type and *rpl12*ΔΔ cells. As shown in Fig 4.8A, the majority of Yvh1 was on the 60S subunits in wild type, but, in contrast, Yvh1 totally lost its interaction with 60S subunits in the *rpl12*ΔΔ mutant cells (Fig 4.8A). This shows that Rpl12 is required for Yvh1 binding to the 60S subunit and suggests that Rpl12 is the binding site of Yvh1 on the large subunit.

If Yvh1 cannot bind 60S subunits in *rpl12*ΔΔ cells, Mrt4 should persist on the 60S subunits in the cytoplasm similar to the *yvh1*Δ situation (Fig 4.4C). I used Nmd3 to immunoprecipitate a predominantly cytoplasmic pool of large subunits from wild type and *rpl12*ΔΔ mutant cells. Similar to the results in *yvh1*Δ, Mrt4 levels on the Nmd3-containing subunits were highly increased in *rpl12*ΔΔ cells (Fig 4.8B). This data supports the idea that Mrt4 cannot be released properly in *rpl12*ΔΔ due to a failure in recruiting Yvh1 to 60S subunits.

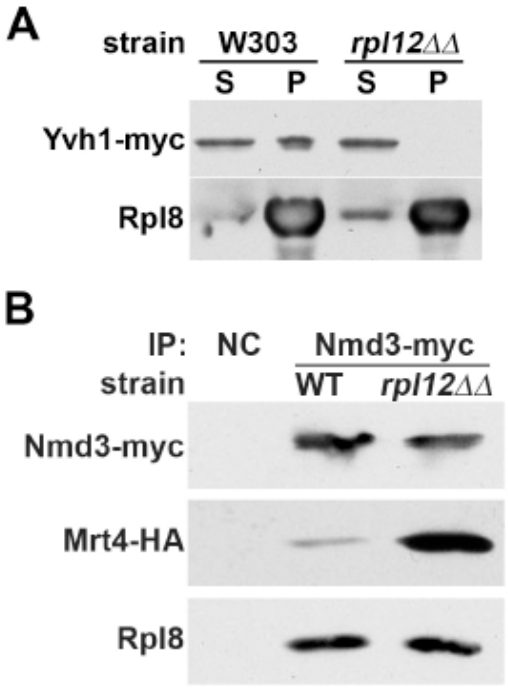

Figure 4.8 Rpl12 is required for Yvh1 binding to the 60S subunit.

(**A**) The binding of Yvh1 to 60S subunits was assayed in W303 (wild-type, WT) and 6EA1 (*rpl12*ΔΔ) cells expressing Yvh1-myc (pAJ2020) by sedimentation through sucrose cushions. Equal amounts of supernatant (S) and pellet (P) were separated by SDS-PAGE and Yvh1 and Rpl8 were detected by western blotting using c-myc (Yvh1) and Rpl8 specific antibodies. (**B**) Extracts were prepared from W303 and 6EA1 containing both pAJ2457 (MRT4-GFP) and Nmd3-myc (pAJ538) and immunoprecipitation was performed with c-myc specific antibody and protein A beads. Immunoprecipitated proteins were eluted in Laemmli buffer and separated by SDS-PAGE. Western blotting was performed against Nmd3-myc, Mrt4-GFP, and Rpl8. NC: Negative control

4.3.6 The order and location of loading Mrt4, Yvh1 and P0 on 60S subunits

To dissect the order and localization of Yvh1 loading, Mrt4 release, and P0 binding on the 60S subunits, Yvh1 was used as a bait protein to immunoprecipitate 60S subunits. Surprisingly, I did not detect either Mrt4 or P0 in Yvh1 complexes. (Fig 4.9A). As controls to show that Mrt4 and P0 can be detected in this experiment, I also immunoprecipitated Nmd3 and Rlp24. Both proteins shuttle, but show a bias toward the cytoplasm and nucleus, respectively. Nmd3 showed enrichment of P0, whereas Rlp24 was enriched for Mrt4. This result was consistent with the cytoplasmic and nuclear localization of P0 and Mrt4, respectively. In Yvh1-containing complexes, I could detect Rpl12 and Rpl8 signals, which indicated that Yvh1 immunoprecipitated with 60S subunits that lacked Mrt4 and P0 (Fig 4.9A). These results suggest a linear series of events in which Mrt4 is released when Yvh1 binds and the subsequent binding of P0 coincides with the release of Yvh1.

Next to determine where the exchange of factors occurs in the cell. Yvh1 is found in the nucleus and cytoplasm while P0 is cytoplasmic at steady state (Fig 4.9B). To test if Yvh1 and P0 shuttle between the nucleus and the cytoplasm, I blocked ribosome export by adding the Crm1 inhibitor leptomycin B (LMB). Under the conditions where Nmd3 and Rpl25 were trapped in the nucleus, Yvh1 also showed nuclear enhancement. However, P0 still localized solely in the cytoplasm (Fig 4.9B).

To preclude the possibility that this was due to sensitivity to LMB rather than from a specific block in 60S export pathway, I monitored Yvh1 and P0 localization in an *nmd3-1* strain (Ho and Johnson, 1999b; Johnson and Kolodner, 1995). *Nmd3-1* is a mutant NMD3 allele, which lacks the C-terminal 50 amino acids, including the nuclear export sequence (NES). It is a very slow growing strain showing strong 60S export defects. Consistent with the LMB results, this mutant showed strong nuclear accumulation of Yvh1, but not P0 (Fig 4.9C). These results suggest that Yvh1 is imported into the nucleus where it loads onto the 60S and releases Mrt4. The 60S subunit is then exported with Yvh1, but without either Mrt4 or P0. In the cytoplasm, Yvh1 is released from the subunit prior to P0 loading.

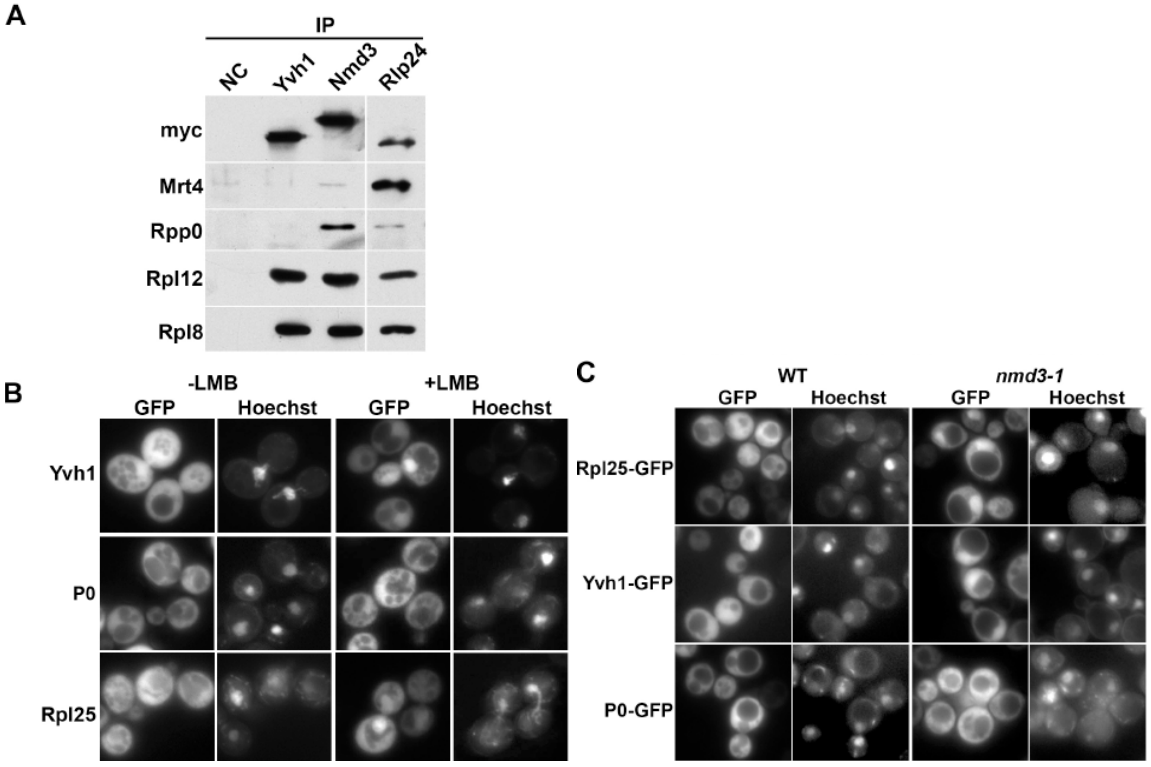

Figure 4.9 Yvh1 shuttles out of the nucleus bound to a 60S subunit that lacks both Mrt4 and P0.

(**A**) Extracts were prepared from cultures of AJY3048 (MRT4-GFP *yvh1*Δ) with Yvh1-myc (pAJ2020) and AJY3040 (MRT4-GFP) with pAJ538 (Nmd3-myc) or pAJ2002 (Rlp24-myc). The myc-tagged bait proteins were immunoprecipitated as described in Materials and Methods, proteins were separated by SDS-PAGE, and Western blotting was performed using antibodies for myc, Mrt4-GFP, P0, Rpl12 and Rpl8. NC: negative control (**B**) AJY1539 (CRM1T539C) with pAJ907 (RPL25-GFP), pAJ2464 (Yvh1-GFP) or pAJ2469 (P0-GFP) was diluted into fresh medium from overnight cultures and incubated at 30°C for 60 minutes. LMB (0.1 μg/ml) was added and the cultures were incubated for another 30 min before microscopy. (**C**) The localization of Rpl25-GFP (pAJ907), Yvh1-GFP (pAJ2464) or P0-GFP (pAJ2469) expressed in an *nmd3-1* mutant (AJY534) was visualized by fluorescence microscopy.

4.3.7 The release mechanism of Mrt4 is conserved in humans.

The structure of the ribosomal stalk is highly conserved from bacteria to mammals. It was previously shown that DUSP12, human Yvh1, complements the slow growing phenotype of yvh1Δ in budding yeast [Fig 4.10A and (Muda et al., 1999)]. Human Mrt4, MRTO4, also complemented the growth defect of *mrt4*Δ in yeast (Fig 4.10A). This suggests that the function of Yvh1 and Mrt4 is conserved from yeast to humans. I determined whether the complementation of DUSP12 in *yvh1*Δ mutant correlates with the Mrt4 release function. Mrt4 localization was monitored in *yvh1*Δ cells expressing DUSP12. As shown in Fig 4.10B, whereas Mrt4 was cytoplasmic in *yvh1*Δ cells containing an empty vector, in the presence of DUSP12 Mrt4 localized to the nucleus and the nucleolus as observed in wild-type cells. This implies that DUSP12 can release Mrt4 from 60S subunits.

To further test if the maturation pathway of the base of the ribosomal stalk is conserved from yeast to humans, I asked if DUSP12 functions in human cells to release MRTO4. This part of the work was collaborated with Edward Marcotte's lab, with assistance from Dr. Zhihua Li. DUSP12 was knocked down by RNAi in HeLa cells and the localization of MRTO4 was monitored by indirect immunofluorescence. In non-treated and control siRNA-transfected cells, MRTO4 localized in the nucleoplasm and nucleolus (Fig 4.10C, first and third panels). After RNAi depletion of DUSP12 in HeLa cells, anti-DUSP12 serum was applied to test the depletion efficiency. The non-specific band in the Western blot was used as a loading control. Compared to control cells, the protein level of DUSP12 was reduced around 70% to 80% (Fig 4.10) when cells were treated with DUSP12-specific siRNA. When DUSP12 was depleted, MRTO4 redistributed to the cytoplasm, but was depleted from the nucleoplasm (Fig 4.10C middle panel). Similar results were observed in HEK293T cells (data not shown). The relocalization of MRTO4 from the nucleoplasm to the cytoplasm is consistent with the results in yeast. However, surprisingly, the nucleolar pool of MRTO4 was not diminished. In wild-type cells, MRTO4 is concentrated in the nucleolus, suggesting that its residence time in the nucleolus is longer than in the nucleoplasm. Because DUSP12 depletion was not complete (Fig 4.10C), MRTO4 is presumably released from subunits in

the cytoplasm, but at a reduced rate. Under these conditions, if the recycling of MRTO4 to the nucleus is slower than its export, the depletion of the nucleoplasmic pool will be greater than that of the nucleolar pool.

DUSP12 is evenly distributed in the cells, whereas P0 is excluded from the nucleus (Fig 4.10D). To determine if DUSP12 or P0 shuttle, we treated HeLa cells with LMB and asked if these proteins would accumulate in the nucleus. Consistent with the results in yeast, DUSP12 was trapped in the nucleus after LMB addition (Fig 4.10D). However, P0 did not display nuclear enhancement in HeLa cells upon LMB treatment. As a control, hNmd3-GFP accumulated in the nucleus after LMB addition, as previously reported (Thomas and Kutay, 2003a; Trotta et al., 2003a). These results in human cells are similar to those in yeast, confirming the conservation of Yvh1 function in regulating the assembly of the ribosome stalk.

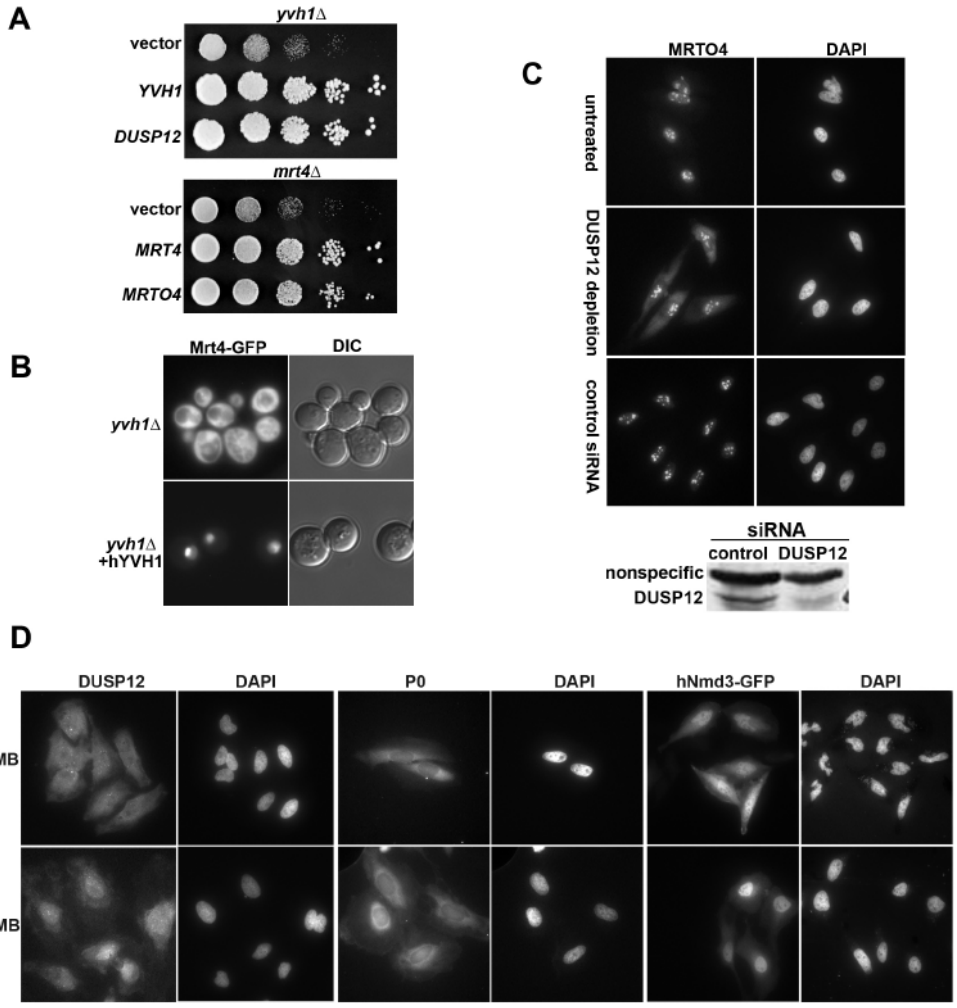

Figure 4.10 The function of Yvh1 to release Mrt4 is conserved in human cells.

(**A**) Ten-fold serial dilutions of cultures of AJY2976 (*yvh1*Δ) with vector, pAJ2020 (Yvh1) and pAJ2476 (DUSP12) and AJY2551 (*mrt4*Δ) with vector, pAJ2475 (MRT4-HA) and pAJ2477 (MRTO4) were spotted on selective plates and incubated at 30°C for 2 days. (**B**) The localization of Mrt4 was observed in AJY3048 (MRT4-GFP *yvh1*Δ) with vector or pAJ2476 (DUSP12). (**C**) HeLa cells were either untreated or transfected with siRNA against DUSP12 or control siRNA. The localization of MRTO4 was detected by indirect immunofluorescence with anti-MRTO4 antibody (Santa Cruz Biotechnology, Inc.) at 48 hours post-transfection. Nuclei were localized by staining with DAPI. The knockdown efficiency of DUSP12 was evaluated by Western blotting with anti-DUSP12

serum (Muda et al., 1999). The non-specific band was used as loading control. (**D**) HeLa cells or HeLa cells transfected with hNMD3-GFP (Trotta et al., 2003a) were treated with 10 nM LMB or vehicle as a control for 18 hours. DUSP12 and P0 were detected by indirect immunofluorescence using anti-DUSP12 (Novus) and P0 specific antibody (Abnova), respectively, whereas hNmd3-GFP was visualized by direct fluorescence.

4.4 Discussion

The assembly of the base of the stalk

The ribosomal stalk is an important functional domain of the large subunit because of its role to recruit translation factors. In this study, I have identified the assembly pathway of the base of the ribosomal stalk. In eukaryotes, Rpl12 interacts with the GTPase center, and P0 binds in close proximity to Rpl12. Mrt4 is a nuclear paralog of P0 and was shown to bind 60S at the same site as P0 (Rodriguez-Mateos et al., 2009), thus necessitating a need to exchange P0 for Mrt4. My results suggest a linear series of events partitioned between the nucleus and cytoplasm (see model, Fig 4.11). In wild-type cells, Mrt4 and Rpl12 assemble into the pre-60S subunit in the nucleolus. Yvh1 is imported into the nucleus, where it binds pre-60S subunits in an Rpl12-dependent fashion to release Mrt4. After export of Yvh1-containing pre-60S subunits to the cytoplasm, Yvh1 is released before P0 loading. Recruitment of P0 allows the assembly of the tetramer of P1 and P2 to form the active stalk (Fig 4.11).

It is unknown if additional factors are needed to assist Yvh1 in removing Mrt4. The binding of Yvh1 could alter the conformation of the Mrt4-binding site, affecting either 25S rRNA or Rpl12 or both, thereby releasing Mrt4. However, attempts to displace Mrt4 from pre-60S particles by the addition of purified Yvh1 in vitro have not been successful (unpublished). In addition, we do not yet know if the removal of Yvh1 requires additional factors or if P0 by itself is capable of displacing Yvh1.

The cellular compartment for P0 assembly into the subunit is controversial. To test if P0 is loaded onto the 60S subunit in the nucleus, I did several localization experiments. I could not detect P0 in the nucleus in wild-type cells, nor could I trap P0 in the nucleus by inhibiting 60S export by various means, either by treating with LMB to inhibit Crm1 function or using an export defective nmd3-1 mutant. I found no evidence that P0 enters the nucleus. However, the compartmentalization inferred from my results is not consistent with some biochemical data. P0 has been identified in several affinity capture experiments with nuclear pre-60S factors (Gavin et al., 2006; Zhang et al., 2007). There are several possibilities to explain this. It is possible that some P0 may load in the nucleus. Indeed, it may be that the location of Mrt4 release and P0 loading is not strictly

controlled, but that the order is tightly regulated. In wild-type yeast, I detected a low signal, but above background, for Mrt4 in Lsg1-containing particles (Fig 4.5D). Thus, some P0 may load in the nucleus, but Mrt4 may not be completely released until the pre-60S particles reaches the cytoplasm. On the other hand, the nucleus might prevent premature P0 loading, but once cells are lysed, P0 would gain access to the nuclear pre-60S subunits previously inaccessible. Thus, these pull-downs experiments may not duplicate *in vivo* situation. Yvh1 interacts with Nop7 (yeast pescadillo protein) in a 2-hybrid assay (Sakumoto et al., 2001). Thus, Nop7 may contribute to Yvh1 recruitment to the pre-60S particle in conjunction with Rpl12. Nop7 is essential for rRNA processing and 60S assembly in the nucleolus and acts earlier than Yvh1. Nop7 was not mislocalized in *yvh1*Δ mutant cells, suggesting that Yvh1 is not needed for release of Nop7.

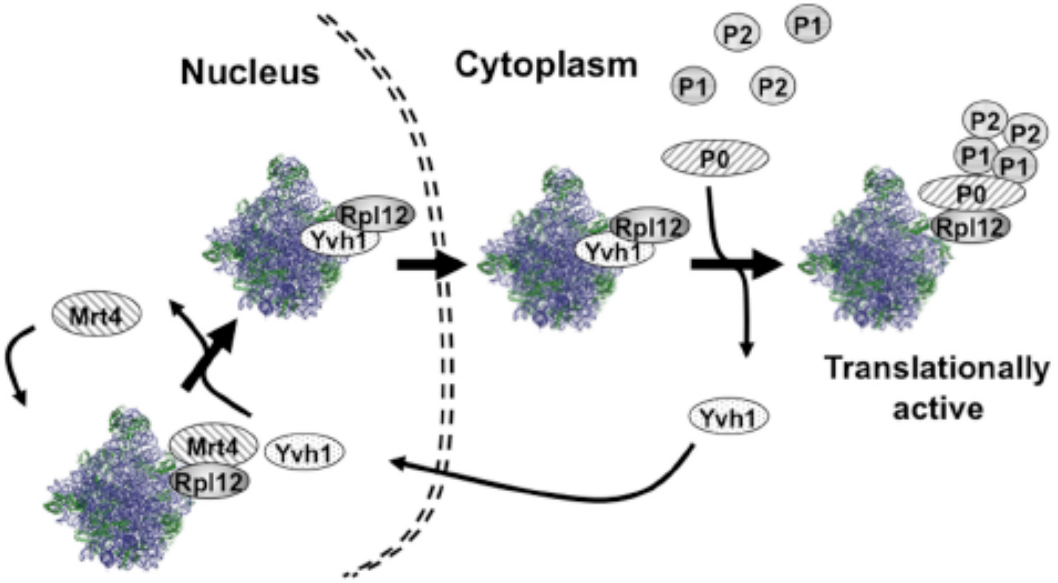

Fig 4.11 Model for the pathway of assembling the stalk base in eukaryotes.

Mrt4 and Rpl12 facilitate the correct folding of the RNA of the stalk base during ribosome biogenesis in the nucleolus. Yvh1 shuttles and binds to pre-60S particles in the nucleus. Its binding depends on Rpl12 and causes the release of Mrt4. P0 loads after export to the cytoplasm where Yvh1 is displaced. The P proteins now assemble onto the subunit.

Is there more than one pathway to release Mrt4?

In the absence of YVH1, Mrt4 cosediments with the 60S subunits, but is not present in 80S ribosomes or in polysomes, indicating that the Mrt4-containing particle is blocked for subunit joining. Since P0 is essential and its binding to the subunit is mutually exclusive with Mrt4, the presence of Mrt4 on cytoplasmic subunits would seem to pose a problem for P0 loading. In yeast, P0 is essential, whereas YVH1 and MRT4 are not. There are two possible explanations for this problem. First, there might be more than one pathway to release Mrt4 in the cells; for example, the loading of P0 itself may displace Mrt4. However, the efficiency of this pathway would not be as robust as Yvh1-dependent release, accounting for the majority of Mrt4 persisting on 60S subunits in the cytoplasm. A second possibility is that Yvh1 is absolutely required for release of Mrt4, but since neither Mrt4 not Yvh1 is essential, cells bypass the need for Mrt4. In this case, the absence of Yvh1 leads to the persistence of Mrt4 on subunits and blocks the loading of P0 on those subunits. This pool of subunits is defective in translation. The absence of Mrt4 recycling to the nucleus depletes the nuclear pool of Mrt4. Now cells synthesize 60S subunits without Mrt4, allowing P0 to load without a need for Yvh1. If Yvh1 is absolutely required for releasing Mrt4, increasing the levels of Mrt4 in the cell should more completely load pre-60S subunits with Mrt4 and further block P0 loading. Indeed, when Mrt4 was overexpressed in a *yvh1*Δ strain, a strong growth defect was observed (Fig 4.6B), supporting this model.

Does Yvh1 have physiological significance in another cellular pathway?

Yvh1 has a conserved phosphatase domain. However, Yvh1 deleted of the phosphatase domain still fully complements a *yvh1*Δ mutant and releases Mrt4 from 60S subunits. What then, is the role of Yvh1 phosphatase function? I considered that Yvh1 is involved in regulation of P1 and P2 phosphorylation, which are identified as phosphoproteins. However, in collaboration with the laboratory of Dr J.P. Ballesta (Madrid, Spain), we found that there was no difference in the phosphorylation status of P1 and P2 when comparing *yvh1*Δ versus wild-type cells. Unexpectedly, the levels of P1α and P2β were significantly decreased in the *yvh1*Δ mutant. An *rpl12*ΔΔ strain shows a

similar but more severe phenotype where P1β and P2α levels were slightly reduced and P1α and P2β were absent from the ribosomes (Briones et al., 1998). This could indicate that Yvh1 is also required for correct assembly of the ribosomal stalk, beyond simply releasing Mrt4. The defects of ribosome stalk assembly in *yvh1*Δ cells may come from several reasons. Yvh1 might stabilize Rpl12 on the 60S subunits in the absence of Mrt4. Alternately the presence of Yvh1 might be critical for the proper loading/function of P0 to further support later P1 and P2 dimer recruitment. Mrt4 may also be required for Rpl12 loading or folding properly. Since most of Mrt4 was present on the 60S subunits in the cytoplasm in *yvh1*Δ cells, Rpl12 may show defects in function due to insufficient Mrt4 in the nucleus. In my hands, RPL12 was a high copy suppressor of *yvh1*Δ, *mrt4*Δ, and *yvh1*Δ*mrt4*Δ (Fig 4.3A and data not shown). This may indicate that both Yvh1 and Mrt4 have roles on function or stability of Rpl12 on the 60S subunits.

Yvh1 might also have a function in cellular signaling by monitoring the metabolite levels, the translational capacity of the cell, or by sensing stress. DUSP12 was shown to interact with glucokinase in rat liver (Munoz-Alonso et al., 2000). DUSP12 can partially dephosphorylate glucokinase in vitro and induce the activity of glucokinase in a dosage-dependent manner. This indicates that Yvh1 may link ribosome biogenesis and glycolysis. Since ribosome biogenesis is energy intensive, mechanisms must exist to coordinate the synthesis of translational capacity of the cell with metabolic needs and energy supplies.

Chapter 5
Ordering the events of cytoplasmic maturation of the 60S ribosomal subunit

5.1 Introduction

In eukaryotic cells, ribosomes are assembled in the nucleolus. The ribosomal subunits must then be transported out of the nucleus for translation. In the cytoplasm, the export factors and several biogenesis factors on the large ribosomal subunits must be released before the large subunits become competent for translation. These events are driven by two different ATPases, Drg1 and Ssa1, and two different GTPases, Lsg1 and Sdo1. In this work, I did an extensively study of these release events and see how they tight to each other.

Truncation of the C-terminus of Rlp24 was dominant-negative and blocked cytoplasmic maturation of the large subunit by blocking the recruitment of Drg1. This led to a secondary defect in the release of Arx1 because of a failure to recruit Rei1. Deletion of REI1 mislocalized Tif6 to the cytoplasm. Depletion of *efl1* or mutant *sdo1* blocked Tif6 release and, surprisingly, Nmd3 release as well. Tif6-V192F has reduced affinity for the ribosome and can bypass the growth defect of *efl1* or *sdo1* mutants. Expression of this mutant suppressed the defect in Nmd3 recycling. On the other hand, expression of mutant Nmd3-I112T, I362T that bypasses *rpl10* or *lsg1* mutants did not bypass the growth defect of *sdo1* or *efl1* mutants. These results show that the release of Tif6 from the 60S subunit is required prior to the release of Nmd3 by Lsg1. In conclusion, Drg1 acts at the first step after ribosome export and is followed by Rei1/Jji1 and then Sdo1/Efl1. Lsg1 function at the last step of ribosome maturation in the cytoplasm. Thus, the two ATPases Drg1 and Ssa work first and then the two GTPases Efl1 and Lsg1 work in a serial event to help 60S maturation in the cytoplasm.

5.2 Background

In eukaryotic cells, the ribosomal subunits are assembled in the nucleolus, a subcompartment of the nucleus that is organized around the rRNA transcription units.

Following extensive RNA processing and protein assembly events, pre-ribosomal particles are released from the nucleolus and must then be exported out of the nucleus (Fromont-Racine et al., 2003; Johnson et al., 2002a; Tschochner and Hurt, 2003; Venema and Tollervey, 1999; Zemp and Kutay, 2007). Although they are assembled from the same primary transcript, the two ribosomal subunits are exported independently of one another. The particles that are exported are not yet fully mature: additional rRNA processing and protein assembly events occur in the cytoplasm. Furthermore, both subunits are exported with a small complement of non-ribosomal trans-acting factors. In particular, the large subunit is known to contain Nmd3, Arx1, Alb1, Rlp24, Nog1 and Tif6 as stably associated factors (Hung and Johnson, 2006; Lebreton et al., 2006; Nissan et al., 2002; Saveanu et al., 2003; Strasser et al., 2000). Some of these factors (Nmd3 and Arx1) facilitate export, whereas others (Tif6) may prevent premature interaction of ribosomal subunits and translation factors. All of these factors must be released in the cytoplasm and shuttled back to the nucleus for subsequent rounds of 60S maturation and export. Because none of these factors are found associated with translating ribosomes, they must be released prior to or during translation initiation. Release of these factors requires the two ATPases, Drg1 and Ssa1/Ssa2, and the two GTPases, Efl1 and Lsg1.

Drg1 contains two AAA-domains and exhibits ATPase activity in vitro (Zakalskiy et al., 2002). Members of this family of ATPases form hexameric ring-like structures (Vale, 2000) and ATP hydrolysis drives conformational changes necessary to disassemble macromolecular complexes. ATPase-defective Drg1 cannot release Rlp24 and several additional pre-ribosomal proteins, including Nog1, Tif6 and Arx1 from the nascent subunits. Consequently, these proteins accumulate in the cytoplasm and are prevented from recycling to the nucleus to support 60S biogenesis and export (Pertschy et al., 2007).

Rei1 and Jjj1 together with the Hsp70 Ssa are responsible for the recycling of Arx1 (Demoinet et al., 2007; Hung and Johnson, 2006; Lebreton et al., 2006; Meyer et al., 2007). Rei1 is a C2H2 zinc-finger protein localized in the cytoplasm, which was reported to be involved in the mitotic signaling pathway (Iwase and Toh-e, 2004). Jjj1 is a J domain-containing chaperone belonging to the Hsp40 family that are binding partners of Hsp70 ATPases. Jjj1 stimulates the ATPase activity of Hsp70 Ssa1, which may be used for remodeling the nascent 60S subunits to facilitate the release of Arx1. Deletion of

either *REI1* or *JJJ1* blocks Arx1 release from nascent 60S subunits in the cytoplasm (Demoinet et al., 2007; Hung and Johnson, 2006; Lebreton et al., 2006; Meyer et al., 2007) , preventing its recycling to the nucleus. *Rei1* and *jjj1* mutants are cold-sensitive and display 60S subunit deficiency at low temperature. Interestingly, the cold-sensitive phenotype can be rescued by deletion of *ARX1* or introduction of mutant Arx1 with decreased 60S binding, implying that the persistence of Arx1 on subunits is detrimental to cells (Hung and Johnson, 2006; Lebreton et al., 2006). Thus, Jjj1 with the Hsp70 Ssa1/Ssa2 act together with Rei1 to recycle Arx1.

Eukaryotic translation initiation factor 6 (eIF6) was initially identified for its ability to prevent subunit joining (Valenzuela et al., 1982), and, more recently, has been proposed to be required for efficient translation initiation in mammals (Gandin et al., 2008). The yeast homolog, Tif6 (Translation initiation factor 6), is required for 60S biogenesis in the nucleus and is retained on the subunit during export. However, this yeast protein has not been shown to act in translation initiation (Basu et al., 2001; Si and Maitra, 1999). The release of Tif6 from 60S subunits in the cytoplasm requires the GTPase Efl1 (elongation factor-like 1) (Becam et al., 2001; Senger et al., 2001), and Sdo1, the yeast ortholog of human Shwachman-Bodian-Diamond syndrome protein, SBDS (Menne et al., 2007). Mutations in Tif6 that reduce its affinity for 60S subunits suppress the growth defect caused by deletion of either *EFL1* or *SDO1* (Becam et al., 2001; Menne et al., 2007; Senger et al., 2001) and restore Tif6 shuttling in *efl1* or *sdo1* mutants. These results support the idea that the main target of Efl1 and Sdo1 is Tif6.

The cytoplasmic GTPase Lsg1 is required for release of Nmd3 (Hedges et al., 2005; Kallstrom et al., 2003a; West et al., 2005). Release also depends on the loading of the ribosomal protein Rpl10. Mutations in either Lsg1 or Rpl10 prevent the release of Nmd3 from 60S subunits blocking its shuttling into the nucleus. Certain mutations in Nmd3 that decrease 60S binding or overexpression of *NMD3* bypasses the export defect of *lsg1* or *rpl10* mutants, indicating that Nmd3 is the primary target of Lsg1 (Hedges et al., 2005).

Although Drg1 acts to release Rlp24 before Rei1 can be recruited to the subunit for subsequent release of Arx1 and Alb1, a more complete understanding of the order of the action of all four release factors has been lacking. In this project, I carried out a comprehensive

analysis of the potential interdependence of these release events. I confirmed previous results showing that a failure to release Rlp24 prevented the loading of Rei1 and, consequently, the release of Arx1. I also showed that mutations in Sdo1 or Efl1 blocked the release of Nmd3 in addition to Tif6. My results place the release of Tif6 by Efl1 and Sdo1 upstream of the release of Nmd3 by Lsg1.

5.3 Results

5.3.1 Deletion of the C-terminal domain of Rlp24 prevents recruitment of Drg1 and inhibits cytoplasmic maturation

Rlp24 is an essential protein that is associated with the pre-60S subunit during export out of the nucleus. It is also critical for recruiting Nog1 to the pre-60S subunit (Saveanu et al., 2003). Depletion of Rlp24 impairs rRNA processing and results in decreased 60S subunit levels (Saveanu et al., 2003). After transport of the pre-60S to the cytoplasm, Rlp24 is removed by the AAA-ATPase Drg1, allowing for the assembly of Rpl24 into the subunit (Pertschy et al., 2007). Rlp24 and Rpl24 share a conserved N-terminal domain that binds to the ribosome (Spahn et al., 2004), but have divergent C-termini, suggesting that Rlp24 has evolved specialized functions for biogenesis or export (Fig 5.1A). To address the role of the C-terminus of Rlp24, we deleted the C-terminal 53 amino acids (rlp24ΔC).

rlp24ΔC was unable to support growth as the sole copy of RLP24 in cells (Fig 5.1B). Western blotting and immunoprecipitation experiments showed that the truncated protein was expressed at a level similar to wild-type protein and that it retained the ability to bind to 60S subunits (Fig 5.1C and data not shown). Since Rlp24ΔC retained 60S binding but was nonfunctional, we considered that excess Rlp24ΔC may compete with wild-type Rlp24ΔC to prevent its binding to the 60S subunit and thereby cause a defect in ribosome biogenesis. Indeed, when Rlp24ΔC was overexpressed under a galactose-inducible promoter, it was strongly dominant-negative (Fig 5.1D) and caused 60S subunit deficiency (data not shown). These data imply that the C-terminal domain of Rlp24 is not required for ribosome binding, but is essential in another function.

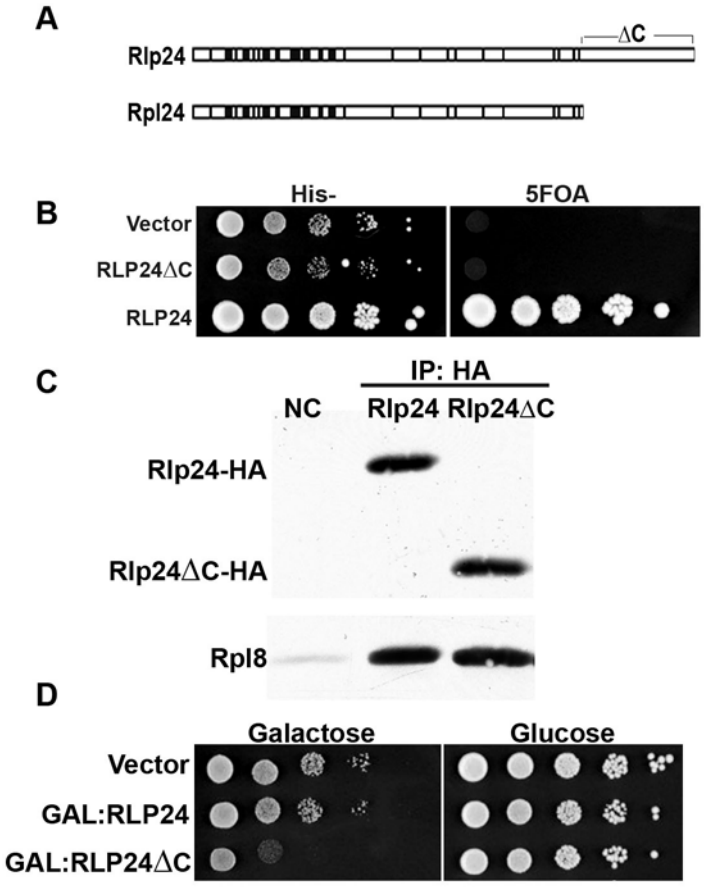

Fig 5.1 The C-terminal domain deletion of Rlp24 still interacts with 60S subunits but cannot complement RLP24 deletion

(A) The diagram of Rpl24 and Rlp24. The N terminus is conserved between Rpl24 and Rlp24. The C-terminus of Rlp24 is extended and not conserved. The C-terminal deletion region of Rlp24 is indicated on the figure. The conserved regions were marked with black lines. Similarity between sequences was analyzed with MACAW. (B) AJY2467 (rlp24Δ with RLP24-HA URA3) was transformed with vector, rlp24ΔC-HA (pAJ1895) and RLP24 (pAJ1875). Spot test was done on the His drop out and 5FOA plate. (C) Rlp24-HA (pAJ1139) and rlp24ΔC-HA (pAJ1895) were immunoprecipitated and detected with anti-HA and anti-Rpl8 antibody. (D) BY4741 with vector, GAL:RLP24 (pAJ2064) and GAL:rlp24ΔC (pAJ2065) were spotted on the glucose or galactose plates.

Surprisingly, whereas wild-type Rlp24 localized predominantly to the nucleus and nucleolus, Rlp24ΔC was cytoplasmic (Fig 5.2A). This might be because its release from the nascent ribosome is blocked, or because Rlp24ΔC cannot be imported to the nucleus. However, Rlp24ΔC cosedimented exclusively at the position of free 60S subunits in sucrose gradients (data not shown), indicating that the protein remains bound to the ribosome. These results suggest that Rlp24ΔC cannot be efficiently released from the subunit in the cytoplasm. To demonstrate that Rlp24ΔC was retained on cytoplasmic subunits, we used immunoprecipitated cytoplasmic pre-60S subunits with Lsg1. As seen in Figure 2B, Lsg1-bound subunits were enriched for Rlp24ΔC, compared to Rlp24. We blocked subunit export with leptomycin B (LMB), a specific inhibitor of the export receptor Crm1 (Kudo et al., 1999). Rlp24ΔC showed a modest accumulation in the nucleus after 30 min in the presence of LMB, indicating that it does recycle to the nucleus, although inefficiently (Fig 5.2A).

To characterize the step at which Rlp24ΔC is defective in the cytoplasm, we used Rei1 and Lsg1 to immunoprecipitate the pre-60S subunits at two different stages of maturation in the cytoplasm. As seen in Figure 2B, Rlp24ΔC could not be detected in the Rei1-bound particles, suggesting that their binding is mutually exclusive. Because these cells continue to express wild-type Rlp24 from their genomic locus, Rei1 can still bind to 60S subunits that contain wild-type Rlp24 and progress through subunit maturation. In contrast to the mutually exclusive binding of Rlp24ΔC and Rei1, Rlp24ΔC was highly enriched on Lsg1 particles (Fig 5.2B).

The AAA-ATPase Drg1 is required for the release of Rlp24 to allow the subsequent recruitment of Rei1 (Pertschy et al., 2007). Thus, one explanation for why Rlp24ΔC remains on ribosomes is that Drg1 cannot load onto Rlp24ΔC-containing subunits. To test this, we immunoprecipitated 60S subunits with Rlp24 or Rlp24ΔC and assayed for the presence of Drg1 by Western blotting. Whereas wild type Rlp24 co-immunoprecipitated Drg1-containing 60S subunits, Drg1 was not detected in the Rlp24ΔC pull down (Fig 5.2C). In contrast, Nog1, whose loading onto the pre-60S particle in the nucleolus requires Rlp24 (Saveanu et al., 2003), was recovered to similar extents in the Rlp24 and Rlp2ΔC samples (Fig 5.2C). Thus, the loss of Drg1 binding

appears specific for Rlp24ΔC. The block in Rlp24 release and in Drg1 binding are consistent with the view that recruitment of Drg1 is necessary for the release of Rlp24 (Pertschy et al., 2007).

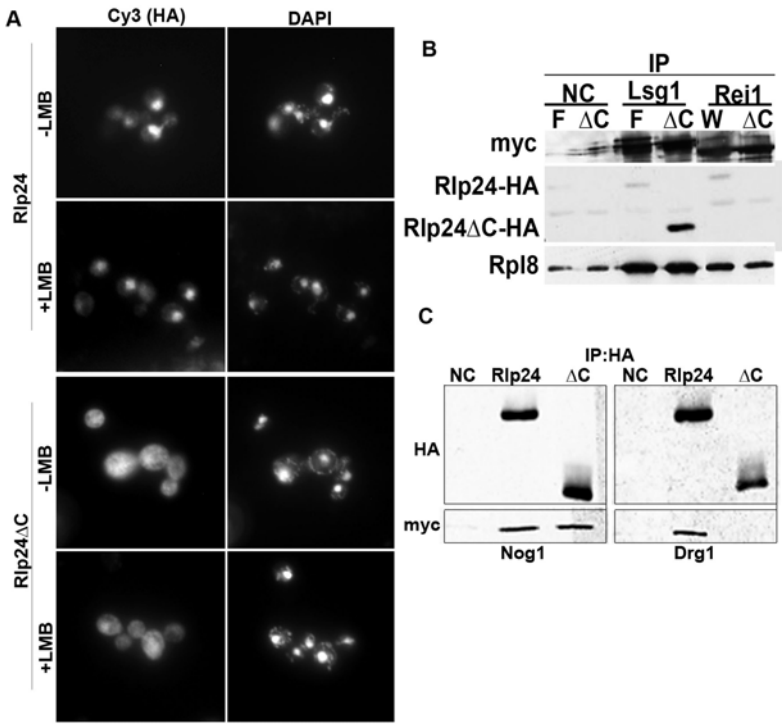

Fig 5.2 Rlp24ΔC was persistent in the cytoplasm

(A) BY4741 with Rlp24-HA (pAJ1139) and rlp24ΔC-HA (pAJ1895) were treated without or with 0.1μg/ml LMB for 30 minutes, fixed with 3.7% formaldehyde and examined with indirect immunofluorescence. (B) BY4741 with LSG1-myc (pAJ903) or REI1-myc (pAJ1028) in combination with Rlp24-HA (pAJ1139) or rlp24ΔC-HA (pAJ1895) were immunoprecipitated with c-myc specific antibody. (C) BY4741 transformed with Rlp24-HA (pAJ1139) or rlp24ΔC-HA (pAJ1895) in combination with either NOG1-myc (pAJ2074) or Drg1-myc (pAJ2075) were immunoprecipitated with HA specific antibody.

5.3.2 Expression of Rlp24ΔC impairs the release of Tif6 and Arx1

It has been reported previously that drg1 mutants accumulate Rlp24, Arx1, and Tif6 in the cytoplasm (Pertschy et al., 2007). Because Rlp24ΔC appears to prevent the recruitment of Drg1 to the nascent subunit, we determined if similar effects could be obtained by overexpression of Rlp24ΔC. Rlp24ΔC or wild-type Rlp24 was overexpressed from a galactose-inducible promoter in cells expressing GFP-tagged Tif6 or Arx1. In raffinose-containing medium (non-inducing), Tif6-GFP and Arx1-GFP showed wild type localization to the nucleolus and nucleus (Fig 5.3B). However, when Rlp24ΔC expression was induced with galactose, Tif6-GFP and Arx1-GFP mislocalized to the cytoplasm (Fig 5.3B). This was similar to the mislocalization observed in *drg1*-mutant cells (Fig 5.3A). We note that the degree of mislocalization was less in the presence of Rlp24ΔC than in *drg1-1* cells. This is probably because of incomplete penetrance of the Rlp24ΔC mutant, which is expressed ectopically to wild-type Rlp24. We did not observe mislocalization of Nmd3, using a nuclear biased mutant that reports defects in cytoplasmic release (data not shown). In parallel with the localization studies we performed coimmunoprecipitations with Lsg1 and Rei1 from wild-type vs *drg1ts* mutant cells. In support of the localization data, we also observed an enrichment of Tif6 and Rlp24 on the Lsg1 and Rei1-containing 60S subunits in the *drg1ts* mutant. The amount of Rpl8 (reflecting 60S subunits) in the Rei1 immunoprecipitation was greatly reduced in the *drg1ts* mutant (Fig 5.3C). This loss of 60S binding by Rei1 in *drg1ts* cells accounted for the loss of Arx1 in the Rei1 immunoprecipitation.

We conclude that deleting the C-terminus of Rlp24 phenocopies a *drg1* mutant, impairing the release of Rlp24 itself and subsequent downstream steps. These results corroborate earlier work (Pertschy et al., 2007) that Drg1 acts upstream of Rei1.

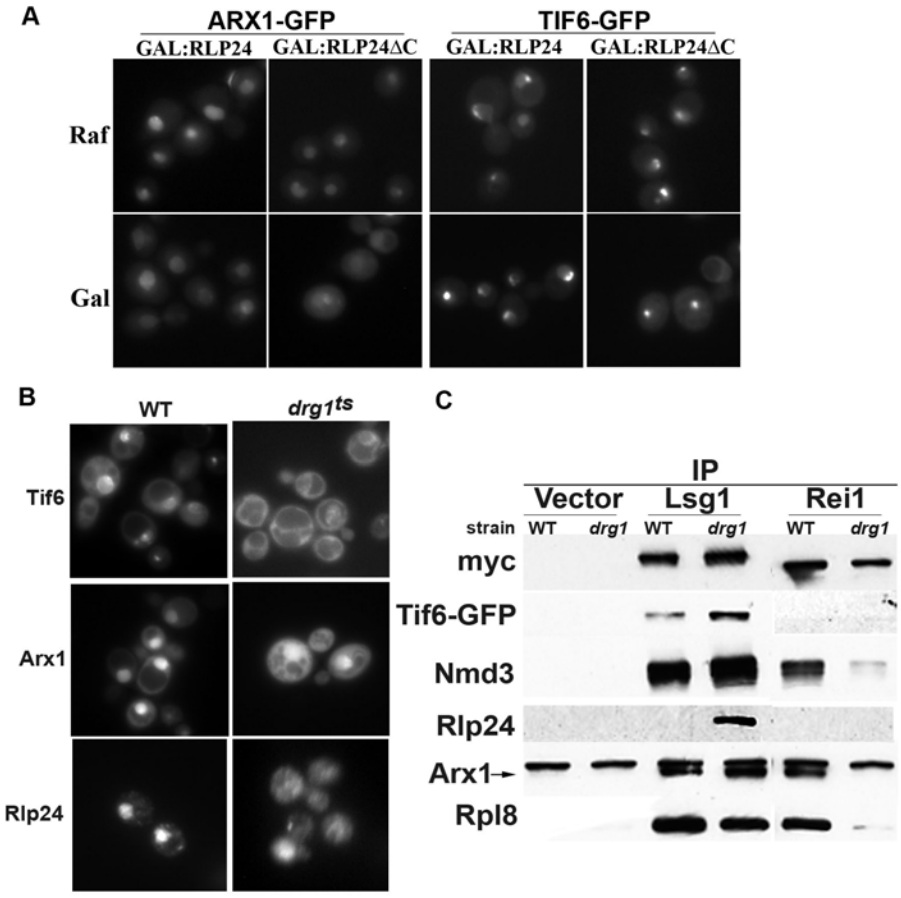

Fig 5.3 The *drg1ts* mutant impaired the release process of Rlp24, Tif6, and Arx1

(A) GAL:RLP24 (pAJ2064) and GAL:rlp24ΔC (pAJ2065) were transformed in Arx1-GFP (AJY1948) and Tif6-GFP (AJY2909) strains. Cells were grown in the drop-out medium with raffinose or induced with galactose for 5 hours. (B) The localization of Arx1-GFP (AJY1948), *drg1ts*Arx1GFP (AJY3088), Tif6-GFP (AJY2909), *drg1ts*Tif6-GFP (AJY3079), Rlp24 (pAJ1139) in W303 and *drg1ts* (FWY111) were visualized. The cells were cultured at 30°C and then shifted to 37°C for 1 hour before microscopy. (C) W303 or *drg1ts* expressing LSG1-myc (pAJ903) or REI1-myc (pAJ1028) were cultured at 30°C until OD_{600} 0.4-0.6 and then shifted to 37°C for 1 hour. Immunoprecipitation was performed using by c-myc-specific antibody and protein A beads. Precipitated proteins were eluted in Laemmli buffer and separated by SDS-PAGE. Western blotting was performed using antibodies to myc, Tif6-GFP, Nmd3, Rlp24, Arx1, and Rpl8.

5.3.3 The release of Arx1 by Rei1 is upstream of Tif6 release by Efl1 and Sdo1

Rei1, Jjj1 and Ssa are needed for the release of Arx1 from the 60S subunit in the cytoplasm (Demoinet et al., 2007; Hung and Johnson, 2006; Lebreton et al., 2006; Meyer et al., 2007), whereas the GTPases Efl1 and Sdo1 are needed for the release of Tif6 (Becam et al., 2001; Menne et al., 2007; Senger et al., 2001). The observation that Tif6 is mislocalized in *rei1* mutant cells suggests that these two events are functionally connected (Lebreton et al., 2006). The Rei1 and Efl1-dependent events could be linked in series, one obligatorily occurring after the other, or they could be interdependent, the progress of one (or both) occurring in concert with the other. We wanted to distinguish between these two possibilities.

We have shown previously that the growth defects of an *rei1*Δ mutant can be partially suppressed by deletion of Arx1, or by point mutations in Arx1 (Hung and Johnson, 2006). Similarly, *efl1* and *sdo1* mutants are suppressed by mutations in Tif6 that weaken its affinity for the subunit. We recapitulated the result (Demoinet et al., 2007; Lebreton et al., 2006) that Tif6 mislocalizes in *rei1*Δ cells and also observed mislocalization of Tif6 in *jjj1*Δ cells as well (Fig 5.4A). The mislocalization fo Tif6-GFP was less pronounced in *jjj1*Δ compared to rei1Δ cells, consistent with the observation that deletion of JJJ1 confers a slightly weaker growth defect than rei1Δ. In contrast, we did not observe mislocalization of Arx1 in EFL1-depleted cells (data not shown), although these cells showed nearly complete mislocalization of Tif6 (see below).

These results imply that the persistence of Arx1 affects the release of Tif6. We reasoned that if Arx1 release were a prerequisite for Tif6 release, deletion of Arx1 from *rei1*Δ cells would bypass the block in Tif6 release. To test this idea, we monitored Tif6 localization in *arx1*Δ*rei1*Δ double deletion mutant cells. Indeed, deletion of *ARX1* restored the nuclear localization of Tif6 (Fig 5.4B). We previously screened for mutations in *ARX1* that suppressed the growth defect of an *arx1*Δ *rei1*Δ double mutant (Lo and Johnson, unpublished). Two such mutants, *arx1-K371E* and *arx1-N428DI*, are shown in Figure 5.4C. Whereas wild-type ARX1 is detrimental to growth of arx1Δ rei1Δ cells, these mutants improve growth (Fig 5.4C). We expressed these mutants in *arx1*Δ *rei1*Δ cells expressing genomic Tif6-GFP. Both mutants weakly suppressed the mislocalization

defect of Tif6, though not nearly as efficiently as deletion of *ARX1* (Fig 5.4B). Thus, Arx1 mutants that suppress the growth defect of *rei1*Δ mutant cells (Fig 5.4C) and complement the function of *arx1*Δ (Fig 5.4C and data not shown) partially restore the mislocalization of Tif6 in *rei1*Δ cells.

TIF6-V192F is a suppressor that bypasses the requirement of its release factors, Sdo1 and Efl1 (Becam et al., 2001; Menne et al., 2007; Senger et al., 2001). If Rei1 works in concert with Sdo1 and Efl1, one might expect that *TIF6-V192F* would also suppress the growth defect of *rei1*Δ or *jjj1*Δ mutants. However, *TIF6-V192F* did not improve the growth of either strain and did not affect the mislocalization of Arx1 in *rei1*Δ cells (data not shown). Together, these data indicate that the release of Arx1 by Rei1/Jjj1/Ssa, is upstream of and a prerequisite for the release of Tif6 by Sdo1 and Efl1.

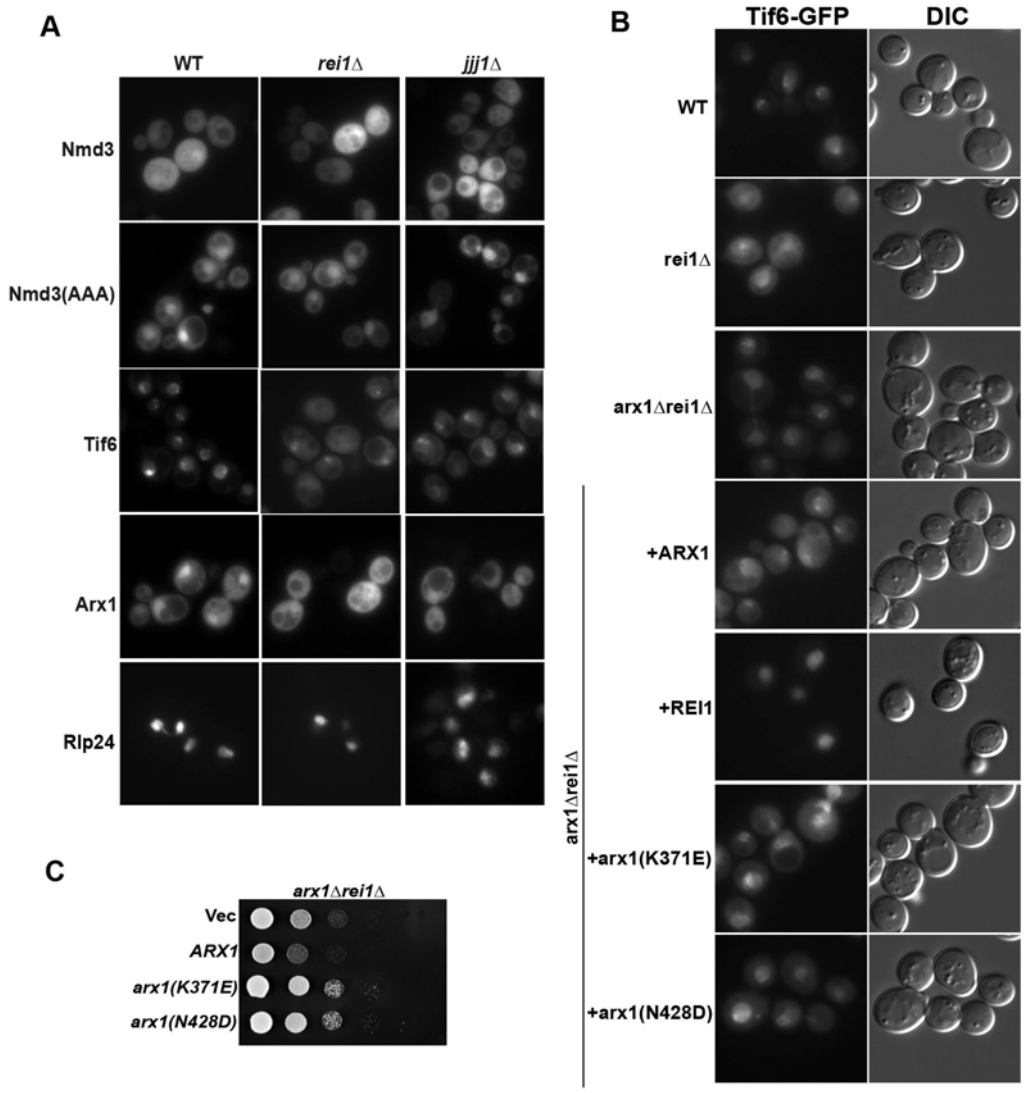

Fig 5.4 rei1Δ/jjj1Δ affects Arx1 and Tif6 release

(A) The localization of NMD3-GFP (pAJ582), Nmd3(AAA)-GFP (pAJ754), Tif6-GFP, Arx1-GFP, and Rlp24HA (pAJ1139) were visualized in BY4741, rei1Δ, or jjj1Δ. The cells were cultured at 25°C to mid-log phase. (B) Tif6-GFP localization was visualized in BY4741, *rei1*Δ, *arx1*Δ*rei1*Δ, and *arx1*Δ*rei1*Δ cells with ARX1, REI1, arx1(K371E), and arx1(N428D) plasmids. (C) *arx1*Δ*rei1*Δ cells with ARX1, arx1(K371E), and arx1(N428D) plasmids were spotted in the plate and incubated at 25°C for 3 days.

5.3.4 The release of Tif6 by Efl1 and Sdo1 is upstream of the release of Nmd3

Sdo1 and Efl1 are both required for the release of Tif6 (Becam et al., 2001; Menne et al., 2007; Senger et al., 2001). Sdo1 is thought to recruit Efl1 to the subunit for subsequent release of Tif6 (Menne et al., 2007). So far, these two factors are reported to function only in Tif6 release. This specificity for Tif6 is supported by the finding that mutations in Tif6 that weaken its affinity for the subunit suppress the growth defect of *sdo1*Δ or *efl1*Δ mutants (Becam et al., 2001; Menne et al., 2007; Senger et al., 2001). We determined whether mutations in *SDO1* or *EFL1* affected the recycling of other trans-acting factors to determine if the release of Tif6 is coupled with other release events.

We monitored the localization of 60S shuttling factors in an *sdo1* temperature-sensitive mutant (Warren, unpublished) at nonpermissive temperature. As previously reported, we observed mislocalization of Tif6 to the cytoplasm (Fig 5.5A). To monitor the localization of Nmd3, we used a mutant that shows a nuclear bias due to point mutations in its Crm1-dependent leucine-rich nuclear export signal (Hedges et al., 2006). Surprisingly, Nmd3(AAA) also strongly mislocalized to the cytoplasm (Fig 5.5A), suggesting that the release of Tif6 and Nmd3 are somehow coupled. This mislocalization of Nmd3(AAA) was qualitatively similar to what we have reported previously for *lsg1* mutants (Hedges et al., 2005). We did not observe appreciable changes in localization of Arx1, Rlp24, and Tif6.

We next tested if the effects of mutant Sdo1 on the release of Nmd3 could be observed after depletion of Efl1, the GTPase that acts with Sdo1 to release Tif6. *EFL1* is not essential, but deletion of *EFL1* causes a severe growth defect. Consequently, a genomic copy of *EFL1* under control of the *GAL1* promoter was used to regulate transcription by carbon source. We also incorporated a hemagglutinin (HA) tag at the amino terminus of Efl1. The effect of depleting Efl1 replicated the phenotypes of an *sdo1ts* mutant: both Tif6 and Nmd3(AAA) showed clear mislocalization to the cytoplasm (Fig 5.5B).

The results thus far suggest that the release of Tif6 and Nmd3 are coupled. These events could be in series, with the release of Nmd3 requiring the prior release of Tif6, or they could be in parallel. We previously reported that the cytoplasmic GTPase Lsg1 is

required for the release of Nmd3 (Hedges et al., 2005). To determine if Lsg1 function is important for the release of Tif6, we monitored the localization of genomic Tif6-GFP in *lsg1-1* mutant cells at restrictive temperature. We observed mislocalization of Nmd3(AAA) but not of Tif6 or Arx1-GFP (data not shown). Similar results were obtained with overexpression of dominant-negative mutants of LSG1 that we have previously reported to prevent Nmd3 recycling to the nucleus [(Hedges et al., 2005) and data not shown].

As an additional means to examine the functional interaction between the release of Tif6 and Nmd3, we used mutant versions of Tif6 and Nmd3 that suppress defects in their respective release factors. As described above, TIF6(V192F) is a dominant-negative mutant that bypasses the requirement for Sdo1 or Efl1 in vivo (Becam et al., 2001; Menne et al., 2007; Senger et al., 2001). Strikingly, TIF6(V192F) fully rescued the mislocalization defect of Nmd3(AAA) when Efl1 was depleted (Fig 5.5C compare panels 2 and 4).

Since Nmd3 mislocalizes in *sdo1* and *efl1* mutants, we tested if expression of NMD3(I112T, I362T), that suppresses mutations in LSG1(Hedges et al., 2006), can also bypass the requirement of Sdo1 and Efl1. NMD3(I112T, I362T) did not suppress the growth defect of either *sdo1* or *efl1* mutants and had no effect on Tif6 mislocalization when Efl1 was depleted (data not shown). These results demonstrate that the failure to recycle Nmd3 in *sdo1* or *efl1* mutants is the indirect consequence of not releasing Tif6. Thus, the release of Tif6 by Efl1 and Sdo1 is upstream and a prerequisite for the release of Nmd3 by Lsg1. Because the *lsg1-1* mutant appears to affect only Nmd3, the Lsg1-dependent release of Nmd3 does not appear to be coupled with release of other factors. This places Lsg1 at the last known step of 60S subunit maturation in the cytoplasm.

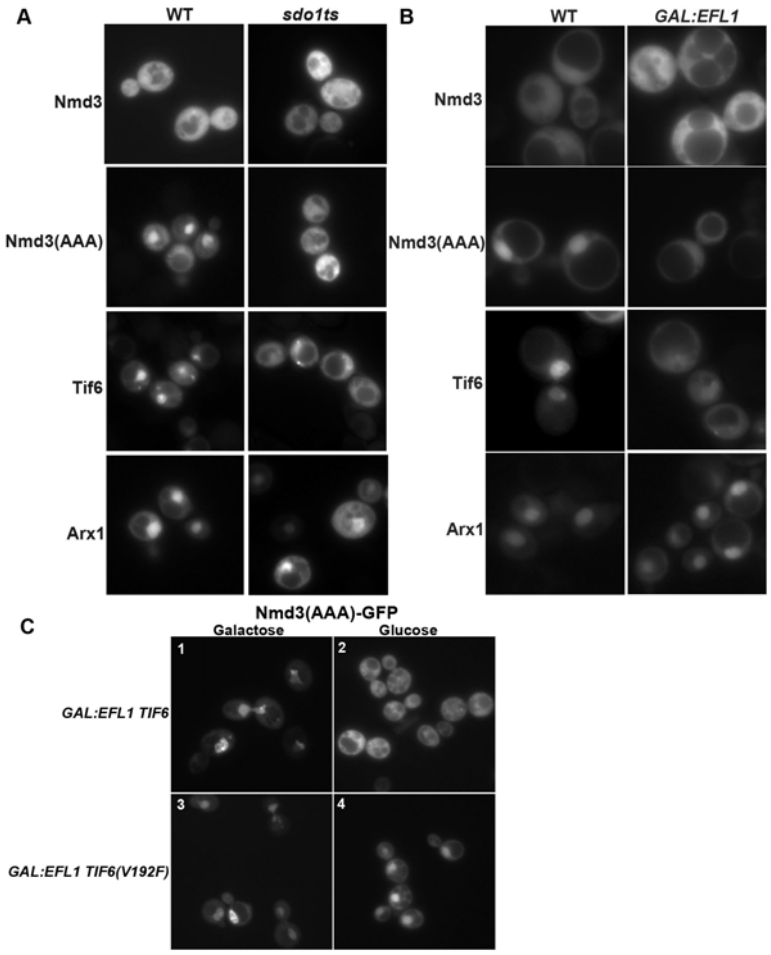

Fig 5.5 The temperature-sensitive sdo1 mutation and depletion of Efl1 block cytoplamic release of Nmd3, whereas the suppressor TIF6(V192F) rescue the defect after *sdo1* or *efl1* inactivation

(A) The localization of Nmd3-GFP (pAJ582), Nmd3(AAA)-GFP (pAJ754), Tif6-GFP (pAJ1003) and Arx1-GFP (pAJ1025) were visualized in S288C or *sdo1ts* strains. The cells were cultured at 30°C and then shifted to 37°C for 30 minutes before microscopy. (B) The localization of Nmd3-GFP (pAJ582), Nmd3(AAA)-GFP (pAJ754), Tif6-GFP (pAJ1003) and Arx1-GFP (pAJ1025) were visualized in W303 or GAL:EFL1 strains. The cells were culture in the galactose-containing medium and then shifted to glucose medium for 26 hours before microscopy. (C) Nmd3(AAA) localization was detected in *GAL:EFL1* with *TIF6* or *TIF6(V192F)* cells in glucose or galactose conditions.

5.4 Discussion

The nascent large ribosomal subunit is exported to the cytoplasm with a handful of non-ribosomal proteins that must be removed before the subunit is competent for translation. In addition, several of these events are associated with assembly of ribosomal proteins into the subunit for its final maturation in the cytoplasm. There are four major unpackaging events that have been characterized in yeast. Drg1 catalyzes the release of Rlp24 and Nog1 to allow for the loading of Rpl24 (Pertschy et al., 2007). Two hybrid interaction between Rpl24 and Rei1 suggests that Rpl24 then recruits the Hsp70 Ssa and its adaptor Jjj1 to release Arx1 and Alb1, and the subsequent release of Arx1 and Alb1 by the combined efforts of Rei1, Jjj1 and Ssa. In addition, the GTPase Efl1 together with the Swachman-Bodian Syndrome protein Sdo1 release Tif6. A second GTPase, Lsg1, releases Nmd3 in conjunction with the loading of Rpl10. Here, we have integrated all these events into a single pathway of linked events, in which each step is dependent on a prior event. Drg1 appears to initiate this pathway while the release of Nmd3 by Lsg1 appears to be the last step before the subunit engages in translation.

The inter-dependence of cytoplasmic release events

A dominant negative RLP24 mutant blocks recruitment of Drg1 and downstream steps

We found that deletion of the C-terminus of Rlp24 resulted in a strongly dominant-negative phenotype, arresting cytoplasmic maturation of the 60S subunit. Notably, the binding of Rei1 and release of Arx1 and Tif6 were inhibited by this mutant. These phenotypes are similar to a *drg1* mutant. Indeed, Drg1 was not recruited to subunits.

Our results with dominant-negative Rlp24 are similar to previously published work showing that Drg1 is required for the release of Rlp24 and Nog1, and that Drg1 activity is required before Rei1, Jjj1 and Ssa act to release Arx1. The results are consistent with Drg1 utilizing the C-terminus of Rlp24 for recruitment to the subunit; however we did not detect interaction between these two factors in a yeast 2-hybrid assay (not shown). The interaction of Rei1 with Rpl24 in a yeast-two-hybrid assay (Lebreton et al., 2006), explains the requirement for Rpl24 loading in the recruitment of Rei1 and

release of Arx1. However, we have observed that an *rpl24a*Δ *rpl24b*Δ double deletion mutant only partially mislocalizes Arx1 and retains Rei1 binding to the ribosome (data not shown), suggesting that the binding site for Rei1 is more complex than Rpl24 alone. Indeed, Rei1 has a high affinity for RNA in vitro (M Parnell, personal communication), suggesting that its binding site may be composed of an RNA element in addition to Rpl24.

Release of Arx1 is required for efficient release of Tif6

As previously reported, Tif6 mislocalizes to the cytoplasm in *rei1*Δ and *jjj1*Δ mutant strains, suggesting that deletion of REI1 and JJJ1 impinges on the Efl1 and Sdo1-dependent release of Tif6. Surprisingly, when Arx1 is deleted from *rei1*Δ cells, Tif6 recycling to the nucleus is restored. This implies that the release of Arx1 rather than the loading of Rei1 or Jjj1 is the step that is important for subsequent release of Tif6. In contrast, inactivation of Sdo1 or depletion of Efl1 did not trap Arx1 in the cytoplasm. Nor did alleles of TIF6 that suppress *efl1* and *sdo1* mutants suppress the growth defect of an *rei1*Δ or *jjj1*Δ mutant. Our results place the Sdo1/Efl1-dependent release of Tif6 downstream of and functionally linked Rei1/Jjj1/Ssa release of Arx1 and Alb1. This is consistent with the observation that Tif6 is partially mislocalized in a *drg1 ts* mutant.

The release Tif6 is a prerequisite for Lsg1 release of Nmd3

We found that inactivation of Efl1 or Sdo1 prevented the release of both Tif6 and Nmd3 from 60S subunits in the cytoplasm. Although the block in Tif6 release was previously well documented (Becam et al., 2001; Menne et al., 2007; Senger et al., 2001), the block in Nmd3 recycling was unexpected. In contrast, an lsg1 mutant blocked the release only of Nmd3. Furthermore, a mutation in Tif6 that weakens its affinity for the 60S subunit and bypasses an *sdo1* or *efl1* mutation also suppressed the release defect of Nmd3. On the other hand, a mutation in *nmd3* that bypasses a mutation in *lsg1* did not suppress *efl1* or *sdo1*. These results show that the release of Tif6 is functionally linked to the release of Nmd3 and that Tif6 must be released prior to the release of Nmd3. Thus, the two GTPases Efl1 and Lsg1 work in series with Efl1 acting upstream of Lsg1.

How do *efl1* or *sdo1* mutants block the release of Nmd3? Because the release of Nmd3 requires Lsg1, one possibility is that the binding of Lsg1 to the subunit is sterically blocked until Tif6 is released. However, Lsg1 can coimmunoprecipitate subunits containing Rlp24 and Tif6 (Fig 5.3C, Lsg1 IP), indicating that it can bind considerably upstream of its point of function. In addition, *lsg1* mutants do not inhibit the release of Tif6, indicating that they do not interfere with Sdo1 or Efl1 function. Another possibility is that the activity of Lsg1 is inhibited by the presence of Tif6. We do not yet know what acts as the effector for the GTPase activity of Lsg1. It may sense a conformational change in the subunit, perhaps associated with the release of Tif6, or it may monitor the assembly of a ribosomal protein such as Rpl10, as we have previously shown that both Rpl10 and Lsg1 are required for the release of Nmd3 (Hedges et al., 2005).

Tif6 was initially identified from mammalian cells as eukaryotic initiation factor 6 (eIF6) based on its biochemical ability to prevent ribosomal subunit association (Si and Maitra, 1999). Recently, Tif6 was reported to be necessary for normal insulin-stimulated translation in mice (Gandin et al., 2008) arguing for a role for eIF6 in translation initiation. Since the release of Nmd3 occurs downstream of Tif6 release, the release of Nmd3 must be close in sequence to translation initiation. Cryo-electron microscopic reconstruction of the Nmd3-60S complex identifies the binding site for Nmd3 on the joining face, adjacent to helix 69 of 25S rRNA and adjacent to Rpl10 (Jayati, Bussiere, Johnson and Frank, unpublished). This location is incompatible with subunit joining and, indeed, Nmd3 cannot bind to 80S complexes in vitro. Taken together, these results suggest that release of Nmd3 is a critical late step in biogenesis or utilization of the subunit.

Taken together, our results demonstrate that the known cytoplasmic maturation events on the 60S subunit can be envisioned as one series of linked events that describe a pathway of cytoplasmic ribosome maturation (Fig 5.6). The first two steps are ATP-dependent, with Drg1 acting upstream of Ssa1. The release of Arx1 by Rei1/Jjj1/Ssa is a prerequisite for the two subsequent GTP-dependent events that, themselves, work in series. We do not know if there is significance to the linkage of two ATPases and two GTPases. Intriguingly, Efl1 is similar in sequence to translation elongation factor 2

(Becam et al., 2001). Elongation factors are recruited to the ribosome through the ribosome stalk, raising the interesting possibility that assembly of the stalk may be necessary for recruitment of Efl1 to initiate the final GTP-dependent steps of 60S maturation.

We have recently determined the position of Nmd3 to be on the joining face of the 60S subunit (unpublished). The binding site of Tif6 on the large subunits is not well established, though its ability to prevent subunit association would likely place it on the joining face as well. Recent work on the eIF6 ortholog aIF6 from the archaea *S. solfataricus* suggests that aIF6 binds between helix 69 of the 23S rRNA and protein L14 (Benelli et al., 2009). This position is overlapping with the position of Nmd3, suggesting that these two factors are close in space on the subunit. Indeed, there is evidence from a genome-wide protein complementation assay for their physical proximity (Tarassov et al., 2008). Thus, GTPases may have evolved from existing translation factors to utilize a common binding platform for maturation of the subunit. It is intriguing as well that the Hsp70 Ssa is involved in a variety of protein remodeling events, including nascent protein folding on the ribosome. Ssa utilization in removing Arx1 in the vicinity of the exit tunnel may derive from having a similar function at this site on the ribosome.

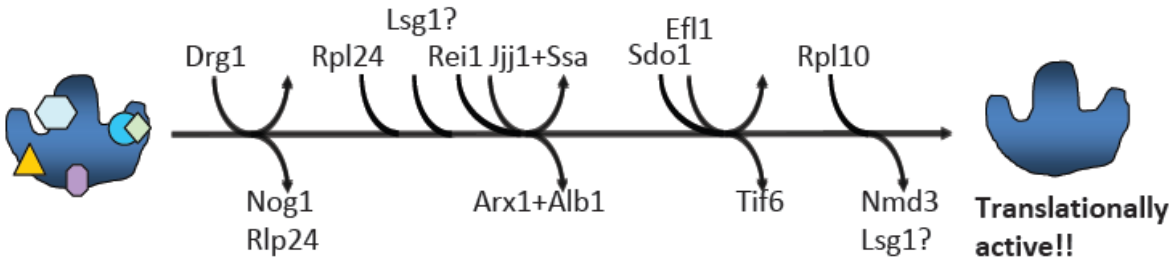

Fig 5.6 Diagram of the ribosome biogenesis events in the cytoplasm

Appendices

Appendix A. Active translation is critical for Nmd3 release

Preliminary data from a previous graduate student in our lab, John Hedges, showed that Nmd3 was trapped in the cytoplasm under cycloheximide treatment. This made us consider if this phenotype was from a non-specific effect of cycloheximide or from the inactivation of translation.

To distinguish between these two possibilities, I put Nmd3(AAA)-GFP as a reporter into different translation mutants or wild-type cells under different growth conditions that inhibit translation.. While wild-type Nmd3 is predominantly cytoplasmic, Nmd3(AAA) is an NES-defective Nmd3 mutant allele and is predominantly nuclear. If Nmd3 persists on the 60S subunits in the cytoplasm, the change from the nucleus to cytoplasm is easily to be monitored.

All results are summarized in Appendixes B and C. When there were defects in the translation, like *fun12*Δ, Nmd3(AAA) was still in the nucleus. However, Nmd3(AAA) was persistent in the cytoplasm when translation was totally stopped. In the mutants of *prt1-1*, *sly1-1*, *sui2-1*, *gcn2-101 gcn3-101 gcd1-502*, *gcn2-101 gcn3-101*, and *sup45-1*, Nmd3 recycling was blocked. Cdc33-1 (*ts* mutant allele of eIF4E) was the only exception of a lethal translation mutant that did not arrest Nmd3 recycling.

I also found that when cells were cultured to high density, Nmd3 was persistent in the cytoplasm. The translation efficiency at stationary phase was significantly lower than that of exponential phase. This may explain why the recycling of Nmd3 was growth stage dependent. To further test if Nmd3 recycling also related to stress caused by nutrition depletion, cells were cultured in low nitrogen medium or ethanol as a major carbon source for growth. Neither the depletion of nitrogen source nor change of carbon source to ethanol trapped Nmd3 in the cytoplasm. These results suggest that Nmd3 release is somehow linked to translation. This is consistent with my conclusion that Nmd3 is released downstream of Tif6, closer to the translation initiation stage.

We do not know how translation regulates the Nmd3 recycling process. Our preferred model is that translation initiation is critical for Nmd3 release. Nmd3 is bound at the joining face of the large 60S subunit. The association between the two ribosomal subunits at translation initiation might be important for triggering Nmd3 release. Although the inactivation of termination steps also prevents Nmd3 from recycling, this result may occur from a halt of the translation process. Thus, it is difficult to distinguish which stage of translation is critical for Nmd3 release. Another possibility for how a block in translation prevents Nmd3 recycling is that a newly translated protein might be important for Nmd3 import.

Beside Nmd3, I also monitored Arx1 and Tif6 localization in these mutants and conditions. Arx1 did not change localization in any of these mutants or cycloheximide treatment. This implies the release of Arx1 is not coupled with translation. Interestingly, Tif6 recycling appeared blocked in *prt1-1*, *sly1-1*, and *sup45ts* mutants. We do not know how to explain the discrimination between Nmd3(AAA) and Tif6 in different translation mutants, but it does imply specificity in the connection between translation and 60S maturation.

Appendix B. Conditions that trap Nmd3(AAA) in the cytoplasm.

Mislocalization: from nucleus to cytoplasm

A. Mutants that change Nmd3(AAA) localization

Mutant allele	Gene product	Strain	Applied condition
prt1-1	eIF3	AJY228	37°C 30min
sly1-1		AJY1207	37°C 120min **PS.** Nmd3(AAA) stays in the nucleus at 30 and 32°C
sui2-1	α subunit of eIF2	AJY2961	37°C 60min
gcn2-101 *gcn3-101* *gcd1-502*	GCN2: Protein kinase that phosphorylates the α subunit of eIF2 GCN3: α subunit of eIF2B GCD1: γ subunit of eIF2B	AJY2963	37°C 60min
gcn2-101 *gcn3-101*		AJY2964	37°C 60min
sup45-1	eRF1	AJY2967	37°C 60min

B. Other conditions

- Cycloheximide (200μg/ml): 15min
- High OD (above 1): Also, at this stage, wild type Nmd3 is less sensitive to LMB.

No Mislocalization

A. Nmd3 in the nucleus

Mutant allele	Gene products	Strain	Applied condition
*fun12*Δ	eIF5B	AJY1505	37°C 30min
cdc33E72G	eIF4E	AJY201	Room temp & 30°C
cdc33-1	eIF4E	AJY217	37°C 30min & 37°C 120min
gcd2L42P	δ subunit of eIF2B	AJY1089	Room temp & 30°C
*pab1*Δ*spb8*Δ	Pab1 and Lsm1	AJY1453	

B. Nmd3 in the vacuole

- Nitrogen starvation (12 hr)
- Ethanol as carbon source

Appendix C. Nmd3(AAA), Arx1 and Tif6 localization in different mutant strains

(A)

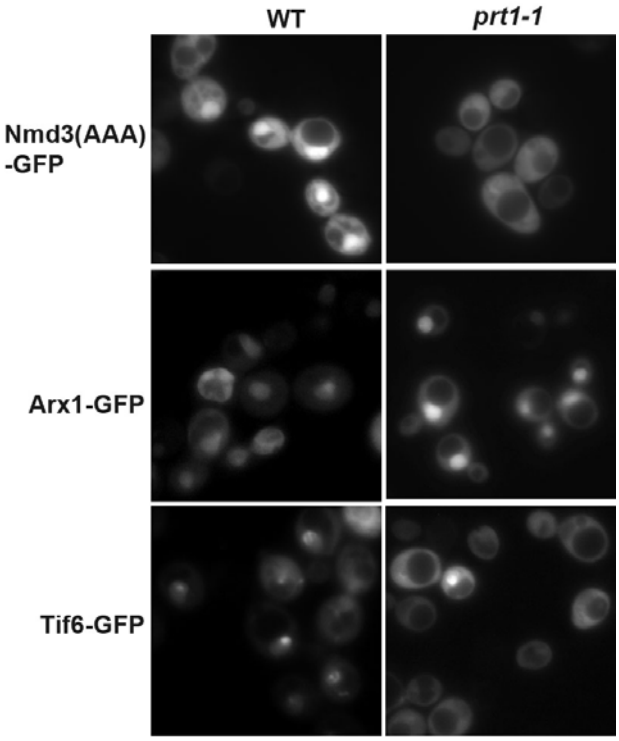

(B)

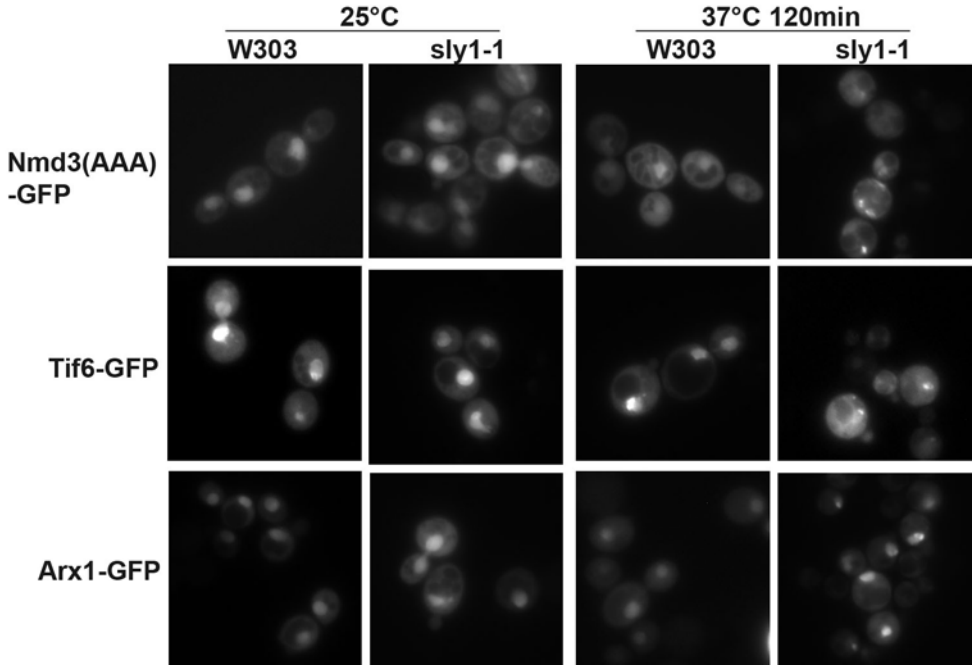

(C)

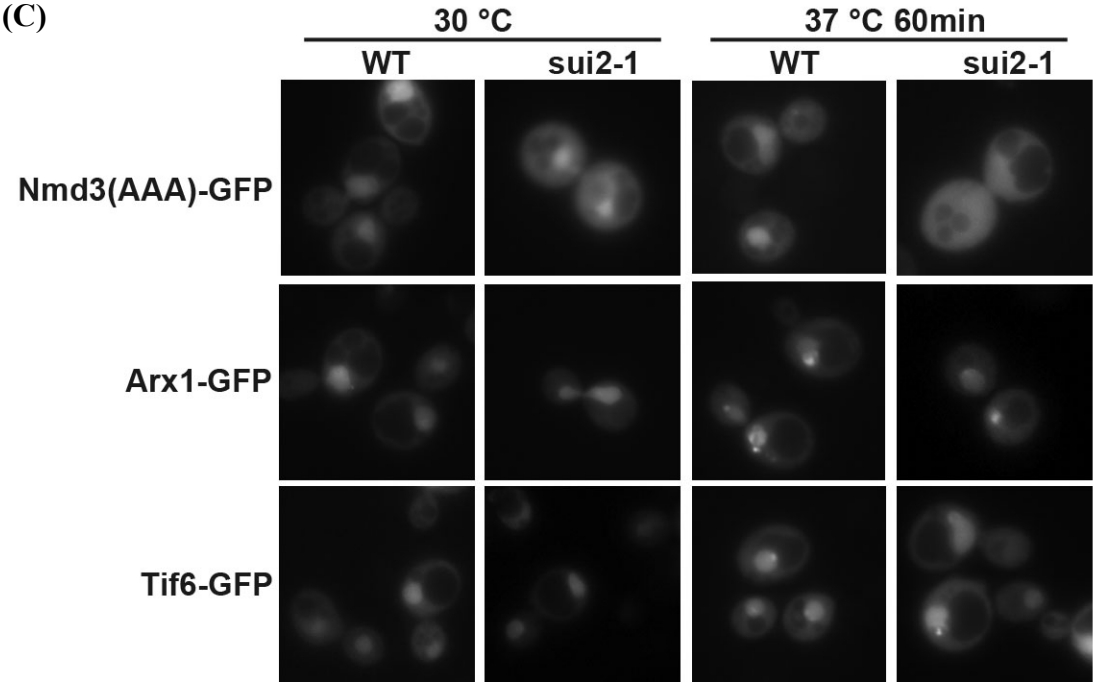
30 °C
37 °C 60min
WT
sui2-1
WT
sui2-1
Nmd3(AAA)-GFP
Arx1-GFP
Tif6-GFP

(D)

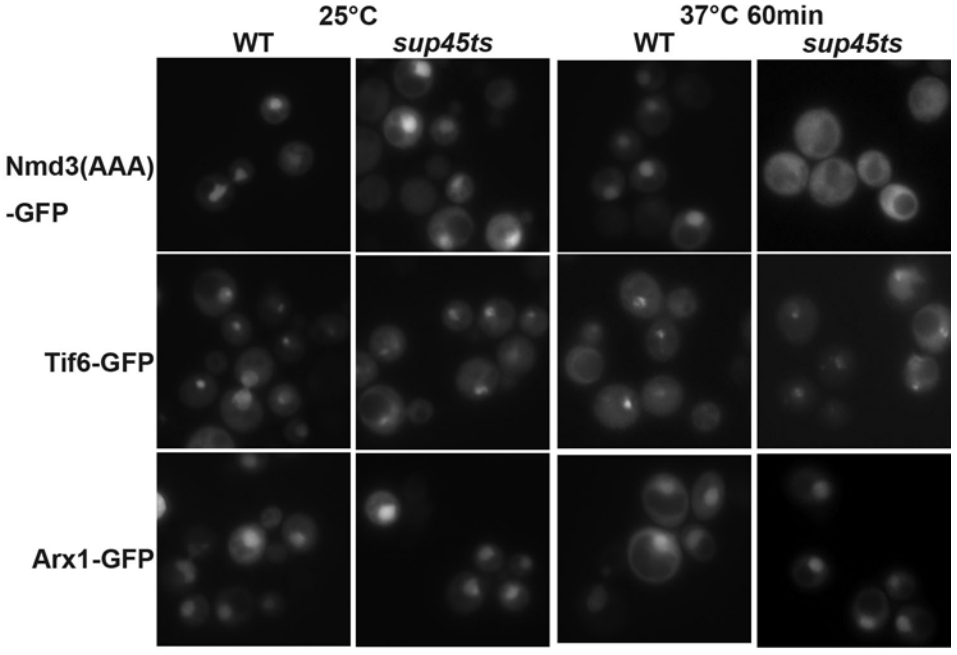
25°C
37°C 60min
WT
sup45ts
WT
sup45ts
Nmd3(AAA)
-GFP
Tif6-GFP
Arx1-GFP

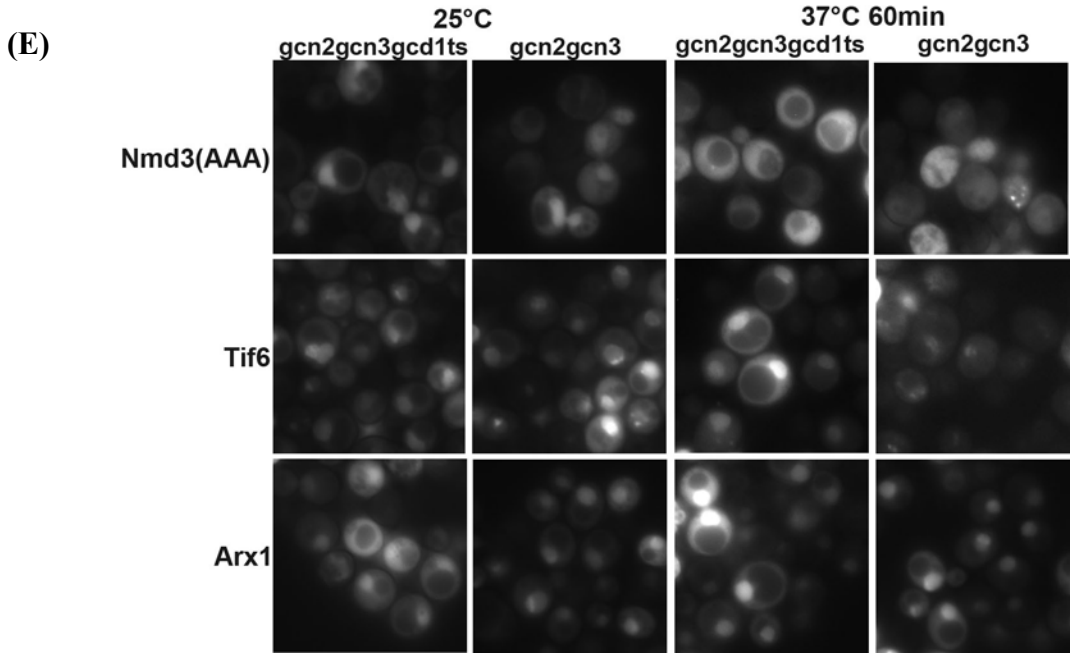
(E)
25°C
37°C 60min
gcn2gcn3gcd1ts
gcn2gcn3
gcn2gcn3gcd1ts
gcn2gcn3
Nmd3(AAA)
Tif6
Arx1

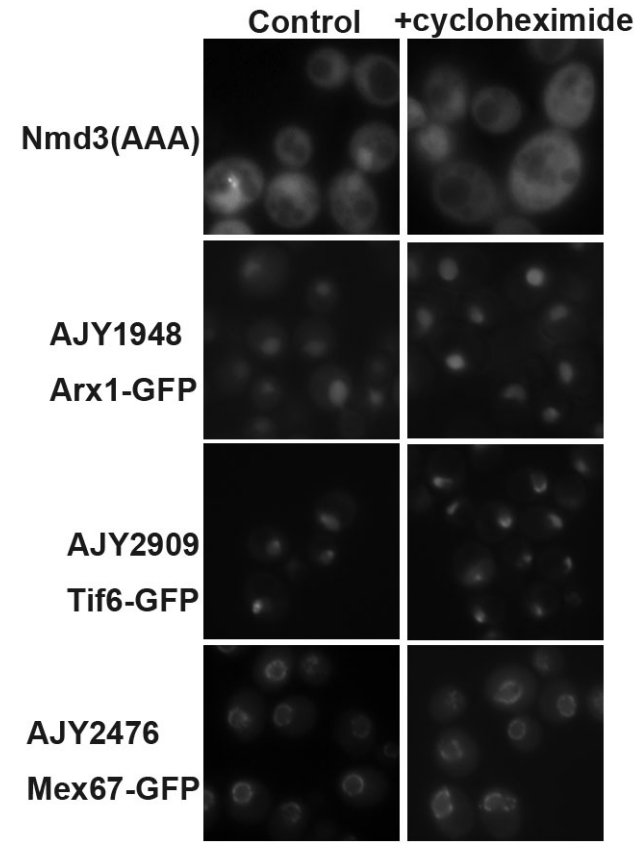
(F)
Control
+cycloheximide
Nmd3(AAA)
AJY1948
Arx1-GFP
AJY2909
Tif6-GFP
AJY2476
Mex67-GFP

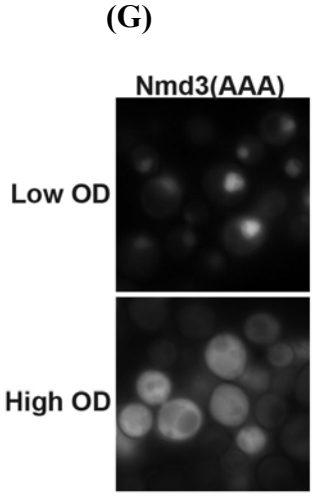
(G)
Nmd3(AAA)
Low OD
High OD

Localization of Nmd3 (AAA)-GFP (pAJ754), Arx1-GFP (pAJ1025), and Tif6-GFP (pAJ1003) was monitored in (A) AJY228 (*prt1-1*), (B) AJY1207 (*sly1-1*), (C) AJY2961 (*sui2-1*), (D) AJY2967 (*sup45-1*), (E) AJY2963 (*gcn2-101 gcn3-101 gcd1-502*) and AJY2964 (*gcn2-101 gcn3-101*). Culture conditions are summarized in Table A in Appendix A. (F) Cycloheximide was added in the culture to 200 μg/ml final concentration and then shaken at 30°C for 60 minutes. (G) BY4741 with pAJ754 was grown until ~OD600 0.3 or above 1 at 30°C.

Appendix D. A mutation in Rpl25 impairs 60S export

Rpl25 is one of the five ribosomal proteins at the exit tunnel of the large subunit. D134 is a conserved residue at the C-terminus of Rpl25. Mutation of this residue to Arg caused severe growth and 60S biogenesis defects at low temperature (unpublished data from Pool lab). Rpl25 shows functional connections with Arx1: fusion of GFP to Rpl25 suppresses an *rei1*Δ mutant, as does deletion of Arx1, and Rpl25-GFP alters Arx1 binding to the subunit (Hung and Johnson, 2006). A potential explanation of these results is that the bulky tag at the C-terminus of Rpl25 perturbs Arx1 binding. Based on these data, we have suggested that Arx1 binds to or near Rpl25. The phenotypes of *rpl25(D134R)* suggested that this Rpl25 mutation disrupted the binding of Arx1.

To explore the mechanism of rpl25(D134R) effects on 60S biogenesis pathway, I did several assays. First, I combined this mutant with *rei1*Δ to test if *rpl25(D134R)* could suppress the growth defect similar to Rpl25-GFP. Contrary to what we expected, *rpl25(D134R)* did not improve the growth rate of *rei1*Δ (data not shown). Interestingly, I found that *rpl25(D134R)* showed strong genetic interactions with several export factors of 60S subunits: *rpl25(D134R)* was synthetic lethal with *arx1*Δ, synthetic sick with *nup120*Δ at 30°C and synthetic lethal at 25°C, and synthetic lethal with Crm1(T539C)-HA (Appendix C). These results suggest that *rpl25(D134R)* has a potential role in 60S export. I visualized Rpl25-GFP and Nmd3-GFP, reporters of 60S subunits, in *rpl25(D134R)*. Consistent with the genetic interactions, *rpl25(D134R)* severely blocked 60S export (Appendix D). The block in Nmd3 export is similar to our previous observations for *arx1*Δ mutants and implies a block in recruiting the 60S subunit to the NPC.

Next, I tested if *rpl25(D134R)* affected Arx1 binding on the 60S subunits. In *rpl25(D134R)*, Arx1 dissociated slightly more from 60S subunits at higher salt concentration compared to that of wild type (Appendix E). It appears unlikely that this minor change of Arx1 on the 60S subunits contributed to such a severe growth phenotype. Another export receptor may be perturbed by *rpl25(D134R)*, or the C-terminus of Rpl25 may be essential in 60S export.

If the major reason for the growth defect of rpl25(D134R) occurs from the defects of 60S export, the slow growth may be suppressed by elevating the copy number of known 60S export receptors. For example, *arx1*Δ and *nmd3*(ΔNES) mutants can be suppressed by high copy *MEX67* (Hung et al., 2008; Yao et al., 2007). I tested several 60S export receptors, *NMD3*, *CRM1*, *MEX67*, *MTR2*, and *ARX1*, as well as those that have been reported as high copy suppressors of 60S export defects, *PAB1* and *SBP1*, but none of them suppressed *rpl25(D134R)* (Appendix F).

Additional experiments will be required to determine if *rpl25(D134R)* disturbs the function of a 60S export receptor or Rpl25 itself is important for 60S export. These results will contribute to our knowledge of the mechanism of 60S export.

Appendix E. Rpl25D134R is synthetic lethal or synthetic sick with *arx1*Δ, *nup120*Δ and *CRM1T539-HA*

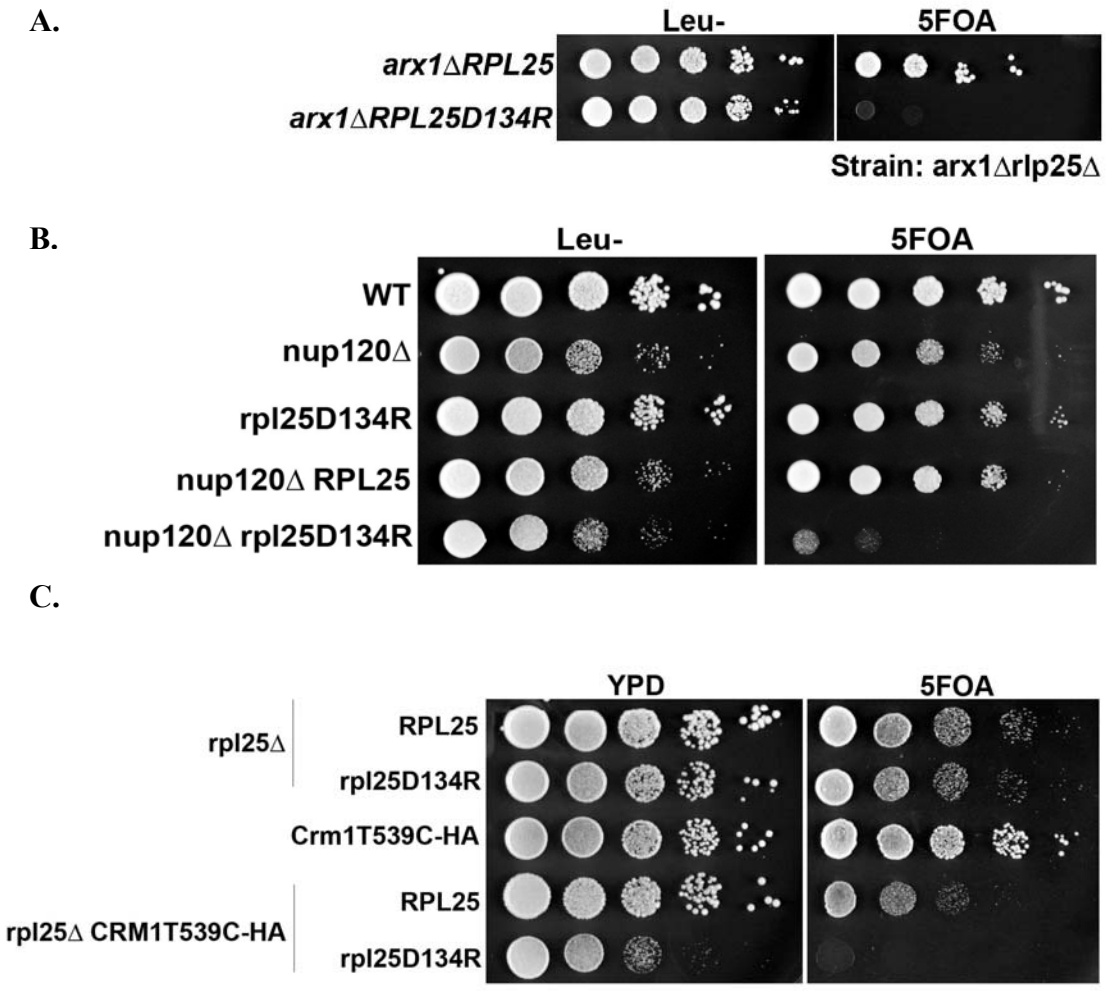

(A)AJY3021 (*arx*Δ*rpl25*Δ *RPL25-HA*), (B) AJY3031 (*nup120*Δ*rpl25*Δ *RPL25*), (C) AJY3042 (rpl25ΔCRM1T539C-HA RPL25) with pAJ2247 (*RPL25*) or pAJ2248 (*rpl25D134R*) were serially diluted and spotted on the plates indicated.

Appendix F. The rpl25(D134R) mutant displays a defect in 60S export

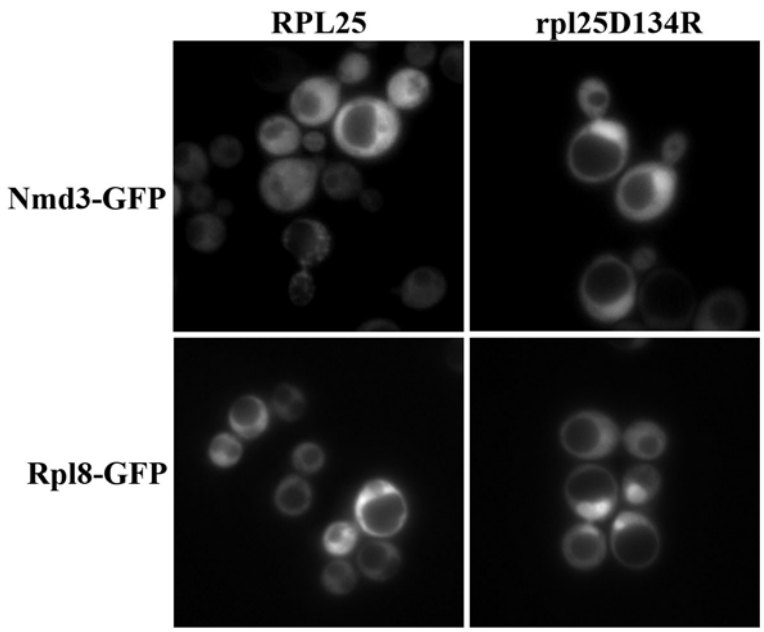

AJY3018 (RPL25) and AJY3019 (RPL25D134R) with Nmd3-GFP (pAJ755) or Rpl8-GFP (pAJ2206) were cultured at 25°C until OD_{600} 0.2 to 0.3. The GFP signal was visualized by fluorescence microscopy.

Appendix G. Arx1 shows weaker association with 60S subunits in the *rpl25D134R* mutant

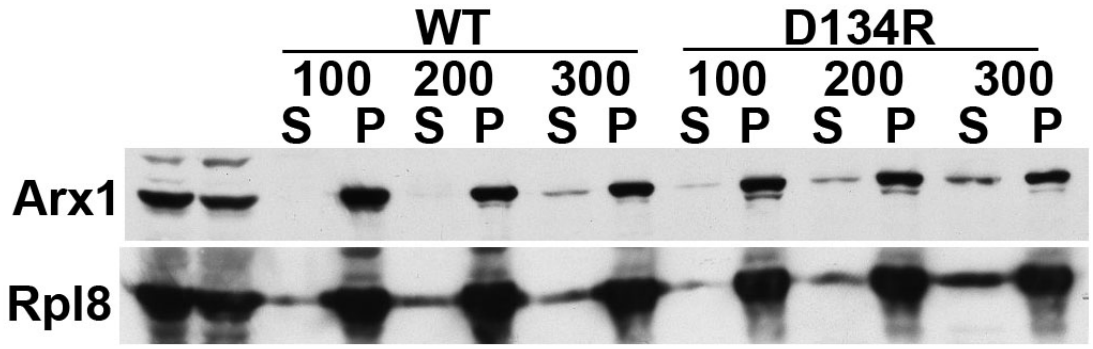

Protein extracts were prepared from AJY2993 and AJY2994 in (20 mM Tris pH 7.4, 100 mM NaCl, 6 mM MgCl2, 10% glycerol, 0.1% NP40, 1 mM PMSF, 1 μM pepstatin A, 1 μM leupeptin) and then overlayed on a 1M sucrose solution. After centrifugation in TLA100.3 rotor at 80,000 rpm for 60 minutes at 4 °C, supernatant (S) and pellet (P) fractions were separated by SDS-PAGE, and the presence of Arx1 and Rpl8 was detected by Western blotting.

Appendix H. Arx1 loss-of-function mutants can bypass the requirement of Rei1

Rei1 is the release factor of Arx1. In the absence of Rei1, Arx1 is persistent on the 60S subunits in the cytoplasm and results in slow growth and the cold-sensitive phenotype. Deletion of Arx1 rescues the growth defects of *rei1*Δ (Hung and Johnson, 2006; Lebreton et al., 2006).

To identify Arx1 suppressors of *rei1*Δ, I set up a mutagenesis of ARX1. The construct was *ARX1* with a C-terminal GFP tag on the *URA3 CEN* vector. *ARX1* mutants were generated by PCR mutagenesis. This *arx1* mutant pool was then gap rescued into the ARX1-GFP vector in *rei1*Δ*arx1*Δ cells. If *arx1* mutants could suppress the growth defects of *rei1*Δ, the mutants would be identified as bigger colonies. To exclude truncation mutants, the GFP signal was monitored by fluorescence microscopy.

Whereas wild type Arx1 showed cytoplasmic signal in *rei1*Δ, these *arx1* suppressor mutants predominantly localized in the nucleus (Appendix G). This suggests that either the Arx1 suppressors can bypass the requirement of Rei1 at the release step and return to the nucleus, or that they do not bind 60S and are never exported.

Surprisingly, these Arx1 suppressors complemented *arx1*Δ. This supports the first assumption that this group of *arx1* suppressors can support the function of Arx1 in ribosome biogenesis and recycle to nucleus without the assistance from Rei1. The mutations in these suppressors are summarized in Appendix G.

Stefan Bresson, an undergraduate student in our lab further characterized these arx1 mutants. If there was wild type-ARX1 in the cells, the growth defects of *rei1*Δ could not be suppressed by these mutants. From previous studies, Tif6 suppressors (Menne et al., 2007; Senger et al., 2001) and Mrt4 suppressors (see Chapter 4) can bypass the requirement of release factors, Efl1/Sdo and Yvh1, respectively, from weaker interaction with 60S subunits. To further determine if these *arx1* mutants also showed weaker 60S binding, salt titration of these mutants was performed using sedimentation through sucrose cushions. However, most of the *arx1* mutants showed similar affinity for 60S subunits as wild type Arx1. One possibility is that Arx1 depends on its binding partner, Alb1, to interact with 60S subunits. As long as is present, Arx1 binds 60S tightly. In the

future, the binding of these mutant Arx1 proteins to the ribosome in the absence of Alb1 will be tested.

Appendix I. Summary of high copy suppressor tests of RPL25D134R

Plasmids	Suppressor of RPL25D134R
2μ NMD3	No
2μ CRM1	No
2μ MEX67	No
2μ MTR2	No
2μ ARX1	No
2μ RLP24	No
2μ PAB1	No
2μ SBP1	No

Appendix J. Summary of ARX1 loss of function mutants

Arx1 LOF mutants	Mutation sites a.a. (nucleotide)	Localization	Growth rate compared to *rei1*Δ*arx1*Δ
#4	371K-E(AAA-GAA 1111)	Nuclear	Better
#5	327E-V(GAG-GTG 980) 388Y-H(TAT-CAT 1162)	Nuclear	Similar
#7	83K-E (AAA-GAA 247) 245R-G (AGA-GGA 733) 408E-G (GAA-GGA 1223)	Nuclear	better
#9	416L-S (TTG-TCG 1247) 417K-R (AAA-AGA 1250)	Nuclear	similar
#12	388Y-C (TAT-TGT 1163)	Nuclear	similar
#14	80Y-H (TAT-CAT 240) 109D-G (GAT-GGT 326) 453N-D (AAT-GAT 1357)	Nuclear	better
#17	375S-P (TCT-CCT 1123)	Nuclear	better
#20	428N-S (AAC-AGC 1283)	Nuclear	better
#22	430Y-H (TAC-CAC 1288)	Nuclear	better
#23	428N-D (AAC-GAC 1281)	Nuclear	better
#24	124T-A (ACT-GCT 370) 475L-S (TTA-TCA 1424)	Nuclear	better
#25	104W-R (TGG-AGG 310)	Nuclear	better
#26	127S-L (TCA-TTA 380)	Nuclear	better
#27	150Y-C (TAC-TGC 449) 278L-S (TTG-TCG 833) D518-G (GAC-GGC 1553)	Nuclear	better
#28	251L-P (CTG-CCG 752) 507I-T (ATC-ACC 1520)	Nuclear	better
#29	318L-S (TTA-TCA 953) 362R-S (AGA-AGT 1086)	Nuclear	better
#30	428N-S (AAC-AGC 1283)	Nuclear	better
#33	285K-E (AAG-GAG 853) 428N-Y (AAC-TAC 1282)	Nuclear	better
#34	464S-P (TCT-CCT 1390)	Nuclear	better
#35	425E-K (GAG-AAG 1273)	Nuclear	better
#36	388Y-H(TAT-CAT 1162)	Nuclear	better
#37	459S-G (AGT-GGT 1375)	Nuclear	better
#38	250F-L (TTC-CTC 748)	Nuclear	better
#39	419F-L (TTT-CTT 1255)	Nuclear	better
#40	430Y-C (TAC-TGC 1289)	Nuclear	better

These mutants were screened in *rei1*Δ*arx1*Δ strain for better growth. All mutants here complemented *arx1*Δ growth.

References

Alkalaeva, E.Z., A.V. Pisarev, L.Y. Frolova, L.L. Kisselev, and T.V. Pestova. 2006. In vitro reconstitution of eukaryotic translation reveals cooperativity between release factors eRF1 and eRF3. *Cell*. 125:1125-36.

Anand, B., S.K. Verma, and B. Prakash. 2006. Structural stabilization of GTP-binding domains in circularly permuted GTPases: implications for RNA binding. *Nucleic Acids Res*. 34:2196-205.

Bassler, J., P. Grandi, O. Gadal, T. Lessmann, E. Petfalski, D. Tollervey, J. Lechner, and E. Hurt. 2001. Identification of a 60S preribosomal particle that is closely linked to nuclear export. *Mol Cell*. 8:517-29.

Basu, U., K. Si, J.R. Warner, and U. Maitra. 2001. The Saccharomyces cerevisiae TIF6 gene encoding translation initiation factor 6 is required for 60S ribosomal subunit biogenesis. *Mol Cell Biol*. 21:1453-62.

Bayliss, R., S.W. Leung, R.P. Baker, B.B. Quimby, A.H. Corbett, and M. Stewart. 2002a. Structural basis for the interaction between NTF2 and nucleoporin FxFG repeats. *Embo J*. 21:2843-53.

Bayliss, R., T. Littlewood, and M. Stewart. 2000. Structural basis for the interaction between FxFG nucleoporin repeats and importin-beta in nuclear trafficking. *Cell*. 102:99-108.

Bayliss, R., T. Littlewood, L.A. Strawn, S.R. Wente, and M. Stewart. 2002b. GLFG and FxFG nucleoporins bind to overlapping sites on importin-beta. *J Biol Chem*. 277:50597-606.

Becam, A.M., F. Nasr, W.J. Racki, M. Zagulski, and C.J. Herbert. 2001. Ria1p (Ynl163c), a protein similar to elongation factors 2, is involved in the biogenesis of the 60S subunit of the ribosome in Saccharomyces cerevisiae. *Mol Genet Genomics*. 266:454-62.

Beeser, A.E., and T.G. Cooper. 2000. The dual-specificity protein phosphatase Yvh1p regulates sporulation, growth, and glycogen accumulation independently of catalytic activity in Saccharomyces cerevisiae via the cyclic AMP-dependent protein kinase cascade. *J Bacteriol*. 182:3517-28.

Benelli, D., S. Marzi, C. Mancone, T. Alonzi, A. la Teana, and P. Londei. 2009. Function and ribosomal localization of aIF6, a translational regulator shared by archaea and eukarya. *Nucleic Acids Res*. 37:256-67.

Bradatsch, B., J. Katahira, E. Kowalinski, G. Bange, W. Yao, T. Sekimoto, V. Baumgartel, G. Boese, J. Bassler, K. Wild, R. Peters, Y. Yoneda, I. Sinning, and E. Hurt. 2007. Arx1 Functions as an Unorthodox Nuclear Export Receptor for the 60S Preribosomal Subunit. *Mol Cell*. 27:767-79.

Briones, E., C. Briones, M. Remacha, and J.P. Ballesta. 1998. The GTPase center protein L12 is required for correct ribosomal stalk assembly but not for Saccharomyces cerevisiae viability. *J Biol Chem*. 273:31956-61.

Collins, S.R., P. Kemmeren, X.C. Zhao, J.F. Greenblatt, F. Spencer, F.C. Holstege, J.S. Weissman, and N.J. Krogan. 2007. Toward a comprehensive atlas of the physical interactome of Saccharomyces cerevisiae. *Mol Cell Proteomics*. 6:439-50.

Demoinet, E., A. Jacquier, G. Lutfalla, and M. Fromont-Racine. 2007. The Hsp40 chaperone Jjj1 is required for the nucleo-cytoplasmic recycling of preribosomal factors in Saccharomyces cerevisiae. *Rna*. 13:1570-81.

Diaconu, M., U. Kothe, F. Schlunzen, N. Fischer, J.M. Harms, A.G. Tonevitsky, H. Stark, M.V. Rodnina, and M.C. Wahl. 2005. Structural basis for the function of the ribosomal L7/12 stalk in factor binding and GTPase activation. *Cell*. 121:991-1004.

Dong, X., A. Biswas, and Y.M. Chook. 2009a. Structural basis for assembly and disassembly of the CRM1 nuclear export complex. *Nat Struct Mol Biol*. 16:558-60.

Dong, X., A. Biswas, K.E. Suel, L.K. Jackson, R. Martinez, H. Gu, and Y.M. Chook. 2009b. Structural basis for leucine-rich nuclear export signal recognition by CRM1. *Nature*. 458:1136-41.

Fornerod, M., and M. Ohno. 2002. Exportin-mediated nuclear export of proteins and ribonucleoproteins. *Results Probl Cell Differ*. 35:67-91.

Fribourg, S., and E. Conti. 2003. Structural similarity in the absence of sequence homology of the messenger RNA export factors Mtr2 and p15. *EMBO Rep*. 4:699-703.

Fried, H., and U. Kutay. 2003. Nucleocytoplasmic transport: taking an inventory. *Cell Mol Life Sci*. 60:1659-88.

Fromont-Racine, M., B. Senger, C. Saveanu, and F. Fasiolo. 2003. Ribosome assembly in eukaryotes. *Gene*. 313:17-42.

Gadal, O., D. Strauss, J. Kessl, B. Trumpower, D. Tollervey, and E. Hurt. 2001. Nuclear export of 60s ribosomal subunits depends on Xpo1p and requires a nuclear export sequence-containing factor, Nmd3p, that associates with the large subunit protein Rpl10p. *Mol Cell Biol*. 21:3405-15.

Gandin, V., A. Miluzio, A.M. Barbieri, A. Beugnet, H. Kiyokawa, P.C. Marchisio, and S. Biffo. 2008. Eukaryotic initiation factor 6 is rate-limiting in translation, growth and transformation. *Nature*. 455:684-8.

Gavin, A.C., P. Aloy, P. Grandi, R. Krause, M. Boesche, M. Marzioch, C. Rau, L.J. Jensen, S. Bastuck, B. Dumpelfeld, A. Edelmann, M.A. Heurtier, V. Hoffman, C. Hoefert, K. Klein, M. Hudak, A.M. Michon, M. Schelder, M. Schirle, M. Remor, T. Rudi, S. Hooper, A. Bauer, T. Bouwmeester, G. Casari, G. Drewes, G. Neubauer, J.M. Rick, B. Kuster, P. Bork, R.B. Russell, and G. Superti-Furga. 2006. Proteome survey reveals modularity of the yeast cell machinery. *Nature*. 440:631-6.

Gleizes, P.E., J. Noaillac-Depeyre, I. Leger-Silvestre, F. Teulieres, J.Y. Dauxois, D. Pommet, M.C. Azum-Gelade, and N. Gas. 2001. Ultrastructural localization of rRNA shows defective nuclear export of preribosomes in mutants of the Nup82p complex. *J Cell Biol*. 155:923-36.

Gonzalo, P., and J.P. Reboud. 2003. The puzzling lateral flexible stalk of the ribosome. *Biol Cell*. 95:179-93.

Gorlich, D., S. Kostka, R. Kraft, C. Dingwall, R.A. Laskey, E. Hartmann, and S. Prehn. 1995. Two different subunits of importin cooperate to recognize nuclear localization signals and bind them to the nuclear envelope. *Curr Biol*. 5:383-92.

Gorlich, D., and U. Kutay. 1999. Transport between the cell nucleus and the cytoplasm. *Annu Rev Cell Dev Biol*. 15:607-60.

Gorlich, D., and R.A. Laskey. 1995. Roles of importin in nuclear protein import. *Cold Spring Harb Symp Quant Biol*. 60:695-9.

Gorlich, D., N. Pante, U. Kutay, U. Aebi, and F.R. Bischoff. 1996. Identification of different roles for RanGDP and RanGTP in nuclear protein import. *Embo J*. 15:5584-94.

Grosshans, H., G. Simos, and E. Hurt. 2000. Review: transport of tRNA out of the nucleus-direct channeling to the ribosome? *J Struct Biol*. 129:288-94.

Guan, K., D.J. Hakes, Y. Wang, H.D. Park, T.G. Cooper, and J.E. Dixon. 1992. A yeast protein phosphatase related to the vaccinia virus VH1 phosphatase is induced by nitrogen starvation. *Proc Natl Acad Sci U S A*. 89:12175-9.

Hanaoka, N., T. Umeyama, K. Ueno, K. Ueda, T. Beppu, H. Fugo, Y. Uehara, and M. Niimi. 2005. A putative dual-specific protein phosphatase encoded by YVH1 controls growth, filamentation and virulence in Candida albicans. *Microbiology*. 151:2223-32.

Hanson, C.L., H. Videler, C. Santos, J.P. Ballesta, and C.V. Robinson. 2004. Mass spectrometry of ribosomes from Saccharomyces cerevisiae: implications for assembly of the stalk complex. *J Biol Chem*. 279:42750-7.

Hedges, J., Y.I. Chen, M. West, C. Bussiere, and A.W. Johnson. 2006. Mapping the functional domains of yeast NMD3, the nuclear export adapter for the 60 S ribosomal subunit. *J Biol Chem*. 281:36579-87.

Hedges, J., M. West, and A.W. Johnson. 2005. Release of the export adapter, Nmd3p, from the 60S ribosomal subunit requires Rpl10p and the cytoplasmic GTPase Lsg1p. *Embo J*. 24:567-79.

Hieda, M., T. Tachibana, F. Yokoya, S. Kose, N. Imamoto, and Y. Yoneda. 1999. A monoclonal antibody to the COOH-terminal acidic portion of Ran inhibits both the recycling of Ran and nuclear protein import in living cells. *J Cell Biol*. 144:645-55.

Ho, J., and A.W. Johnson. 1999a. NMD3 encodes an essential cytoplasmic protein required for stable 60S ribosomal subunits in Saccharomyces cerevisiae. *Mol Cell Biol*. 19:2389-2399.

Ho, J.H., and A.W. Johnson. 1999b. NMD3 encodes an essential cytoplasmic protein required for stable 60S ribosomal subunits in Saccharomyces cerevisiae. *Mol Cell Biol*. 19:2389-99.

Ho, J.H., G. Kallstrom, and A.W. Johnson. 2000a. Nascent 60S ribosomal subunits enter the free pool bound by Nmd3p. *Rna*. 6:1625-34.

Ho, J.H., G. Kallstrom, and A.W. Johnson. 2000b. Nmd3p is a Crm1p-dependent adapter protein for nuclear export of the large ribosomal subunit. *J Cell Biol*. 151:1057-66.

Ho, J.H.N., G. Kallstrom, and A.W. Johnson. 2000c. Nmd3p is a Crm1p-dependent adapter protein for nuclear export of the large ribosomal subunit. *J Cell Biol*. 151:1057-1066.

Hofer, A., C. Bussiere, and A.W. Johnson. 2007. Mutational analysis of the ribosomal protein RPL10 from yeast. *J Biol Chem*.

Hung, N.J., and A.W. Johnson. 2006. Nuclear recycling of the pre-60S ribosomal subunit-associated factor Arx1 depends on Rei1 in Saccharomyces cerevisiae. *Mol Cell Biol*. 26:3718-27.

Hung, N.J., K.Y. Lo, S.S. Patel, K. Helmke, and A.W. Johnson. 2008. Arx1 Is a Nuclear Export Receptor for the 60S Ribosomal Subunit in Yeast. *Mol Biol Cell*. 19:735-44.

Hurt, E., S. Hannus, B. Schmelzl, D. Lau, D. Tollervey, and G. Simos. 1999. A novel in vivo assay reveals inhibition of ribosomal nuclear export in ran-cycle and nucleoporin mutants. *J Cell Biol*. 144:389-401.

Iwase, M., and A. Toh-e. 2004. Ybr267w is a new cytoplasmic protein belonging to the mitotic signaling network of Saccharomyces cerevisiae. *Cell Struct Funct*. 29:1-15.

Izaurralde, E., U. Kutay, C. von Kobbe, I.W. Mattaj, and D. Gorlich. 1997. The asymmetric distribution of the constituents of the Ran system is essential for transport into and out of the nucleus. *Embo J*. 16:6535-47.

Johnson, A.W., and R.D. Kolodner. 1995. Synthetic lethality of sep1 (xrn1) ski2 and sep1 (xrn1) ski3 mutants of Saccharomyces cerevisiae is independent of killer virus and suggests a general role for these genes in translation control. *Mol Cell Biol*. 15:2719-27.

Johnson, A.W., E. Lund, and J. Dahlberg. 2002a. Nuclear export of ribosomal subunits. *Trends Biochem Sci*. 27:580-5.

Johnson, A.W., E. Lund, and J. Dahlberg. 2002b. Nuclear Export of Ribosomal Subunits. *TiBS*. 11:580-585.

Kallstrom, G., J. Hedges, and A. Johnson. 2003a. The putative GTPases Nog1p and Lsg1p are required for 60S ribosomal subunit biogenesis and are localized to the nucleus and cytoplasm, respectively. *Mol Cell Biol*. 23:4344-55.

Kallstrom, G., J. Hedges, and A.W. Johnson. 2003b. The putative GTPases Nog1p and Lsg1p are required for 60S ribosomal subunit biogenesis and are localied to the nucleus and cytoplasm, respectively. *Mol Cell Biol.* 23:in press.

Katahira, J., K. Strasser, A. Podtelejnikov, M. Mann, J.U. Jung, and E. Hurt. 1999. The Mex67p-mediated nuclear mRNA export pathway is conserved from yeast to human. *Embo J*. 18:2593-609.

Kavran, J.M., and T.A. Steitz. 2007. Structure of the base of the L7/L12 stalk of the Haloarcula marismortui large ribosomal subunit: analysis of L11 movements. *J Mol Biol*. 371:1047-59.

Kohrer, K., and H. Domdey. 1991. Preparation of high molecular weight RNA. *Methods Enzymol*. 194:398-405.

Kowalinski, E., G. Bange, B. Bradatsch, E. Hurt, K. Wild, and I. Sinning. 2007. The crystal structure of Ebp1 reveals a methionine aminopeptidase fold as binding platform for multiple interactions. *FEBS Lett*. 581:4450-4.

Kressler, D., P. Linder, and J. de La Cruz. 1999. Protein trans-acting factors involved in ribosome biogenesis in Saccharomyces cerevisiae. *Mol Cell Biol*. 19:7897-912.

Krokowski, D., A. Boguszewska, D. Abramczyk, A. Liljas, M. Tchorzewski, and N. Grankowski. 2006. Yeast ribosomal P0 protein has two separate binding sites for P1/P2 proteins. *Mol Microbiol*. 60:386-400.

Krokowski, D., M. Tchorzewski, A. Boguszewska, and N. Grankowski. 2005. Acquisition of a stable structure by yeast ribosomal P0 protein requires binding of P1A-P2B complex: in vitro formation of the stalk structure. *Biochim Biophys Acta*. 1724:59-70.

Kudo, N., N. Matsumori, H. Taoka, D. Fujiwara, E.P. Schreiner, B. Wolff, M. Yoshida, and S. Horinouchi. 1999. Leptomycin B inactivates CRM1/exportin 1 by covalent modification at a cysteine residue in the central conserved region. *Proc Natl Acad Sci U S A*. 96:9112-7.

Kutay, U., and S. Guttinger. 2005. Leucine-rich nuclear-export signals: born to be weak. *Trends Cell Biol*. 15:121-4.

la Cour, T., L. Kiemer, A. Molgaard, R. Gupta, K. Skriver, and S. Brunak. 2004. Analysis and prediction of leucine-rich nuclear export signals. *Protein Eng Des Sel*. 17:527-36.

Lebreton, A., C. Saveanu, L. Decourty, J.C. Rain, A. Jacquier, and M. Fromont-Racine. 2006. A functional network involved in the recycling of nucleocytoplasmic pre-60S factors. *J Cell Biol*. 173:349-60.

Liu, Y., and A. Chang. 2008. A Mutant Plasma Membrane Protein Is Stabilized Upon Loss of Yvh1, a Novel Ribosome Assembly Factor. *Genetics*.

Lo, K.Y., and A.W. Johnson. 2009. Reengineering ribosome export. *Mol Biol Cell*. 20:1545-54.

Macara, I.G. 2001. Transport into and out of the nucleus. *Microbiol Mol Biol Rev*. 65:570-94, table of contents.

Mager, W.H., R.J. Planta, J.G. Ballesta, J.C. Lee, K. Mizuta, K. Suzuki, J.R. Warner, and J. Woolford. 1997. A new nomenclature for the cytoplasmic ribosomal proteins of Saccharomyces cerevisiae. *Nucleic Acids Res*. 25:4872-5.

Mattaj, I.W., and L. Englmeier. 1998. Nucleocytoplasmic transport: the soluble phase. *Annu Rev Biochem*. 67:265-306.

Menne, T.F., B. Goyenechea, N. Sanchez-Puig, C.C. Wong, L.M. Tonkin, P.J. Ancliff, R.L. Brost, M. Costanzo, C. Boone, and A.J. Warren. 2007. The Shwachman-Bodian-Diamond syndrome protein mediates translational activation of ribosomes in yeast. *Nat Genet*. 39:486-95.

Meyer, A.E., N.J. Hung, P. Yang, A.W. Johnson, and E.A. Craig. 2007. The specialized cytosolic J-protein, Jjj1, functions in 60S ribosomal subunit biogenesis. *Proc Natl Acad Sci U S A*. 104:1558-63.

Monecke, T., T. Guttler, P. Neumann, A. Dickmanns, D. Gorlich, and R. Ficner. 2009. Crystal structure of the nuclear export receptor CRM1 in complex with Snurportin1 and RanGTP. *Science*. 324:1087-91.

Monie, T.P., A.J. Perrin, J.R. Birtley, T.R. Sweeney, I. Karakasiliotis, Y. Chaudhry, L.O. Roberts, S. Matthews, I.G. Goodfellow, and S. Curry. 2007. Structural insights into the transcriptional and translational roles of Ebp1. *Embo J*. 26:3936-44.

Moy, T.I., and P.A. Silver. 1999. Nuclear export of the small ribosomal subunit requires the ran-GTPase cycle and certain nucleoporins. *Genes Dev*. 13:2118-33.

Muda, M., E.R. Manning, K. Orth, and J.E. Dixon. 1999. Identification of the human YVH1 protein-tyrosine phosphatase orthologue reveals a novel zinc binding domain essential for in vivo function. *J Biol Chem*. 274:23991-5.

Munoz-Alonso, M.J., G. Guillemain, N. Kassis, J. Girard, A.F. Burnol, and A. Leturque. 2000. A novel cytosolic dual specificity phosphatase, interacting with glucokinase, increases glucose phosphorylation rate. *J Biol Chem*. 275:32406-12.

Neville, M., and M. Rosbash. 1999. The NES-Crm1p export pathway is not a major mRNA export route in Saccharomyces cerevisiae. *Embo J*. 18:3746-56.

Nissan, T.A., J. Bassler, E. Petfalski, D. Tollervey, and E. Hurt. 2002. 60S pre-ribosome formation viewed from assembly in the nucleolus until export to the cytoplasm. *Embo J*. 21:5539-47.

Paine, P.L., L.C. Moore, and S.B. Horowitz. 1975. Nuclear envelope permeability. *Nature*. 254:109-14.

Park, H.D., A.E. Beeser, M.J. Clancy, and T.G. Cooper. 1996. The S. cerevisiae nitrogen starvation-induced Yvh1p and Ptp2p phosphatases play a role in control of sporulation. *Yeast*. 12:1135-51.

Pemberton, L.F., and B.M. Paschal. 2005. Mechanisms of receptor-mediated nuclear import and nuclear export. *Traffic*. 6:187-98.

Pertschy, B., C. Saveanu, G. Zisser, A. Lebreton, M. Tengg, A. Jacquier, E. Liebminger, B. Nobis, L. Kappel, I. van der Klei, G. Hogenauer, M. Fromont-Racine, and H. Bergler. 2007. Cytoplasmic recycling of 60S pre-ribosomal factors depends on the AAA-protein Drg1. *Mol Cell Biol*.

Pestova, T.V., V.G. Kolupaeva, I.B. Lomakin, E.V. Pilipenko, I.N. Shatsky, V.I. Agol, and C.U. Hellen. 2001. Molecular mechanisms of translation initiation in eukaryotes. *Proc Natl Acad Sci U S A*. 98:7029-36.

Petosa, C., G. Schoehn, P. Askjaer, U. Bauer, M. Moulin, U. Steuerwald, M. Soler-Lopez, F. Baudin, I.W. Mattaj, and C.W. Muller. 2004. Architecture of CRM1/Exportin1 suggests how cooperativity is achieved during formation of a nuclear export complex. *Mol Cell*. 16:761-75.

Planta, R.J., and W.H. Mager. 1998. The list of cytoplasmic ribosomal proteins of Saccharomyces cerevisiae. *Yeast*. 14:471-7.

Reichelt, R., A. Holzenburg, E.L. Buhle, Jr., M. Jarnik, A. Engel, and U. Aebi. 1990. Correlation between structure and mass distribution of the nuclear pore complex and of distinct pore complex components. *J Cell Biol*. 110:883-94.

Ribbeck, K., and D. Gorlich. 2001. Kinetic analysis of translocation through nuclear pore complexes. *Embo J*. 20:1320-30.

Rodriguez-Mateos, M., D. Abia, J.J. Garcia-Gomez, A. Morreale, J. de la Cruz, C. Santos, M. Remacha, and J.P. Ballesta. 2009. The amino terminal domain from Mrt4 protein can functionally replace the RNA binding domain of the ribosomal P0 protein. *Nucleic Acids Res*.

Rosendahl, G., and S. Douthwaite. 1995. Cooperative assembly of proteins in the ribosomal GTPase centre demonstrated by their interactions with mutant 23S rRNAs. *Nucleic Acids Res*. 23:2396-403.

Rout, M.P., J.D. Aitchison, A. Suprapto, K. Hjertaas, Y. Zhao, and B.T. Chait. 2000. The yeast nuclear pore complex: composition, architecture, and transport mechanism. *J Cell Biol*. 148:635-51.

Rout, M.P., and G. Blobel. 1993. Isolation of the yeast nuclear pore complex. *J Cell Biol*. 123:771-83.

Sakumoto, N., H. Yamashita, Y. Mukai, Y. Kaneko, and S. Harashima. 2001. Dual-specificity protein phosphatase Yvh1p, which is required for vegetative growth and sporulation, interacts with yeast pescadillo homolog in Saccharomyces cerevisiae. *Biochem Biophys Res Commun*. 289:608-15.

Salas-Marco, J., and D.M. Bedwell. 2004. GTP hydrolysis by eRF3 facilitates stop codon decoding during eukaryotic translation termination. *Mol Cell Biol*. 24:7769-78.

Santos-Rosa, H., H. Moreno, G. Simos, A. Segref, B. Fahrenkrog, N. Pante, and E. Hurt. 1998. Nuclear mRNA export requires complex formation between Mex67p and Mtr2p at the nuclear pores. *Mol Cell Biol*. 18:6826-38.

Satya Nugroho, N.S., Satoshi Harashima. 2003. Mutant MRT4 is capable of restoring normal growth rate to the yvh1 protein phosphatase disruptant mutant of Saccharomyces cerevisiae. *In* YGM conference.

Saveanu, C., A. Namane, P.E. Gleizes, A. Lebreton, J.C. Rousselle, J. Noaillac-Depeyre, N. Gas, A. Jacquier, and M. Fromont-Racine. 2003. Sequential protein association with nascent 60S ribosomal particles. *Mol Cell Biol*. 23:4449-60.

Segref, A., K. Sharma, V. Doye, A. Hellwig, J. Huber, R. Luhrmann, and E. Hurt. 1997. Mex67p, a novel factor for nuclear mRNA export, binds to both poly(A)+ RNA and nuclear pores. *Embo J*. 16:3256-71.

Senay, C., P. Ferrari, C. Rocher, K.J. Rieger, J. Winter, D. Platel, and Y. Bourne. 2003. The Mtr2-Mex67 NTF2-like domain complex. Structural insights into a dual role of Mtr2 for yeast nuclear export. *J Biol Chem*. 278:48395-403.

Senger, B., D.L. Lafontaine, J.S. Graindorge, O. Gadal, A. Camasses, A. Sanni, J.M. Garnier, M. Breitenbach, E. Hurt, and F. Fasiolo. 2001. The nucle(ol)ar Tif6p and Efl1p are required for a late cytoplasmic step of ribosome synthesis. *Mol Cell*. 8:1363-73.

Sengupta, J., J. Nilsson, R. Gursky, C.M. Spahn, P. Nissen, and J. Frank. 2004. Identification of the versatile scaffold protein RACK1 on the eukaryotic ribosome by cryo-EM. *Nat Struct Mol Biol*. 11:957-62.

Si, K., and U. Maitra. 1999. The Saccharomyces cerevisiae homologue of mammalian translation initiation factor 6 does not function as a translation initiation factor. *Mol Cell Biol*. 19:1416-26.

Spahn, C.M., M.G. Gomez-Lorenzo, R.A. Grassucci, R. Jorgensen, G.R. Andersen, R. Beckmann, P.A. Penczek, J.P. Ballesta, and J. Frank. 2004. Domain movements of elongation factor eEF2 and the eukaryotic 80S ribosome facilitate tRNA translocation. *Embo J*. 23:1008-19.

Stage-Zimmermann, T., U. Schmidt, and P.A. Silver. 2000. Factors affecting nuclear export of the 60S ribosomal subunit in vivo. *Mol Biol Cell*. 11:3777-89.

Strasser, K., J. Bassler, and E. Hurt. 2000. Binding of the Mex67p/Mtr2p heterodimer to FXFG, GLFG, and FG repeat nucleoporins is essential for nuclear mRNA export. *J Cell Biol*. 150:695-706.

Stutz, F., A. Bachi, T. Doerks, I.C. Braun, B. Seraphin, M. Wilm, P. Bork, and E. Izaurralde. 2000. REF, an evolutionary conserved family of hnRNP-like proteins, interacts with TAP/Mex67p and participates in mRNA nuclear export. *Rna*. 6:638-50.

Tarassov, K., V. Messier, C.R. Landry, S. Radinovic, M.M. Serna Molina, I. Shames, Y. Malitskaya, J. Vogel, H. Bussey, and S.W. Michnick. 2008. An in vivo map of the yeast protein interactome. *Science*. 320:1465-70.

Thomas, F., and U. Kutay. 2003a. Biogenesis and nuclear export of ribosomal subunits in higher eukaryotes depend on the CRM1 export pathway. *J Cell Sci*. 116:2409-19.

Thomas, F., and U. Kutay. 2003b. Biogenesis and nuclear export of ribosomal subunits in higher eukaryotes depend on the CRM1 export pathway. *J Cell Sci*. 116:2409-2419.

Tran, E.J., Y. Zhou, A.H. Corbett, and S.R. Wente. 2007. The DEAD-box protein Dbp5 controls mRNA export by triggering specific RNA:protein remodeling events. *Mol Cell*. 28:850-9.

Trotta, C.R., E. Lund, L. Kahan, A.W. Johnson, and J.E. Dahlberg. 2003a. Coordinated nuclear export of 60S ribosomal subunits and NMD3 in vertebrates. *Embo J*. 22:2841-51.

Trotta, C.R., E. Lund, L. Kahan, A.W. Johnson, and J.E. Dahlberg. 2003b. Coordinated nuclear export of 60S ribosomal subunits and NMD3 in vertebrates. *Embo J*. 22:2841-2851.

Tschochner, H., and E. Hurt. 2003. Pre-ribosomes on the road from the nucleolus to the cytoplasm. *Trends Cell Biol*. 13:255-63.

Vale, R.D. 2000. AAA proteins. Lords of the ring. *J Cell Biol*. 150:F13-9.

Valenzuela, D.M., A. Chaudhuri, and U. Maitra. 1982. Eukaryotic ribosomal subunit anti-association activity of calf liver is contained in a single polypeptide chain protein of Mr = 25,500 (eukaryotic initiation factor 6). *J Biol Chem*. 257:7712-9.

Venema, J., and D. Tollervey. 1999. Ribosome synthesis in Saccharomyces cerevisiae. *Annu Rev Genet*. 33:261-311.

Warner, J.R. 1999. The economics of ribosome biosynthesis in yeast. *Trends Biochem Sci*. 24:437-40.

Weis, K. 2003. Regulating access to the genome: nucleocytoplasmic transport throughout the cell cycle. *Cell*. 112:441-51.

West, M., J.B. Hedges, A. Chen, and A.W. Johnson. 2005. Defining the order in which Nmd3p and Rpl10p load onto nascent 60S ribosomal subunits. *Mol Cell Biol*. 25:3802-13.

West, M., J.B. Hedges, K.Y. Lo, and A.W. Johnson. 2007. Novel interaction of the 60S ribosomal subunit export adapter Nmd3 at the nuclear pore complex. *J Biol Chem*. 282:14028-37.

Yang, Q., M.P. Rout, and C.W. Akey. 1998. Three-dimensional architecture of the isolated yeast nuclear pore complex: functional and evolutionary implications. *Mol Cell*. 1:223-34.

Yao, W., M. Lutzmann, and E. Hurt. 2008. A versatile interaction platform on the Mex67-Mtr2 receptor creates an overlap between mRNA and ribosome export. *Embo J*. 27:6-16.

Yao, W., D. Roser, A. Kohler, B. Bradatsch, J. Bassler, and E. Hurt. 2007. Nuclear export of ribosomal 60S subunits by the general mRNA export receptor Mex67-Mtr2. *Mol Cell*. 26:51-62.

Zakalskiy, A., G. Hogenauer, T. Ishikawa, E. Wehrschutz-Sigl, F. Wendler, D. Teis, G. Zisser, A.C. Steven, and H. Bergler. 2002. Structural and enzymatic properties of the AAA protein Drg1p from Saccharomyces cerevisiae. Decoupling of intracellular function from ATPase activity and hexamerization. *J Biol Chem*. 277:26788-95.

Zemp, I., and U. Kutay. 2007. Nuclear export and cytoplasmic maturation of ribosomal subunits. *FEBS Lett*. 581:2783-93.

Zhang, J., P. Harnpicharnchai, J. Jakovljevic, L. Tang, Y. Guo, M. Oeffinger, M.P. Rout, S.L. Hiley, T. Hughes, and J.L. Woolford, Jr. 2007. Assembly factors Rpf2 and Rrs1 recruit 5S rRNA and ribosomal proteins rpL5 and rpL11 into nascent ribosomes. *Genes Dev*. 21:2580-92.

Zuk, D., J.P. Belk, and A. Jacobson. 1999. Temperature-sensitive mutations in the Saccharomyces cerevisiae MRT4, GRC5, SLA2 and THS1 genes result in defects in mRNA turnover. *Genetics*. 153:35-47.

Vita

Kai-Yin Lo was born on November 21th, 1978 in Taipei, Taiwan, the daughter of Fan-Ching Lo and Li-Hui Hsieh. After graduating from Taipei First Girls' high school, she attended National Taiwan University from 1997 to 2001. After earning her Bachelors drgree, she joined in Dr. Chia-Yin Lee's Lab and got her Master degree in Microbiology in Department of Agricultural Chemistry, NTU. After one year as a research assistant in Dr. Hsin-Chih Lai's Lab in Department of Clinical laboratory science and Medical Biotechnology, NTU, she entered the Ph.D. program in Microbiology at the University of Texas at Austin in Fall 2004 and joined Dr Arlen Johnson's Lab in the summer of 2005.

Permanent address: 5F, No5, Aly1, Ln203, Sec1, Shiou-Lang Rd, Yung-He City, Taipei 234, Taiwan

This dissertation was typed by the author.

Publication

Lo KY, Li Z, Wang F, Marcotte E, and Johnson AW. Ribosome stalk assembly requires the dual specificity phosphatase Yvh1 for the exchange of Mrt4 with P0 (Manuscript under review [Journal of Cell Biology])

Lo KY and Johnson AW. Unpackaging the pre-60S particle in the cytoplasm (Manuscript in preparation)

Lo KY and Johnson AW. Reengineering ribosome export. Mol Biol Cell. 2009. 20(5):1545-1554

Hung NJ, **Lo KY**, Patel SS, Helmke K, Johnson AW. Arx1 is a nuclear export receptor for the 60S ribosomal subunit in yeast. Mol Biol Cell. 2008. 19(2):735-44

West, M, Hedges J, **Lo KY**, Johnson A. 2007. Novel interaction of the 60S ribosomal subunit export adapter Nmd3p at the nuclear pore complex. J Biol Chem. 2007. 282(19):14028-37

Horng YT, Soo PC, Shen BJ, Hung YL, **Lo KY**, Su HP, Wei JR, Hsieh SC, Hsueh PR, Lai HC. Development of an improved PCR-ICT hybrid assay for direct detection of *Legionellae* and *Legionella pneumophila* from cooling tower water specimens. Water Res. 2006. 40(11):2221-9.

Abstracts

Lo KY and Johnson AW. Reengineering ribosome export. Meeting on Translational Control. CSH. (2008)

West, M, Hedges J, **Lo KY**, Johnson A. Novel interaction of the 60S ribosomal subunit export adapter Nmd3p at the nuclear pore complex. 11th annual meeting of the RNA society. (2006)

Lo, KY and Lee CY. Analysis of amidohydrolase operon from *Variovorax paradoxus* Iso1. The 36th Conference of Chinese Society of Microbiology (2002)

Lin, HY, **Lo KY**, Peng IC, and Lee CY. Gene regulation and protein expression of collagenase gene of *Vibrio parahaemolytics*. The 35th Conference of Chinese Society of Microbiology (2001)